ENVIRONMENTAL ASSESSMENT OF *IN SITU* GROUNDWATER REMEDIATION WITH REDUCED IRON REACTIVE MEDIA

by

Monica R Higgins

A dissertation submitted in partial fulfillment
of the requirements for the degree of
Doctor of Philosophy
(Environmental Engineering)
in The University of Michigan
2011

Doctoral Committee:

Associate Professor Terese M. Olson, Chair
Professor Kim F. Hayes
Professor Gregory A. Keoleian
Professor Nancy G. Love

Acknowledgements

Financial support for the research conducted in this dissertation came from the Rackham Engineering Award, the GEM Fellowship with Pacific Northwest National Laboratory, and the Elizabeth C. Crosby Award.

Life-Cycle Case Study Comparison of Permeable Reactive Barrier versus Pump-and-Treat Remediation (Chapter 4), is adapted from an article of the same name published in *Environemntal Science & Technology* in 2009.

Thank you to my committee members Dr. Kim Hayes, Dr. Gregory Keoleian, and Dr. Nancy Love, for their time and discussions on this work, and in particular Dr. Terese Olson, thank you for support and guidance in research and for being an advisor, teacher, and mentor over these five years.

To my PhD Support Group Members: Dr. Andrew Henderson, Jeremy Guest, Sherri Cook, Matthew Fadden, and Carol Girata, thank you for all of the conversations, easy and difficult, and for never letting me get away with "reading" as a weekly goal. Two down, four to go.

Finally, and most importantly, thank you to Elizabeth. Your love, support, and patience made this dissertation and this degree possible. We did it.

Table of Contents

List of Figures

List of Tables

List of Appendices

List of Abbreviations

CERCLA	Comprehensive Environmental Response, Compensation, and Liability Act
CFU	Colony Forming Units
E. coli	*Escherichia coli*
Fe^{0}	Iron in the 0 Oxidation State
Fe^{II} or Fe(II)	Iron in the +II Oxidation State
Fe^{II} or Fe(III)	Iron in the +III Oxidation State
FeS	Iron Sulfide
M	Molar; moles/liter
MOPS	3-(N-morpholino)propanesulfonic acid
Na-MOPS	3-(N-morpholino)propanesulfonic acid Sodium Salt
pe	-log[e-]
pH	-log[H+]
PMF	Proton Motive Force
PRB	Permeable Reactive Barrier
PTS	Pump-and-Treat System
SSA_{ext}	External Specific Surface Area
ZVI	Zero Valent Iron

Chapter 1

Introduction

Groundwater is the largest reservoir of liquid freshwater on earth (Oki and Kanae 2006), making it an important natural resource and source of potable water for individual homes and municipalities. In assessments of water use in 2000 and 2005, 36% and 33% of public water supply in the United States was obtained from groundwater aquifers, respectively (Hutson et al. 2004; Kenny et al. 2009). Despite the importance of groundwater to the supply of potable and irrigation water, across the United States there is significant groundwater contamination resulting from natural and anthropogenic processes. These contaminants range from naturally-occurring deposits of arsenic-bearing minerals (Focazio et al. 2000) to atrazine contamination due to pesticide application (Stackelberg et al. 2005). There are several other issues currently threatening the sustainable use of groundwater in the future, including global climate change (Goderniaux et al. 2009), increasing population (United Nations Environment Programme (UNEP) 2006) and urbanization (Haase 2009), all of which must be considered when designing a remediation technology.

Remediation of contaminated groundwater in the United States began in the 1980s following the passage of the Comprehensive Environmental Response,

Compensation, and Liability Act, passed in response to public tragedies such as Love Canal, NY (National Research Council 1994). Originally, it was conceived that the physical removal of the contaminated groundwater from the subsurface would result in the flow of clean groundwater into the area and remediation of the site; this formed the basis for the design of pump-and-treat systems. Such designs require that groundwater be pumped from the subsurface into aboveground treatment facilities (National Research Council 1994). A major economic and environmental cost of pump-and-treat systems is the need for continuous and long term extraction of groundwater, and therefore the continuous input of energy (National Research Council 1994; Bayer and Finkel 2006).

Permeable reactive barriers were introduced as an alternative to pump-and-treat systems in 1991 (Gillham and O'Hannesin 1994). Permeable reactive barriers treat the groundwater *in situ* by allowing the water to flow naturally through a biologically or chemically engineered cell that is designed to remove targeted contaminants from the aqueous phase. The long-term success of permeable reactive barriers remains uncertain, as the first permeable reactive barrier was installed in 1991, though there is documented operation of over ten years for chromium remediation (Wilkin, Puls, and Sewell 2003) ten years for chlorinate solvent remediation (Phillips et al. 2010) and fifteen years for the remediation of nitrate (Robertson, Vogan, and Lombardo 2008). Though permeable reactive barriers have eliminated the need for continuous energy input to a remediation system, an area of uncertainty is the longevity of reactive media.

Permeable reactive barrier designs have employed a variety of reactive media, including granular activated carbon, surface-modified zeolites, and dithionite solutions, to transform contaminants in the subsurface (Scherer et al. 2000). However, the vast

majority of permeable reactive barriers installed at field-scale or monitored for long time periods have used a single reactive media, zero-valent iron. Zero-valent iron is a strong reducing agent that has been employed for the conversion of organic compounds and metals in the environment (Cantrell, Kaplan, and Wietsma 1995/7). Zero-valent iron is not applicable at all contaminated sites, such as sites with high alkalinity or carbonate concentrations where the formation of precipitates and loss of permeability may cause premature failure (Henderson and Demond 2007).

Other reduced iron solids have been investigated for use in permeable reactive barriers, including ferrous sulfate and ferrous sulfide minerals (Scherer et al. 2000). Mackinawite is a naturally-occurring, iron sulfide mineral that has been proposed as an alternative to zero-valent iron as a permeable reactive medium for the treatment of arsenic (Han et al. 2011), trichloroethylene and tetrachloroethylene (Butler and Hayes 1999). In a mechanism similar to zero-valent iron, mackinawite can reduce contaminants, but also dissolves to produce sulfide ions in solution (Pankow and Morgan 1979) that may remove metal contaminants through the formation of insoluble sulfide solids.

A recent advance in the implementation of the permeable reactive barrier technology has been the use of nanoscale reactive media (Tratnyek and Johnson 2006b; Li, Elliot, and Zhang 2006). Nanoparticles offer many advantages over granular media, such as ease of emplacement or regeneration, because of their size and the ability to employ individual nanoparticles or particles anchored to a support medium (Zhang 2003). Zero-valent iron nanoparticles have been successfully employed on many sites in the United States and around the world for the treatment of many common pollutants

including trichloroethene and chromium (Li, Elliot, and Zhang 2006). Bimetallic iron nanoparticles (Fe/Pd) has also been tested in a four-week field applications for the treatment of trichloroethene (Elliott and Zhang 2001; 2001). Iron-sulfide nanoparticle-coated sand has been studied in laboratory columns for the removal of arsenic from solution (Han et al. 2011).

The continued use of permeable reactive barriers will rely on the technology's ability to satisfy an increasingly complicated set of design objectives. Remediation technologies must remove contaminants from the aqueous phase such that the public is protected from contamination of the water supply and delicate ecosystems can be maintained (National Research Council 1994). In order to provide for this requirement, reactive media must be chemically suitable for the transformation of contaminants to non-hazardous levels, as determined by project goals. In addition to providing treatment, regulatory agencies (USEPA 2008) and researchers (Bayer and Finkel 2006) are pushing for remediation technology designs to minimize the environmental burden placed on the local and global environment. This additional objective requires analysis of the environmental impacts of permeable reactive barriers and reactive media with respect to environmental considerations including resource use and possible toxicity. In the future, designs will likely be based on both performance and environmental impact, maximizing treatment and environmental performance, for each individual contaminated site. This dissertation seeks to answer key questions necessary for determination of the environmental impact of permeable reactive barriers which employ reduced iron reactive media.

Objectives of Research

The primary objectives of this research were as follows:

1. **Investigation of the Relative Environmental Impacts of *In Situ* Remediation with Reduced Iron Reactive Media: Life Cycle Assessment Case Study**

   A comparative study of the environmental sustainability of a pump-and-treat-system and permeable reactive barrier was conducted based on thirty years of treatment, allowing for the quantification of environmental impacts (global warming potential, acidification potential, human health effect, eutrophication potential, ozone depletion potential and smog formation potential), determination of the environmentally-preferable technology, and identification of materials and processes that most influence the sustainability of each technology.

2. **Investigation of the Local Environmental Impacts of *In Situ* Remediation with Reduced Iron Reactive Media: Toxicity to Microorganisms**

   a. **Investigation of the Effect of Zero-Valent Iron Nanoparticles on Bacterial Growth;**

      The effect of zero-valent iron nanoparticles and dissolved ferrous iron on bacterial cultures growing under anaerobic conditions was examined. The effect of nZVI age was also examined. Equilibrium speciation modeling provided insight into the chemical changes in the presence of nZVI and the aqueous species responsible for observed effect.

   b. **Investigation of the Effect of Iron Sulfide Nanoparticles on Bacterial Growth;**

The effect of iron sulfide nanoparticles and dissolved sulfide on bacterial growth was investigated. The dissolution of FeS in the microbial growth medium was also examined. Equilibrium speciation modeling provided insight into the chemical changes in the presence of FeS and the aqueous species responsible for observed effect.

Dissertation Organization

This dissertation is divided into six chapters in addition to this introduction. Chapter 2 provides necessary background and theoretical information related to the research conducted. Chapter 3 outlines the materials, methods of chemical analysis and approach used in dissertation reserach. Chapter 4 addresses the first objective and presents the life cycle assessment case study results. Chapter 5 addresses the second objective and presents the results related to the effect of zero-valent iron nanoparticles on bacterial growth. Chapter 6 focuses on the final objective and describes the effect of iron sulfide nanoparticles on bacterial growth. Chapter 7 gives the conclusions from the research conducted and provides insight into future needs in this area. Appendices are provided and contain Life Cycle Assessment Assumptions (Appendix A), nanoparticle exposure experimental data (Appendix B), Equilibrium Modeling Codes (Appendix C-F), selected thermodynamic database used in speciation modeling (Appendix G), and additional speciation modeling results for zero-valent iron exposure (Appendix H). References are provided following the Appendices.

Chapter 2

Background and Theory

Groundwater Remediation Technologies

Contaminated groundwater can be restored using an *ex situ* remediation technology, an *in situ* remediation technology, or natural attenuation. *Ex situ* technologies remove groundwater from the subsurface for treatment while *in situ* technologies provide treatment in the subsurface. Two common groundwater remediation technologies, a pump-and-treat system and a permeable reactive barrier, are introduced in this section.

Pump-and-Treat Systems

A pump-and-treat system (PTS) is the most common *ex situ* treatment technology employed for groundwater remediation. A PTS uses established water treatment unit processes to transform contaminants in aboveground facilities (National Research Council 1994). The design of a PTS involves the design of both the extraction system and the treatment facilities, which is detailed in several government guidance documents (U.S. EPA 1996; Cohen et al. 1997; U.S. EPA 2005). PTS is the most widely applied groundwater remediation technology in the United States (National Research Council

1994; U.S. EPA 1996) and has been used at a variety of sites since the 1980s (U.S. EPA 2001).

Permeable Reactive Barriers

A permeable reactive barrier (PRB) is a common in situ remediation technology. PRBs are an engineered reactive zone which is placed in the subsurface to provide adequate treatment of contaminants (Morrison et al. 2002). A PRB using metallic iron was first introduced as an alternative to a PTS in 1991 (Gillham and O'Hannesin 1994). PRB design depends on the types and distribution of contaminants, hydrologic flow characteristics, site conditions, and the reactive media used (Gavaskar 1999). Design variables include the dimensions of the barrier and the amount of reactive material (Scherer et al. 2000). PRBs are designed in several configurations, including funnel-and-gate, continuous trench, injection emplacement, and injection. Geotechnical techniques for barrier construction, including slurry trenching, deep soil mixing, and grouting have been proposed and tested for PRB installation (Day, O'Hannesin, and Marsden 1999).

Reactive Media. The reactive zone of a PRB is often maintained in the subsurface by a reactive media, which provides geochemical or biologically-mediated reaction gradients which mediate the treatment of contaminants (Scherer et al. 2000; Blowes et al. 2000). The selection of a reactive medium for PRB applications is dependent on the contaminants of interest and the geochemical conditions at the site. The medium is usually a granular (micrometer-sized) solid phase that is capable of creating reducing or oxidizing conditions in the subsurface, with most common reactive medium chosen being zero-valent iron (ZVI) (Scherer et al. 2000). Other reactive media that are

employed include activated carbon, iron minerals, as well as oxygen- or nitrate-releasing compounds. Chemical reactive media have a fixed lifetime based on the interaction of the medium with contaminants and groundwater constituents.

Nanosized Reactive Media. Recently, the use of nanosized reactive media, specifically nanosized zero valent iron (nZVI), has become more common. Nanomaterials, defined as materials with at least one dimension that is less than 100 nanometers (10^{-9} m) (Nel et al. 2006), are present in both natural and engineering form in our environment (Klaine et al. 2008). Nanomaterials exhibit specific properties that distinguish them from bulk-phase materials and dissolved solutes (Hochella and Madden 2005), which can be exploited in engineering applications in electrical, biomedical, energy, and environmental applications (Nowack and Bucheli 2007).

Performance of Remediation Technologies

Remediation technologies are employed at a contaminated site to meet site-specific goals including removal of contaminant mass or hydraulic containment, or both. Initially, the primary goal of remediation was to restore contaminated aquifers to drinking water quality standards through the removal of contaminant, but the performance goals have changed to reflect the unexpected challenges in contaminant extraction (National Research Council 1994). Both PTS and PRB technologies have been applied at field-scale with variable success.

Pump and Treat System Performance. The long-term success of PTS applications has been low, due to complex geochemical conditions and contaminant-aquifer material interactions (Mackay and Cherry 1989). Several authors have applied computer modeling to PTS design and optimized extraction systems (Kuo, Michel, and

Gray 1992; Guan and Aral 1999; Matott, Rabideau, and Craig 2006). The reinjection of treated water, called pump-treat-inject (PTI) strategies have also been proposed to increase the hydraulic gradients through the treatment zone (Bear and Sun 1998). Other innovative strategies include the combined use of a PTS with additional chemical or biological treatment (U.S. EPA 1996)or the inclusion of physical barriers (Bayer, Finekel, and Teutsch 2005). Though optimization is possible, any PTS has a high energy demand and cost due to the operation of the extraction system for more than 30 years.

Permeable Reactive Barrier Performance. Assessment of the long-term performance of the PRB technology suggest that while failures are limited, there are a variety of factors that contribute to risk of failure at many sites (Henderson and Demond 2007). Failure of permeable reactive barriers implemented at field-scale can be mainly attributed to inappropriate site characterization and subsequent construction (Korte 2000). Issues with permeable reactive barriers include loss of reactivity due to passivation or loss of the reactive media (Phillips et al. 2000) and loss of permeability or porosity due to poor clogging (Kamolpornwijit et al. 2003), with both processes taken together described as the barriers longevity. The longevity of a PRB is determined by the chemical properties of the reactive media together with the contaminants present and the geochemical conditions on site (Phillips et al. 2010).

Environmental Assessment of Remediation Technologies

Criticism of *ex situ* technologies has been based on the long treatment times and the continuous use of energy resources, but framed in terms of cost rather than impact on the environment (National Research Council 1994; Travis and Doty 1990). Similarly, at the outset of permeable reactive barrier technology implementation, the manufacture of

zero-valent iron was inefficient such that cost of the material was prohibitively high for some configurations or applications (Day, O'Hannesin, and Marsden 1999; Gavaskar 1999). Though in previous applications of remediation technologies, the choice of one technology over another has been made based only on technical or economic comparisons (Diamond et al. 1999), regulatory agencies are beginning to emphasize the consideration of environmental impacts in decision-making and design (USEPA 2008).

Remediation of contaminated groundwater represents the restoration of one natural resource at the expense of many other resources. The incorporation of environmental impacts into the determination of a site-specific remediation strategy requires a method through which to quantitatively compare various environmental impacts of alternatives. Life cycle assessment (LCA) is such a method for the quantification of environmental impacts (International Organization for Standardization 1997).

LCA and Site Remediation. The application of LCA methodology to remediation technologies for site restoration has been presented in a number of studies. A review of life cycle assessment for site remediation is presented by Suér and colleagues (Suer, Nilsson-Paledal, and Norrman 2004). Diamond and colleagues developed a life cycle framework for the assessment of site remediation options, and applied the framework to a hypothetical case-study (Diamond et al. 1999). The same framework was also applied to the excavation and disposal for the remediation of lead-contaminated soil (Page et al. 1999). Similar methods were used to select a remediation technology for a diesel-contaminated site (Cadotte, Deschênes, and Samson 2007). The only published life cycle assessment of groundwater remediation alternatives compares a pump-and-treat

technology and permeable reactive barrier technology both employing granular activated carbon for the remediation of PAH-contaminated groundwater (Bayer and Finkel 2006). The high energy demand of active systems suggests that there may be an environmental benefit of choosing a PRB as opposed to a PTS, as indicated in previous studies (Bayer and Finkel 2006), but the impacts of the most common ZVI reactive medium have not been determined.

Geochemistry of Reduced Iron Permeable Reactive Barrier Media

The manipulation of solution chemistry by reduced iron reactive media will determine the effectiveness of treatment and longevity of a PRB as well as the effects on the local soil ecosystem. The chemistry of ZVI, nZVI, and FeS at near-neutral pH in the presence of common groundwater ions is briefly reviewed in this section.

Zero Valent Iron and Nanosized-Zero Valent Iron

Granular ZVI, or metallic iron, is a manufactured material produced by reducing natural iron ores in a blast furnace, often using coke or coal to provide necessary heat to reduce ferrous and ferric iron to metallic iron (GeoChemTec). Nano-sized ZVI (nZVI) can be made from granular ZVI by conventional ball milling techniques, or can be manufactured or synthesized as nanoparticles (Nurmi et al. 2005). The most commonly reported nZVI particles are synthesized according to the borohydride reduction method, shown as equation (1) (Wang and Zhang 1997)(Macé et al. 2006b) or by reducing iron oxides with hydrogen gas (Macé et al. 2006a).

(1)

Corrosion. ZVI and nZVI are thermodynamically unstable in air or aqueous solution, which causes the corrosion of iron on the surface. Upon exposure to air or water, ZVI or nZVI will corrode to produce ferrous iron and electrons according to equation (2).

(2)

In aerobic solutions iron will be oxidized by dissolved oxygen shown in equation (3), while in anaerobic solutions iron will be oxidized by water itself (known as anaerobic corrosion), shown in equation (4).

(3)

(4)

In a PRB, and any dissolved oxygen present in influent is expected to be removed within the first few centimeters of an installed barrier, making anaerobic corrosion the important process to consider. ZVI with a size between 10-32 mesh initially corroded with a rate of $1.5.x\ 10^{-5}$ mol kg^{-1} day^{-1} $kPa^{-0.5}$ and decreased to 9×10^{-6} mol kg^{-1} day^{-1} $kPa^{-0.5}$ after 150 days under anaerobic conditions (Reardon 1995). The anaerobic corrosion rate was affected by carbonate, sulfate, and chloride, with a rate of 7×10^{-4} mol Fe kg^{-1} day^{-1} in saline groundwater at 25 °C (Reardon 1995). The rates for nZVI anaerobic corrosion are much greater, reported as 1.9 mol Fe kg^{-1} day^{-1} for the reaction of nZVI in water and 0.5 mol Fe kg^{-1} day^{-1} in quartz sand (Reardon et al. 2008). The half-life of nZVI in aqueous solution is between 78 days (Reardon et al. 2008) and 90-180 days (Liu and Lowry 2006). The anaerobic corrosion of ZVI and nZVI will influence both barrier longevity and the local solution chemistry, but will also determine the rate at

which secondary solids form on the reactive surface, a processes described as ZVI or nZVI aging.

Aging. The surface of ZVI or nZVI will transform during exposure to aqueous solution under aerobic or anaerobic conditions due to the corrosion of iron metal and the release of ferrous iron. The progression of the ZVI surface from more reduced phases (Fe^0) to a more oxidized phase (Fe^{II} and/or Fe^{III}) depends on the conditions of the aging solution. One solid phase that is often assumed to form on the surface of nZVI is magnetite (Fe_3O_4) (Liu and Lowry 2006), though the mineralogical characterization of a field-scale ZVI PRB identified akaganeite (β-FeOOH), goethite (α-FeOOH), lepidocrocite (γ-FeOOH), magnetite (Fe_3O_4), maghemite (γ-Fe_2O_3) after 3 years of operation (Phillips et al. 2003). These iron oxide phases may be less likely to form in the presence of common groundwater anions, due to the competition with iron carbonate solids.

In the presence of other anions, the formation of a variety of solids may be induced by ZVI or nZVI because of the redox and pH conditions that will prevail inside of a barrier. The formation of carbonate minerals, siderite ($FeCO_3$) and calcite ($CaCO_3$), has been observed in laboratory columns with granular ZVI in solutions with 1×10^{-3} and 5×10^{-3} M $CaCO_3$ (Jeen, Gillham, and Blowes 2006). In simulated groundwater conditions, the nZVI aged for six month in the presence of nitrate, chloride, phosphate and sulfate produced a mixture of iron oxide phases, as well as vivanite ($Fe_3(PO_4)_3$-$8H_2O$) and schwertmannite ($Fe^{3+}{}_{16}O_{16}(OH\text{-}SO_4)_{12\text{-}13}$-10-$12H_2O$) phases (Reinsch et al. 2010). The formation of secondary phases can reduce the reactivity of ZVI and nZVI with contaminants of interest and can reduce the ability to control solution chemistry.

Mackinawite (FeS)

Mackinawite is a naturally-occurring reduced iron sulfide mineral found under anoxic conditions. It has been determined that mackinawite is stoichiometric iron (II) monosulfide (FeS) (Rickard and Luther 2007), though it has been reported in the literature as both iron- ($Fe_{1-x}S$) and sulfur-deficient (FeS_{1-x}) (Mullet et al. 2002). Laboratory synthesis of mackinawite commonly follows one of two reaction mechanisms, using either metallic iron (Berner 1964) or ferrous iron (Rickard and Luther 2007), and experimental results suggest that some properties are dependent on the synthesis method (Jeong, Lee, and Hayes 2008). FeS has a layer structure with an average particle size of 21.7 nm x 7.5 nm and an external specific surface area (SSA_{ext}) of 103 m^2/g based on Transmission Electron Microscopy (TEM) observations or diameter of 3.5 nm and SSA_{ext} = 424 ±124 m^2/g based on photocorrelation spectroscopy (Jeong, Lee, and Hayes 2008). The point of zero charge for FeS has been reported at pH ~5 (Gallegos 2007), meaning that at near-neutral pH the surface of FeS will be negatively charged.

Dissolution. The kinetics of FeS dissolution was studied by Pankow and Morgan (Pankow and Morgan 1979). The dissolution was monitored in terms of change in pH assuming the stoichiometric composition of mackinawite. Mackinawite disks were prepared from synthetic mackinawite prepared from metallic iron, and reacted with constant temperature solution in a specially-designed experimental reactor. The authors found that the dissolution rate depended on the solution pH below pH 5, while the rate between 4.7 < pH < 7.5 was pH-independent. The effect of ionic strength was investigated from 0.05 M to 0.20 M but the effect on dissolution rate was slight. The two-term equation for the dissolution of mackinawite is given:

(5)

where $[S]_{tot}$ is the total dissolved sulfide calculated from the pH and ionization fractions for sulfide species, A is the disk area, V is the volume, and constants $k_{1,\ 25\ C} = 0.18 \pm 0.06$ cm/min and $k_{2,\ 25\ C} = 1.9 \times 10^{9}$ mol/cm^2·min.

Solubility. Unlike zero-valent iron, at room temperature and atmospheric pressure mackinawite is metastable in an Fe-S-O system with $S_{total} = 1 \times 10^{-3}$ and $Fe_{total} = 1 \times 10^{-6}$ with $Na_{total} = Cl_{total} = 0.1$ M between pH 6 and 11 and pe between -5 and -12 (Gallegos 2007). The equilibrium solubility of mackinawite in acid and alkaline solutions has been investigated by Rickard, and is summarized (Rickard and Luther 2007). The solubility of mackinawite is pH-dependent in acid solutions and pH-independent in neutral to alkaline solutions. The pH-dependent reaction can be described by equation (6), which has an equilibrium constant (Log K) between -3.5 and -4.93. A summary of log K values obtained for equation (6) is shown in Table 1.

(6)

Table 1:Summary of FeS Solubility Product Values.

Log K	Reference
-3.6 ±0.2*	(Davison 1991)
-3.5 ±0.25	(Rickard and Luther 2007)
3.9 to -4.93	(Gallegos 2007)

***This value is consistent with the MINTEQ.V4 Database and PHREEQC Modeling conducted in this dissertation.**

Oxidation. Oxidation of mackinawite exposed to air and aqueous solutions has been studied. There is general consensus that the formation of pyrite requires the oxidation of an iron monosulfide through either an iron-loss or sulfidification pathway,

which has fueled research into the reaction pathways and intermediates, including mackinawite and greigite. In anoxic H_2S-saturated solutions, XRD patterns of solid samples showed the characteristic peaks of mackinawite and no peaks for both greigite and pyrite for more than four months (Benning, Wilkin, and Barnes 2000). A high-temperature (100-200 °C), in-situ XRD study of the transformation of mackinawite to pyrite through greigite also concluded the mechanism was a solid-state transformation and concluded that the reaction followed zero-order kinetics as described by Equation (7) (Hunger and Benning 2007).

(7)

The proposed mechanism in hydrothermal system involves electron-transfer from the mackinawite surface to adsorbed polysulfide species (Hunger and Benning 2007). At low temperature (< 200 °C), the formation of greigite occurs upon oxidation of the mackinawite in aqueous solutions only after the introduction of an oxidant (Benning, Wilkin, and Barnes 2000). This suggests that mackinawite will be stable relative to greigite in groundwater and laboratory solutions in the absence of an external oxidant.

Bacterial Cell Structure and Function

In toxicity experiments with bacterial cells, the changes in cell structure or function are observed as a function of exposure to the chemical of interest. Therefore, it is important to understand the general structure and function of bacterial cells and how they may influence experimental design and results. The structure, metabolism, and growth of bacteria are introduced in this section, with an emphasis on cellular components and processes that respond to chemical and particle exposure.

Bacterial Structure

Bacteria are able to survive in a variety of environments because of their relatively simple structure, allowing them to quickly adapt to changing surroundings (Maier, Pepper, and Gerba 2009). The major structures or components that define a bacterial cell are the cell envelope (cell membrane or cell wall), the cytoplasm, the chromosome, the plasmid, and ribosomes. The cell envelope defines the boundary of the cell and protects the cell contents from the environment. The cytoplasm is the fluid inside of the bacterial cell where all cellular processes occur. The chromosome contains all of the genetic information necessary for cell replication and growth. Extrachromosomal DNA is stored on the plasmid. The ribosomes transcribe messenger RNA into proteins involved in cell metabolism.

Bacterial Cytoplasmic Membrane. The cytoplasmic membrane of bacteria serves a number of important structural and functional roles including defining the cell boundary and containing cellular contents, regulating the movement of substances into or out of the cell, and energy transduction through the maintenance of ion and solute gradients (Denich et al. 2003). Bacterial cells can be classified into two groups based on the structure of the cell envelope: gram-positive or gram-negative. Whether a bacterium is gram-positive or gram-negative indicates how well cell survival will be in different environments (Maier, Pepper, and Gerba 2009). A gram-positive cell, such as *Bacillus*, has a cell envelope composed of a cytoplasmic membrane and a thick peptidoglycan cell wall. A gram-negative cell, such as *Escherichia*, has a cell envelope composed of a cytoplasmic membrane, a thin peptidoglycan cell wall and a outer membrane with a layer of lipopolysaccharides extending into the environment. The cell envelope plays an

important role in maintaining homoeostasis of the cell and contributes to necessary cellular functions including metabolism and replication.

The cytoplasmic membrane has a lipid-bilayer structure, composed of glycerophospholipid molecules that have both a hydrophilic and hydrophobic regions (Denich et al. 2003). Under normal physiological conditions, this membrane allows diffusion of non-polar and non-charged molecules into and out of the cell. The transport of charged molecules, such as metal ions, into and out of the cell is carried out by proteins that are associated or imbedded within the membrane (Denich et al. 2003).

A variety of environmental factors can alter the structure and function of membrane lipids and proteins, including temperature, pressure, pH, nutrients, ions and chemicals (Denich et al. 2003). Chemicals can alter both the structure and function of membranes, through accumulation within the membrane or at the interface or membranes and solutions or membranes and imbedded proteins (Denich et al. 2003). The extracellular redox potential or electron activity can also influence the cytoplasmic membrane structure and function, where a decrease in the electron activity can increase the permeability of the cytoplasmic membrane with respect to protons, affecting the internal pH and the pH-gradient of the membrane (Riondet et al. 1999).

Bacterial Metabolism

A cell's metabolism defines the chemical reactions that occur for the generation of energy and the maintenance of cell structure and function (Maier, Pepper, and Gerba 2009). There are many types of metabolism, depending on the form of energy that is used by cells, but most bacteria are chemoheterotrophs, meaning they derive their energy from chemical compounds but cannot fix carbon as organic molecules. Depending on the electron donors and acceptors present in the system, bacteria may undergo oxidative

phosphorylation or fermentation. Under aerobic conditions, most bacteria will undergo oxidative phosphorylation with oxygen as the terminal electron acceptor and an organic compound as the electron donor. Under anaerobic conditions, bacteria may use other terminal electron acceptors such as nitrate, or sulfate to complete oxidative phosphorylation. Much of the energy produced during oxidative phosphorylation is the result of the membrane process known as the proton motive force (PMF) where the charge imbalance across the membrane provides energy for phosphorylation.

In the absence of other electron acceptors, some bacteria can undergo fermentation, where organic compounds serve as the electron donors and conjugate organic acids act as the terminal electron acceptors. Fermentation yields much less energy than oxidative metabolism, generating only 4 ATP per glucose molecule compared to the 36 ATP per glucose molecule of oxidative phosphorylation in the presence of oxygen. This results in slower bacterial growth under anaerobic conditions and lower bacterial yields in anaerobic systems.

Bacterial Growth

Growth of bacterial cultures follows the general relationship:

—— (8)

where X is the cell mass, and μ is the specific growth rate. For a constant specific growth rate, the cell mass will increase exponentially and the final concentration is given by:

(9)

Bacterial growth occurs in four phases: lag phase, growth phase, stationary phase, and death phase. The description of bacterial growth related to substrate concentration is the given by the classic Monod equation (Monod 1949):

(10)

where is the maximum specific growth rate which occurs when substrate is not limiting. In situations where the substrate is not limiting bacterial growth, several mathematical models have been introduced to model the characteristic curve of bacterial growth as reviewed by Zwietering and colleagues (Zwietering et al. 1990).

The structure and function of cells can change dramatically during different growth phases. For example, the formation of cyclopropane fatty acids in the membrane occurs as cells enter the stationary phase (Wang 1994). Another example of growth-dependent structure is the variation in the abundance of nucleoid-associated proteins reported in the literature (Bradley 2007). The changes that occur in cells as a function of growth state necessitate the use of a single growth state in experiments, such as an overnight culture or mid-log culture.

Iron Homeostasis in Bacteria

Iron is an essential micronutrient for bacterial growth, and is involved in a variety of biological processes including respiration, the trichloroacetic acid cycle, gene regulation and DNA biosynthesis (Andrews, Robinson, and Rodriguez-Quinones 2003). Despite the importance of iron in biological processes, there are many environments where bioavailable iron concentrations are very low (as low as 10^{-18} M at pH = 7), creating the need for an iron-regulatory system in bacteria to accumulate, store, and manage iron within a cell (Andrews, Robinson, and Rodriguez-Quinones 2003). This regulatory system allows for the chelation and transport of iron into the cell under conditions of iron-deficiency and the management of reactive oxygen species that may result from iron-rich conditions (Crichton and Ward 1995). Within a bacterial cell, iron

can be stored in proteins and bacterioferritins as ferric or heme-iron (Andrews, Robinson, and Rodriguez-Quinones 2003; Crichton and Ward 1995).

Many aspects of the iron-regulatory system in bacteria depend on the ability of the cell to change the redox state of iron between Fe(II) and Fe(III) to create stored or usable iron within the cell (Yang et al. 2000; Braun and Braun 2002). Iron stored in bacterioferritins is present in a iron oxide core within the proteins and the rate of storage depends on the oxidation of ferrous iron to produce an insoluble iron (III) oxide phase (Yang et al. 2000). Similarly, in environments with limited iron, bacteria can employ siderophores (Braun and Braun 2002) that bind with ferric iron and facilitate transport into the cell where reduction of the ferri-siderophore can occur (Andrews, Robinson, and Rodriguez-Quinones 2003). Due to the direct relationship between iron availability and redox state, it is expected that changes in solution electron activity may significantly influence the iron homeostasis in bacterial cells.

Toxicity of Reduced Iron Nanoparticle Reactive Media

Nanoparticles may interact with bacteria in the environment, in water and wastewater treatment plants, and inside of other organisms, and may have a variety of effects depending on the nanoparticle chemistry and the exposure solution composition. There are three mechanisms extensively discussed in the literature: physical membrane disruption, generation of radical oxygen species, and toxic ion release (Klaine et al. 2008). In this section, these mechanisms will be briefly discussed and then a review of reduced iron nanoparticle particle toxicity is presented.

Mechanisms of Nanoparticle Toxicity

Membrane Disruption. When nanoparticle-bacterium interactions result in close-contact, it can be anticipated that some change to membrane structure or function may occur. Nanoparticles may diffuse into or through membranes changing membrane structure or integrity may cause rupture of the cell and cell lysis, or the leaking of cellular contents into the environment (Klaine et al. 2008). The formation of pits in bacterial membranes has been reported for *E. coli* treated with silver nanoparticles (Sondi and Salopek-Sondi 2004) and ZnO nanoparticles (Brayner et al. 2006; Zhang et al. 2007).

Nanoparticles may also compromise membranes through sorption such that they can no longer generate the ion or pH gradient necessary for the PMF or may allow entry of toxic ions into the cell resulting in cell death (Klaine et al. 2008). The adsorption of ceria (CeO2) nanoparticles (Thill et al. 2006) and iron oxide nanoparticles (Schwegmann, Feitz, and Frimmel 2010) to bacterial membranes has been implicated in the adverse effects observed during nanoparticle exposure.

Reactive Oxygen Species. The generation of reactive oxygen species (ROS) is often given as the mechanism of nanoparticle toxicity in the literature. ROS such as the superoxide anion radical, hydrogen peroxide, and the hydroxyl radical can damage all major biological molecules, and have been linked to cellular damage including membrane disruption through lipid attack, protein and amino acid oxidation, and DNA damage (Demple 1991). The ROS generation can be caused by photocatalytic activity (Adams, Lyon, and Alvarez 2006), or may be induced by the release of ferrous iron to solution (Lee et al. 2008).

Toxic Ion Release. There are many naturally-occurring ions that are toxic to bacteria at low concentrations, including mercury, cadmium, and silver ions (Nies 1999;

Silver 1996). There are also ions that are not toxic at low concentrations but prove toxic at higher concentrations, including zinc, nickel, and copper ions (Nies 1999). Of particular importance is the interesting case of iron, which is necessary for life but toxic in high concentrations under oxic conditions because of the generation of reactive oxygen species (Andrews, Robinson, and Rodriguez-Quinones 2003). Other studies suggest that sulfide may be harmful to bacteria by limiting metals in solution (Caffrey and Voordouw 2010).

Cytotoxicity of Nanoparticulate Reduced Iron Reactive Media

Like other nanoparticles, nZVI and FeS may have an adverse effect on the microorganisms, specifically those in the subsurface where PRBs may be installed. The inactivation of bacteria under aerobic and deaerated conditions has been studied in carbonate buffer (Lee et al. 2008; Auffan et al. 2008; Li et al. 2010; Chen et al. 2010) and ultra pure water conditions (Auffan et al. 2008; Diao and Yao 2009). A summary of relevant studies on the adverse effects experienced by bacteria when exposed to nZVI is presented in Table 2. The adverse effects on mixed-microbial populations has been examined in simulated groundwater (Barnes et al. 2010a) and river water (Barnes et al. 2010b) as well as in a growth medium (Xiu et al. 2010). The minimum inhibitory concentration for nZVI and *E. coli* in LB growth medium has also been reported (Li et al. 2010). The effect of nZVI on actively-growing pure cultures is still largely unknown, though these studies can provide insight into possible mechanisms of inhibition.

Inactivation of Bacteria by nZVI. The presence of nZVI in solution can significantly inactivate bacteria, or render the cells biologically-inert, under both aerobic and deaerated conditions. After 10 minutes of exposure to 9 mg/L nZVI under deaerated conditions in a carbonate buffer, viable *E. coli* were reduced 3.4 orders of magnitude

(Lee et al. 2008). Under aerobic conditions, however, 60 minutes of exposure to 90 mg/L nZVI only produced a 2.6-log reduction in *E. coli* viability (Lee et al. 2008). In a similar carbonate buffer system,100 mg/L nZVI produced a 5-log and 0.8-log reduction in *E. coli* were reported under deaereated and aerated conditions, respectively (Li et al. 2010). Exposure in ultrapure water also produces significant inactivation (Auffan et al. 2008; Diao and Yao 2009).

The mechanisms of cellular damage are likely related to the ability of nZVI to create oxidative stress conditions. Oxidative stress is a condition of redox disequilibrium with the cell, generally one where the production of ROS overwhelms cellular defenses (Xia et al. 2006). The mechanism of ROS production reported in an nZVI-*E. coli* system is Fenton-type chemistry where the presence of Fe(II) in solution and inside of the cell catalyzes the production of ROS, represented by equations (11) and (12) (Imlay 2008).

(11)

(12)

The effect of nZVI did not change in the presence of superoxide ($O_2^{\cdot}$) and hydrogen peroxide (H_2O_2) scavengers, suggesting that the effective oxidants may be intracellular hydroxyl radicals (OH·) or ferryl radicals (Fe(IV)) (Kim et al. 2010). The greater effect of nZVI under deaerated conditions may have to do with a slower or lesser degree of passivation of the nZVI surface in the absence of oxygen (Lee et al. 2008) or the increased cycling of Fe(II)/Fe(III) in the absence of oxidants causing increased ROS production (Duesterberg, Cooper, and Waite 2005).

Inhibition of Mixed Cultures by nZVI. The effect of nZVI on mixed microbial communities, including communities of dechlorinating bacteria that would be present in the subsurface on a site contaminated with chlorinated solvents, has also been studied. Monitored over 200 days, concentrations of nZVI from 0.1 to 1 g/L reduced the growth of the natural dechlorinating and sulfate-reducing bacteria and concentrations over 0.3 g/L reduced growth completely (Barnes et al. 2010a). Similar results were obtained when a mixed dechlorinating culture was exposed to 1 g/L nZVI and the dechlorination was completely inhibited (Xiu et al. 2010). The effect of nZVI on the community structure in a river water microcosm over 36 days showed that while certain populations declined initially, the communities recovered within 3 days (Barnes et al. 2010b). The inhibition of mixed-communities in the presence of nZVI, and the ability of populations to recover from initial stresses, suggests that pure cultures may also recover from the effects of nZVI if exposed under growth conditions.

Inactivation of Bacteria by FeS. The effect of FeS on microbial survival or growth has not been explicitly studied in the literature. However, there have been several studies of Fe(II) and Fe(III) solids including oxidized nZVI, iron oxide nanoparticles and ferrous and ferric salts (Lee et al. 2008; Auffan et al. 2008; Li et al. 2010; Diao and Yao 2009). A summary of relevant experiments examining the inactivation of bacteria in the presence of Fe(II) and Fe(III) solids is presented in Table 3. The Fe(III) solids and nZVI oxidized by exposure to oxygen show little effect on bacteria survival under aerobic or deaerated conditions (Lee et al. 2008; Auffan et al. 2008; Li et al. 2010; Diao and Yao 2009). For the mixed Fe(II)/Fe(III) solids, exposure to 700 mg/L of magnetite nanoparticles (nFe_3O_4) could reduce viable cells by 80% under aerobic conditions, but no

significant effect was observed at lower concentrations (Auffan et al. 2008). The only study of an Fe(II) salt, $FeSO_4$, found that under deaerated conditions in a carbonate buffer, the viable *E. coli* cells were reduced by 3 orders of magnitude in 60 minutes (Lee et al. 2008). The results of inactivation experiments with Fe(II) and Fe(III) solids suggests that FeS may be less inhibitory than nZVI, but may still have an adverse effect.

The dissolution of FeS will also produce sulfide ions in solution that may have an adverse effect on microbial growth. Monitoring the decomposition of deoxyribose under anaerobic conditions in the presence of hydrogen peroxide, iron sulfide was found to be more efficient than ferrous iron or sodium sulfide in catalyzing the generation of hydroxyl radicals, and the authors suggest that the coordination chemistry of iron sulfide may leave a free coordination site in the structure, though the effect of FeS alone was not studied (Berglin and Carlsson 1985). In an investigation of the effect of sulfide on the growth of *Desulfovibrio vulgaris* growth, it was determined that high sulfide (10 mM) reduced both the growth rate and the final cell density compared with low sulfide (1 mM) condition (Caffrey and Voordouw 2010). The authors conclude that the high sulfide condition is a significant stress condition, and that the reduced bioavailability of metals may be the reason for reduced growth (Caffrey and Voordouw 2010). Therefore, while there may be less of an effect due to the redox state of iron in FeS, the additional effect of sulfide must also be considered in the inhibitory effect of FeS.

Table 2: Summary of nZVI Inactivation or Inhibition Experiments

nZVI	Culture	Exposure Solution	pH	Exposure Time	Exposure Concentration	Effect	Citation
TOXICITY EXPERIMENTS WITH NON-GROWING CULTURES							
nZVI[1]	E. coli	2 mM Carbonate Buffer	8	60 mins	90 mg/L	2.6 log reduction	Lee et al 2008
nZVI[2]	*E. coli*	*2 mM Carbonate Buffer [Deaerated]*	*8*	*10 mins*	*9 mg/L*	*3.4 log reduction*	*Lee et al 2008*
nZVI[2]	E. coli	Ultrapure Water	5-5.5	60 mins	7, 70, 175, 350, 700 mg/L	Significant effect from 70 - 700 mg/L <50 % viable cells	Auffan et al 2008
nZVI[2]	B. subtilis	DI Water		5 mins	0.1, 1, and 10 mg/mL	80-100% Inactivation	Diao and Yao 2009
nZVI[2]	P. fluorescens	DI Water		5 mins	0.1, 1, and 10 mg/mL	Complete Inactivation	Diao and Yao 2009
RNIP (Toda)	E. coli	5 mM Bicarbonate Buffer	8.2	60 mins	100 mg/L	0.8 log reduction after 60 minutes	Li et al 2010
RNIP (Toda)	*E. coli*	*5 mM Bicarbonate Buffer[Deaerated]*	*8.2*	*60 mins*	*100 mg/L*	*5 log reduction after 60 minutes*	*Li et al 2010*
RNIP (Toda)	E. coli	2 mM Bicarbonate Buffer	8.1	4 hours	1 g/L	35.9% Survival after 60 minutes	Chen et al 2011
RNIP (Toda)	B. subtilis	2 mM Bicarbonate Buffer	8.1	4 hours	1 g/L	80.2% Survival after 60 minutes	Chen et al 2011
TOXICITY EXPERIMENTS WITH GROWING CULTURES							
RNIP (Toda)	E. coli	LB Miller Broth	SP	12 hours	0.001 - 1 g/L	Minimum Inhibitory Concentration is 5 mg/L	Li et al 2010
nZVI[2]	*Mixed Culture - Groundwater Microcosm*	*Groundwater [Anaerobic]*	*6.94*	*200 days*	*0.1 - 1 g/L*	*nZVI was inhibitory to indigenous dechlorinating and sulfate reducing bacteria; > 0.3 g/L completely inhibitory*	*Barnes et al 2010*
RNIP (Toda)	*Mixed Culture - Anaerobic methanogenic*	*Growth Medium [Anaerobic]*	*8.1*	*500 hours*	*1 g/L*	*Dechlorination activity was inhibited in the presence of nZVI*	*Xiu et al 2010*
nZVI[3]	Mixed Culture – River Microcosm	River Water	8.5	36 days	100 mg/L	nZVI and ZVI had impact on community structure initially but not long-term	Barnes et al 2010

nZVI synthesized in laboratory based on the method of Lowry and Johnson (1996)[1], Wang and Zhang (1997)[2], Barnes et al (2010)[3]
Deaerated or Anaerobic studies are indicated in italics.

Table 3: Summary of Bacterial Inactivation with Fe(II)- of F(III)-containing Salts or Particles

	Culture	Exposure Solution	pH	Exposure Time	Exposure Concentration	Effect	Citation
Fe(II) or Fe(II)/Fe(II)							
nFe_3O_4	*E. coli*	*2 mM Carbonate Buffer [Deaerated]*	*8*	*60 mins*	*9 mg/L*	*< 0.1 log inactivation*	*Lee et al 2008 EST*
nFe_3O_4	E. coli	Ultrapure Water	5-5.5	60 mins	7, 70, 175, 350, 700 mg/L	< 20 % viable Cells only in 700 mg/L	Auffan et al 2008 EST
Ox-nZVI	*E. coli*	*2 mM Carbonate Buffer [Deaerated]*	*8*	*60 mins*	*9 mg/L*	*< 0.1 log inactivation*	*Lee et al 2008 EST*
Ox-nZVI	E. coli	2 mM Carbonate Buffer	8	60 mins	90 mg/L	< 0.1 log inactivation	Lee et al 2008 EST
Ox-nZVI	B. subtilis	DI Water		5 mins	0.1, 1, and 10 mg/mL	No effect	Diao and Yao 2009 Wat Res
Ox-nZVI	P. fluorescens	DI Water		5 mins	0.1, 1, and 10 mg/mL	No Effect	Diao and Yao 2009 Wat Res
Ox-nZVI	*E. coli*	*5 mM Bicarbonate Buffer [Deaerated]*	*8.2*	*60 mins*	*100 mg/L*	*Aging reduced Fe0 content and increased viability at 60 mins*	*Li et al 2010 EST*
$FeSO_4$	E. coli	2 mM Carbonate Buffer	8	60 mins	0.1 mM	< 0.1 log inactivation	Lee et al 2008 EST
$FeSO_4$	*E. coli*	*2 mM Carbonate Buffer [Deaerated]*	*8*	*60 mins*	*0.1 mM*	*> 3 log inactivation*	*Lee et al 2008 EST*
Fe(III)							
nFe_2O_3	E. coli	Ultrapure Water	5-5.5	60 mins	7, 70, 175, 350, 700 mg/L	No effect	Auffan et al 2008 EST
$FeCl_3$	*E. coli*	*2 mM Carbonate Buffer [Deaerated]*	*8*	*60 mins*	*1 mM*	*< 0.1 log inactivation*	*Lee et al 2008 EST*
$FeCl_3$	E. coli	2 mM Carbonate Buffer	8	60 mins	1 mM	< 0.1 log inactivation	Lee et al 2008 EST

Deaerated or Anaerobic studies are indicated in italics.

Summary of Literature Reviewed and Research Needs

Following the review of current literature, the following conclusions and research needs were identified:

1. **The Effect of Reactive Media Longevity on the Relative Environmental Benefit of PRBs is Uncertain.**

   It is likely that the longevity of reactive media will significantly influence the environmental performance of a permeable reactive barrier, because there is an inherent trade-off between the higher energy burden associated with an active groundwater remediation technology and the higher material burden of a passive technology. An assessment of current groundwater remediation strategies is needed to provide information on the elements of remediation strategies which influence environmental sustainability and inform the future development of both active and passive groundwater remediation technologies.

2. **The Effect of Zero-Valent Iron Nanoparticles on Bacterial Cultures under Anaerobic Growth Conditions is Unknown.**

   Zero-valent iron nanoparticles have been shown to exhibit cytotoxic behavior in aerated and deaerated conditions when bacteria are in a non-growth state. However, there is evidence to suggest that bacteria in a growth state may recover from initial adverse effects, possibly as a function of changing particle and solution chemistry. An assessment of the effect of zero-valent iron nanoparticles on the growth of bacterial cultures under anaerobic conditions is needed to understand the possible environmental effects of employing zero-valent iron for groundwater remediation.

3. **The Effect of FeS Nanoparticles on Bacterial Cultures under Anaerobic Growth Conditions is Unknown.**

   Reduced iron nanoparticles, specifically ferrous- and zero-valent iron phases, have been shown to be cytotoxic under various conditions when bacteria are in a non-growth state. Hydrogen sulfide and dissolved sulfide have also been implicated as a possible toxic ions. However, FeS may be less harmful because solubility in the growth medium may limit the exposure to toxic aqueous species. A study of the effect of FeS nanoparticles on the growth of bacterial cultures under anaerobic conditions can provide information on whether potential ecotoxicity of iron sulfide nanoparticles is greater or less than that of zero-valent iron nanoparticles.

Chapter 3

Materials, Analyses and Approach

The research presented in this dissertation involved modeling of the environmental impacts through a life cycle assessment and laboratory experiments to understand the effects of nanoscale reactive media on bacterial growth. The general approach and methods used are described in this chapter. Detailed methods for the Life Cycle Assessment are presented in Chapter 4.

Materials

Mackinawite (FeS)

Synthetic nanocrystalline mackinawite was synthesized by precipitation of $FeCl_2$ with Na_2S according to the method described by Butler and Hayes (Butler and Hayes 1998). A 1.1 M $FeCl_2$ (Fisher Chemical, ACS Reagent Grade) solution was added to 1.0 M Na_2S (Fisher Chemical, ACS Reagent Grade) under anoxic conditions (3% Hydrogen, 97% Nitrogen), which immediately precipitates FeS as a viscous slurry. The suspension was aged for 3 days before centrifugation to collect particles. The slurry was centrifuged at 10000 rpm for 20 minutes, the supernant is decanted, and the particles were re-suspended in fresh deoxygenated water. After eight washings, the mackinawite was

freeze-dried and stored under anoxic conditions in crimp-sealed vials until use. Nanocrystalline mackinawite synthesized with similar methods has particle dimensions 21.7 nm x 7.5 nm and a specific surface area of 103 m^2/g according to TEM observations (Jeong, Lee, and Hayes 2008).

Nano-scale Zero-Valent Iron (nZVI)

Synthetic nano-scale zero-valent iron was synthesized through the reduction of ferrous iron solution using borohydride (Lee et al. 2008). A solution of 8 mg/L of $NaBH_4$ (Fisher Chemical, ACS Reagent Grade) was slowly added to 1 g/L solution of $FeSO_4$ (Fisher Chemical, ACS Reagent Grade) while the solution was stirred and purged with N_2 gas (>99%, Cryogenic Gases). The suspension was transferred to 50 mL centrifuge tubes (Corning, USA) and centrifuged for 4 minutes at 4000 rpm (2197*g*). The supernant was decanted and the particles were resuspended in 10^{-4} N HCl three times to rinse synthesis ions from solution. After the final rinse, the particles were re-suspended in 5 mL of 10^{-4} N HCl and stored as a suspension in an anaerobic chamber in 50 mL centrifuge tubes prior to use in experiments. The concentration of the nZVI stock was measured by nitric acid digestion and ICP-MS and determined to be 5.37±0.05 grams Fe^0 per liter.

Particle Preparation

Prior to experiments, FeS powder was weighed, and re-suspended in sterile, deoxygenated Milli-Q water on a magnetic stir plate for 72 hours. MOPS buffer was added 24 hours prior to experiment to allow equilibration at the experimental pH. Particle suspensions were allowed to settle quiescently for 30 minutes prior to use in experiments. Suspensions of nZVI were prepared for experiments by vortexing for 60 seconds in the 5 mL of 10^{-4} M HCl, before being diluted 1:10 into a solution of MOPS buffer at pH = 7.

No visible oxidation occurred during this transfer (no orange color developed). Buffered nZVI suspensions were vortexed for 60 seconds prior to use in experiments.

Ferrous Chloride ($FeCl_2$) and Sodium Sulfide (Na_2S)

Ferrous chloride (Fisher Chemical, ACS Reagent Grade) and sodium sulfide (Fisher Chemical, ACS Reagent Grade) were used as received from the manufacturer. Ferrous chloride was stored in an anaerobic chamber at room temperature and the sodium sulfide was stored in open atmosphere at 4 °C. Prior to experiments, ferrous chloride or sodium sulfide was dissolved in anoxic Milli-Q water and allowed to equilibrate for at least 12 hours under anaerobic conditions.

Anaerobic Solutions

Aqueous solutions were prepared in deaerated, deionized distilled water which was prepared by bringing distilled, deionized (Milli-Q) water (> 18 MΩ-cm) to a boil, and purging with high-purity (>99.999%) $N_{2\,(g)}$ during cooling. This deaerated water was transferred to an anaerobic chamber and allowed to equilibrate in the atmosphere for 24 hours. Sterile deaerated water was prepared by autoclaving Milli-Q water in media bottles that were sealed upon completion of the sterilization cycle (121 °C, 1 bar for 20 minutes) placed into an anaerobic chamber, opened and then allowed to equilibrate for 24 hours. Anaerobic media was prepared by mixing stock solutions, autoclaving, and equilibrating in the anaerobic chamber for 24 hours.

Chemical Analyses

Particle Digestion

In experiments where reduced iron nanoparticles were quantified, 0.5 or 1 mL of particle suspensions was digested in 2% nitric acid and vortexed at 3000 rpm at room

temperature for 60-90 seconds. Following the digestion procedure, the samples were diluted for iron analysis. A similar digestion in 20% nitric acid was tested, but it was determined in experiments that the recovery with 2% nitric acid digestion of reduced iron nanoparticles was reproducible and that no additional recovery was gained by using 20% nitric acid.

Aqueous Iron Analysis

Aqueous total iron in experimental samples was determined with inductively-coupled plasma mass spectrometry (ICP-MS). Samples were acidified to 2% HNO_3 for storage and analysis. Iron concentrations were determined relative to prepared calibration standards. ICP-MS analysis was calibrated linearly between 75 ppb and 1000 ppb using certified standard solutions ($R^2 = 0.9975$). The minimum reporting level for analysis was 111 ppb and the average percent recovery of standards during analysis was 102 ± 1.62 %.

Aqueous Sulfate Analysis.

Aqueous sulfate in experimental samples was determined using the Barium Sulfate Turbidimetry method according to Standard Method 426.C (Franson and American Public Health Association 1985). Briefly, 12 mL of sample was added to 31.75 mL Milli-Q water and 6.25 mL of a 100 mg/L Na_2SO_4 standard to make up 50 mL of solution for analysis. The 6.25 mL of standard solution was added because sample SO_4^{2-} concentrations were anticipated to be below method detection limit of 10 mg/L. Buffer solution (30 g/L $MgCl_2$-$6H_20$, 1 g/L KNO_3, and 20 mL CH_2COOH (99%)) was added to the 50 mL sample just prior to the addition of a spoonful of $BaCl_2$ crystals (> 99%, for analysis) was added during stirring with a magnetic stir bar. After stirring for 60 seconds, the solution was transferred into a 5-cm spectrophotometric cell and the

absorbance was measured 5 minutes after stirring ended at 420 nm with a UV/Vis Spectrophotometer (Varian). An eight-point linear calibration range from 0 – 35 mg/L SO_4^{2-} was established with a $R^2 = 0.983$. The minimum reporting level was 25 mg/L SO_4^{2-}.

Approach

Environmental Impact of in situ and ex situ Remediation Technologies

A life cycle assessment case study comparison was conducted to explore the global environmental impacts of a pump-and-treat system and permeable reactive barrier that were designed and implemented at field-scale.

Criteria for Site Selection. Three main factors informed the selection of case study site. First, the comparison of *in situ* and *ex situ* technologies would be most informative if the technologies were compared on a similar basis, such as the provision of equivalent treatment (Diamond et al. 1999). Second, the development of a life cycle assessment model required knowledge of components, materials, and construction processes for both technologies. Finally, the case study would have the most impact if the technologies were tested at pilot- or field-scale and represented common groundwater contaminants, and common remediation strategies, methods, and reactive materials. Therefore, the selection of case study site was based on a number of desirable characteristics including: (1) the ability to compare technologies designed to provide identical (or similar) treatment, (2) the availability of design documents including material requirements and process descriptions, and (3) the incorporation of the most common contaminants, remediation strategies and reactive media. After considering these objectives, Dover Air Force Base, Area 5, was chosen as the case study site. Area 5

was contaminated with several volatile organic compounds including dichlorooethylene, dichloroethane, trichloroethylene and vinyl chloride (Kim et al. 1994).

Life Cycle Assessment. The life cycle assessment methods used was based on ISO 14040 (International Organization for Standardization 1997), United States Environmental Protection Agency guidance documents (Scientific Applications International Corporation 2006), and published frameworks (Bayer and Finkel 2006; Diamond et al. 1999) . The life cycle assessment was conducted using SimaPro software with associated life cycle inventory databases (Pre Consultants 2006). Inventory information which was unavailable within the databases was estimated from literature or calculation. An effort was made to use inventory data that is representative of the United States. Similarly, the life cycle impact assessment was conducted using the Tool for the Reduction and Assessment of Chemical and other environmental Impacts (TRACI), developed by the United States Environmental Protection Agency (Bare et al. 2003; Bare, Gloria, and Norriss 2006). Impact categories including global warming, acidification, human health, eutrophication, ozone depletion and smog were used in the analysis, chosen based on environmental relevance and previous studies. Monte Carlo simulations with set stop factors was used to generate 95% confidence intervals, with uncertainty values assigned to system input data based on perceived quality. From the available design information (Kim et al. 1994; Gavaskar et al. 2000b) the PTS and PRB were analyzed, revealing major design elements, materials, and energy usage. Based on this analysis, a treatment system model was developed, which was used as input to the life cycle assessment program. Each technology was examined, such that the products of the

analysis not only provide a comparison of the two technologies, but also examine which design elements of each technology produce the greatest environmental impact.

Effect of Reduced Iron Nanoparticles on Bacterial Growth

The effect of reduced iron nanoparticles on bacterial growth was investigated to explore the local environmental impacts of employing groundwater remediation technologies with nanoscale reactive media.

Toxicity Terminology. Wherever possible, the effect of reduced iron nanoparticles on bacterial growth were described by the terms suggested by the International Union of Pure and Applied Chemistry (IUPAC) (Duffus, Nordberg, and Templeton 2007), and definitions for terms not included in the glossary are defined here. The phrase "adverse effects" was used to describe any change in growth, in accordance with the IUPAC definition, while "cytotoxic" refers specifically to cellular damage. The phrase, "change in limiting nutrient" will be used to describe changes in the microbial growth medium that may result in reduced growth due to the loss of a specific nutrient. The term "inactivation" is not explicitly defined in the IUPAC guidelines, but was be used in this dissertation to describe the effect of rendering non-living cells biologically inert.

Model Organism. *Escherichia coli* K12 was used as a model organism for toxicity tests. *E. coli* is a gram-negative bacterium that is commonly-used in nanoparticle toxicity tests in the literature (Sondi and Salopek-Sondi 2004; Adams, Lyon, and Alvarez 2006; Lee et al. 2008). Furthermore, a majority of studies that examine the effect of reduced iron nanoparticles on bacterial survival or growth use *E. coli* as a model bacterium (see Table 2 and Table 3), such that choosing *E. coli* in this study allows for

discussion of findings in the context to published reports. As a gram-negative bacterium, *E. coli* may be more sensitive to reduced iron nanoparticles than gram-positive bacteria, which have thicker peptidoglycan layers (Chen et al. 2010).

Bacterial Culture Methods. The *E. coli* K12 selected for the toxicity tests was obtained as an environmental isolate (courtesy of Dr. Nancy G. Love) and maintained in Luria-Bertani (LB) broth and on LB agar plates. *E. coli* was kept at -80 °C in a 1:1 glycerol:LB media for the duration of experiments. *E. coli* was plated from the freezer culture onto LB agar plates and grown aerobically at 37 °C overnight before storage at 4 °C for use during experiments. *E. coli* was maintained in a liquid minimal media derived from a Minimal Davis (MD) Medium reported in the literature (Adams, Lyon, and Alvarez 2006; Lyon et al. 2006; Mahendra et al. 2008; Brunet et al. 2009).

Microbial Growth Medium. Modification to the MD Medium reported in the literature were made to accommodate the specific needs of this study. First, the concentration of phosphate in the medium was reduced to 5.52×10^{-3} M to 1.0×10^{-3} M to reduce the precipitation of $Fe_3(PO_4)_{2(s)}$ following the addition of nZVI or FeS to the medium. Second, 3-(N-morpholino)propanesulfonic acid (MOPS) buffer was added to buffer the medium at pH = 7 (Neidhardt, Bloch, and Smith 1974). To increase yield under both aerobic and anaerobic conditions, a divalent metals solution and a trace metals solution were added to the medium. Finally, to anaerobic minimal media 5 mg/L peptone was added, which was necessary for survival of the aerobic-anaerobic transition. The final growth medium used in this dissertation is described in Table 4.

Table 4. Microbial Growth Medium Components and Recipe.

Component	[g/L]	[M]	Purpose
K_2HPO_4	0.12749610000	7.32E-04	Phosphate for Growth
KH_2PO_4	0.03647351360	2.68E-04	Phosphate for Growth
$NaC_7H_{15}NO_4S$ (Na-MOPS)	0.44621600000	1.93E-03	Buffer at pH = 7
$C_7H_{16}NO_4S$ (MOPS)	0.64242985780	3.07E-03	Buffer at pH = 7
NH_4Cl	0.80962000000	1.51E-02	Ammonium for Growth
$C_6H_{12}O_6$ (D-Glucose)	1.00000000000	5.55E-03	Carbon for Growth
$MgSO_4$-$7H_2O$	0.12432400932	3.54E-04	Magnesium for Growth
$CaCl_2$-$2H_2O$	0.02195819958	1.49E-04	Calcium for Growth
H_3BO_3	0.00012432401	2.01E-06	Trace Metals for Growth
$CoCl_2$-$6H_2O$	0.00124324009	3.79E-06	Trace Metals for Growth
Na_2MoO_4-$2H_2O$	0.00041441336	1.52E-06	Trace Metals for Growth
$CuCl_2$-$2H_2O$	0.00041441336	2.07E-06	Trace Metals for Growth
$ZnCl_2$	0.00124324009	9.12E-06	Trace Metals for Growth
$MnSO_4$-H_2O	0.00364084814	1.59E-05	Trace Metals for Growth
Na_2-EDTA	0.15420000000	4.14E-04	Chelating Agent
$FeCl_2$-$4H_2O$	0.00911709402	3.52E-05	Trace Metals for Growth
Peptone	0.00500000000		Peptone for Anaerobic Growth

Bacterial Enumeration. Enumeration of bacteria was obtained by plating *E. coli*-containing solutions on LB-agar plates (10 g/L Tryptone, 5 g/L Yeast Extract, 10 g/L NaCl, 15 g/L Agar) and counting colony forming units (CFU). Solutions were diluted 1:10, 1:100, or 1:1000 in phosphate buffer solution (8.5 g/L NaCl, 0.3 g/L KH_2PO_4 ,0.6 g/L Na_2HPO_4, 0.1 g/L Peptone) to obtain 30-300 CFU/plate with 50 μL aliquot. Agar plates were spread and allowed to grow for 96 hours under anaerobic conditions prior to counting. A colony counter with magnifier was used to obtain the number of CFUs per plate. Abiotic (negative) and biotic (positive) controls were run with every experiment to detect contamination and standardize results. Samples were run in duplicate or triplicate, and reported values are the mean with error bars representing one standard deviation

unless otherwise noted. Data tables for toxicity experiments are presented in Appendix B.

Protocol for Toxicity Tests. The effect of nZVI and FeS on *E. coli* growth under anaerobic conditions was examined by preparing nanoparticle suspensions buffered at pH 7 with MOPS buffer and added to anaerobically-growing *E. coli* cultures in a well-defined growth medium inside of an anaerobic chamber. The chamber was maintained under positive pressure and contained a platinum catalyst to scavenge oxygen.

E. coli were grown aerobically to a mid-log optical density measured at 600 nm (OD_{600} = 0.162), and transferred to the anaerobic chamber in a culture tube with a screw-top cap. A representative aerobic growth curve is presented in Figure 1. The aerobic culture was added to anaerobic growth medium with a 1:10 dilution ratio and grown to a mid-log optical density (OD_{600} = 0.027) before transfer to the experimental solution using a 1:100 dilution ratio. A representative anaerobic growth curve is presented in Figure 2. In all experiments, particle suspensions or salt solutions were added to growth medium immediately prior to inoculation.

The adverse effects of zero-valent iron nanoparticles, iron sulfide nanoparticles, sodium sulfide and ferrous chloride to *Escherichia coli* were evaluated by measuring the colony forming units after 24 hours of growth (CFU_{24}) of bacterial cultures with particle or salt amendments and compared with CFU_{24} of bacterial cultures grown in absence of amendments. Based on the anaerobic growth of *E. coli* in minimal media, 24 hours was roughly the time to mid-log growth in the medium without amendments.

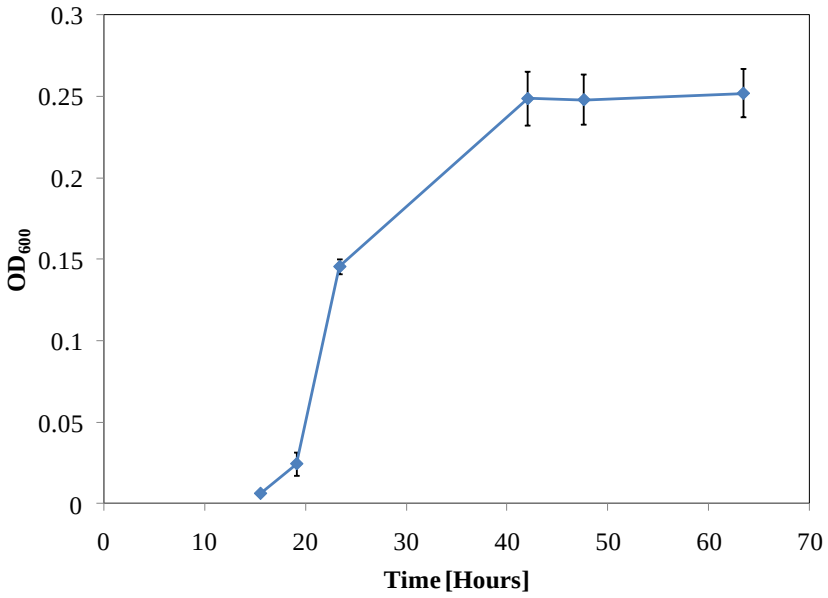

Figure 1. Representative aerobic growth curve for *E. coli* in microbial growth medium without peptone (see Table 4) at 37 °C. Error bars represent the standard deviation of biological replicates conducted in the same experiment (*n*=3).

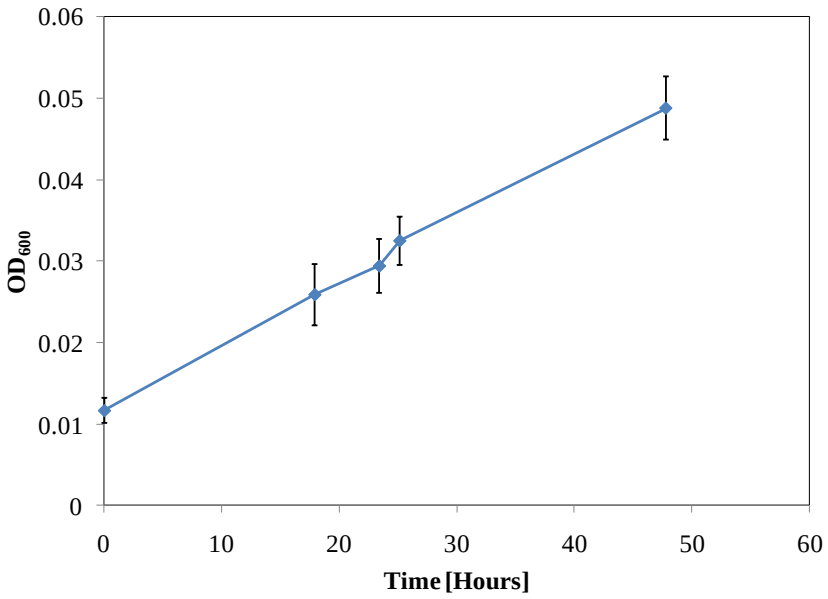

Figure 2. Representative anaerobic growth curve for *E. coli* in microbial growth medium (see Table 4) at 21 °C. Error bars represent the standard deviation of biological replicates conducted in the same experiment (*n*=4).

FeS Dissolution Studies. The dissolution of FeS nanoparticles in the microbial growth medium was determined by measuring changes in the total and dissolved iron as a function of time. FeS stock solutions were prepared at pH 7 as described above. Stock suspension was allowed to settle for 30 minutes to remove large aggregates and 10 mL were withdrawn from the top of suspension for use in experiments. FeS stock suspensions were added to microbial growth medium to achieve the desired final solid phase concentration of FeS. Samples were distributed to individual tubes and were allowed to sit without mixing in the anaerobic chamber. At designated time points an entire sample tube was sacrificed for analysis. 1 mL of the sample was acidified to 2% HNO_3, and analyzed for iron content by ICP-MS (Perkin Elmer). The remaining 4 mL of the sample was centrifuged (Eppendorf 5810R) for 20 minutes at 10000*g* to remove particles from suspension. The supernatant was withdrawn with a pipette, acidified to 2% HNO_3, and analyzed for iron content.

Equilibrium Speciation Modeling. Equilibrium speciation of the microbial growth medium was modeled using PHREEQC geochemical modeling software (Parkhurst, Appelo, and Geological Survey (US) 1999) using the MINTEQ.V4 thermodynamic database (HydroGeoLogic. and Allison Geoscience Consultant 1998). Speciation modeling was carried out in batch mode, with equilibrium among solution species with the solid phases listed in Table 5. Of the 139 solid phases with a chemical composition consistent with the species added, only 39 were predicted to precipitate during any of the model runs (10^{-6} to 10^{-2} M nZVI, FeS, Na_2S, or $FeCl_2$ added).

The set of solid phases considered, 23 of the 39 solids, was chosen to suppress the formation of stable iron sulfide phases in favor of mackinawite and to suppress the

formation of iron oxide phases. The suppression of iron oxide phases represents a conservative assumption because the model attempts to describe a kinetic process (corrosion) with in an equilibrium model. Toxicity experiments were conducted for 24 hours and the formation of appreciable iron oxide phases during that time was assumed not to occur. Inclusion of magnetite as a solid phase did not change the predicted solution chemistry at concentrations below 2 x 10^{-3} M nZVI added, and is described in Appendix H.

Table 5: List of Solid Phases Considered in Speciation Modeling

MINTEQ.V4 Phase	Formula
Anilite	$Cu_{0.25}Cu_{1.5}S$
BlaubleiI	$Cu_{0.9}Cu_{0.2}S$
BlaubleiII	$Cu_{0.6}Cu_{0.8}S$
CaHPO4	$CaHPO_4$
CaHPO4:2H2O	$CaHPO_4{:}2H_2O$
Chalcocite	Cu_2S
Chalcopyrite	$CuFeS_2$
CoFe2O4	$CoFe_2O_4$
CoS(alpha)	CoS
CoS(beta)	CoS
Covellite	CuS
Cuprite	Cu_2O
Cuprousferrite	$CuFeO_2$
Djurleite	$Cu_{0.066}Cu_{1.868}S$
FeMoO4	$FeMoO_4$
Fe(OH)2.7Cl.3	$Fe(OH)_{2.7}Cl_{0.3}$
Hydroxylapatite	$Ca_5(PO_4)_3OH$
Mackinawite	FeS
MnHPO4	$MnHPO_4$
MoS2	MoS2
Sphalerite	ZnS
Vivianite	$FePO_4$
ZnS(am)	ZnS(am)

Several modifications to the database were made to add or control species based on the procedure or results. ZVI was added to the model according to equation (2) with the equilibrium constant Log K = 14.9 (Stumm and Morgan 1996). This assumption allows for ZVI to be added as an equilibrium phase, though it defines an equilibrium constant for a non-equilibrium reaction and likely over-estimates the concentrations of Fe^{2+} and e^- in solution. The abiotic reduction of sulfate to sulfide assumed not to occur in the presence of nZVI or $FeCl_2$, and was therefore suppressed during model runs by modification of the equilibrium constant. This assumption was tested experimentally and the results are presented in Chapter 5. The aqueous species MOPS and H-MOPS were added to the model to control pH but no reactions were allowed with media components. Glucose and peptone were not included in the model. The PHREEQC codes used to generate model results are provided in Appedices C, D, E and F for nZVI, $FeCl_2$, FeS, and Na_2S, respectively. Appendix G contains the thermodynamic data from the Minteq.v4 database.

Chapter 4

Life-Cycle Case Study Comparison of Permeable Reactive Barrier versus Pump-and-Treat Remediation

Introduction

Groundwater resources are critical to meeting current and future global water needs, but are threatened by extensive contamination, as illustrated by the more than 900 sites on the US National Priorities List (U.S. EPA 2007), with chlorinated solvents occurring most frequently at industrial sites (Stroo et al. 2003). Selection of remediation technologies to restore groundwater depends on site-specific conditions as well as technology performance, cost, and environmental impacts. One technology often considered is a pump-and-treat system (PTS), which removes the contaminated groundwater by pumping and use of aboveground treatment facilities. A PTS provides quick initial reductions in contaminant concentrations, but often results in a slow, steady reduction for the long term (Mackay and Cherry 1989). If conditions are suitable for PTS, remediation goals can be achieved in reasonable time scales (Cohen et al. 1997). However, a 2001 summary of experiences at groundwater remediation sites found that of the 32 sites surveyed only two had met remediation goals with an average capital cost of $4.9 million and $26 per thousand gallons treated (U.S. EPA 2002).

A permeable reactive barrier (PRB) was first tested in 1991 as an alternative for remediation (O'Hannesin and Gillham 1998). PRBs are installed *in situ*, allowing groundwater to flow under the natural gradient through a reactive cell where a reactive medium degrades or captures contaminants (U.S. EPA 2002). A variety of PRB configurations have been employed. The two most common designs are 'continuous trench' configurations, in which the reactive medium is continuously placed in an excavated trench, or 'funnel and gate' arrangements, where impermeable surfaces direct flow through smaller cells of reactive material (Gavaskar 1999). According to an US EPA survey, approximately 30% of PRB installations use the former design, 30% the latter, with the remainder consisting of several less common configurations (U.S. EPA 2002). PRB installations have also been designed with several types of reactive media, although the most common reactive medium has been zero valent iron (ZVI). Approximately 55% of the PRB installations surveyed in 2002 relied on ZVI to effect treatment (U.S. EPA 2002). These surveys indicate that the length of time over which the reactive medium remains effective, the longevity, is a major factor in the long-term success of the technology. Though some field-scale barriers have been in operation for more than ten years (Wilkin, Puls, and Sewell 2003)(), the absolute longevity of ZVI and the factors which control longevity at PRB installations are relatively unknown (Henderson and Demond 2007).

Due to its minimal material and energy requirements during operation, a PRB system offers potential economic and environmental advantages over a PTS (Wilkin, Puls, and Sewell 2003; Scherer et al. 2000; Day, O'Hannesin, and Marsden 1999; Gavaskar 1999). However, a thorough evaluation of environmental advantages must be

made with respect to all relevant life-cycle stages. Life-cycle assessment (LCA) is used to quantify and compare environmental impacts of products or systems over the entire life cycle (International Organization for Standardization 1997). Applications of LCA to site remediation, including remediation of contaminated soil and/or groundwater, have been investigated in generic applications and through case studies (Bayer and Finkel 2006; Diamond et al. 1999; Suer, Nilsson-Paledal, and Norrman 2004; Page et al. 1999; Cadotte, Deschênes, and Samson 2007). A conceptual framework for the application of LCA to site remediation technologies was developed by Diamond et al. (Diamond et al. 1999), which was subsequently applied to a case study involving excavation and disposal of lead-contaminated soil (Page et al. 1999). Suer and colleagues reviewed the methods and results of eight case studies on the application of LCA to site remediation (Suer, Nilsson-Paledal, and Norrman 2004) and found that energy consumption was a major cause for environmental impact. However, of the eight case studies examined, only two of the assessments included technologies for groundwater remediation and neither considered PRB or other passive technologies among the alternatives ((Suer, Nilsson-Paledal, and Norrman 2004). In the sole published LCA comparison of a PRB and a PTS system (Bayer and Finkel 2006), a relatively atypical reactive medium, activated carbon, was considered for the remediation of acenaphthene, a polycyclic aromatic hydrocarbon (PAH).

Although ZVI is one of the most common reactive media employed in PRBs, no LCA comparisons involving this type of PRB have been reported. In this study an LCA of a ZVI-type PRB was compared to a PTS for a case study site contaminated with chlorinated solvents. The assessment was designed to examine the impact of medium

longevity on the life-cycle impacts of a PRB, and thereby quantify the design life at which the two remediation approaches are equivalent from an LCA perspective. The LCA comparison was also used to identify specific components of PRB design which, if improved, would result in the greatest environmental benefit.

Methods

Case Study Description

The case study was conducted using publicly-available design documents for two remediation strategies designed by Battelle for Dover Air Force Base (AFB) in Dover, DE (Kim et al. 1994; Gavaskar et al. 2000a). Contaminants on site include several volatile organic compounds (VOCs) including 1,2-dichloroethylene (DCE), 1,2-dichloroethane (DCA), trichloroethylene (TCE), perchloroethylene (PCE), and vinyl chloride (VC) (Kim et al. 1994). Though the geochemical conditions on site are representative of many contaminated sites, some hydraulic conditions (specifically low hydraulic gradient, 0.0018, and high depth to aquitard, 11 m) are somewhat atypical for PRB applications (ESTCP 2003). Since these characteristics make the site a more difficult PRB application, the life-cycle assessment of the PRB's environmental impacts may be less favorable than sites with shallower water tables and greater hydraulic gradients.

Pilot scale testing of both PTS (Kim et al. 1994) and PRB (Gavaskar et al. 2000a) technologies was carried out on-site. Although these technologies were never installed on-site at full scale, full-scale designs of both systems were developed by Battelle. These completed designs have served as the basis for engineering and economic comparisons of the two technologies in several publications (Gavaskar et al. 2000b; Gavaskar et al.

2000a; ESTCP 2003). Acknowledging that there is general uncertainty in the validity of design assumptions, especially with respect to the design life of a PRB, the effect of design life on its life-cycle environmental impacts was examined in this study.

The full-scale PRB was designed as a funnel-and-gate configuration with a 36.6 m length of funnel and four - 2.4 m diameter cylindrical gates, as shown in Figure 3. The funnel was to be constructed from pre-fabricated steel sheet piling sealed together with cementitious grout. The gates were to be constructed by excavating within a 2.4 m diameter steel caisson, installing a 1.2 m by 1.2 m column of ZVI, and backfilling the outer pretreatment and exit zones with sand. The ZVI used in the pilot-scale unit and recommended for use in the full-scale PRB was commercially-available, high quality granular iron. The design of the full-scale PRB was similar to the pilot-scale PRB unit tested; the most significant differences were the size (the full-scale PRB was twice as large), and modifications to the pretreatment zones (the full-scale PRB used only sand while the pilot-scale unit employed sand/iron mineral mixtures).

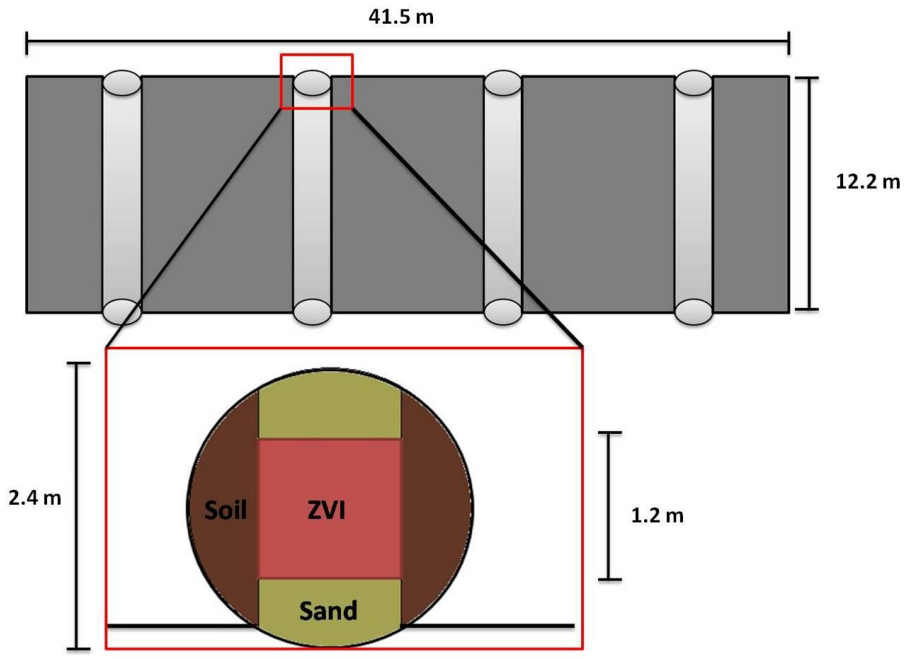

Figure 3: Illustration of Dover Air Force Base permeable reactive barrier, showing the 41.5 m total length, 12.2 m depth. Water flow is into the paper. Enlarged gate shows the 1.2m by 1.2m column of ZVI and the total 2.4 m diameter.

The full-scale PTS was designed to remove groundwater from three pumping wells using electric pumps. It included a packed-tower air-stripping unit that was housed aboveground in a building. Air emissions from the tower were to be treated using catalytic oxidation and the effluent water stream was further polished using GAC adsorption before re-injection to the aquifer. The pilot PTS facility evaluated two air-stripper tower configurations at 190 L min^{-1} (50 gpm) each, and four different catalytic oxidation units. In the full scale design the assumed process flow rate for the selected configuration was 76 L min^{-1} (20 gpm).

Permeable Reactive Barrier System Model

The PRB was modeled as three subsystems: funnel, gate, and reactive medium. The model PRB funnel was constructed using a vibratory hammer mounted on a 100-ton

crane (nominal capacity of 835 kW at 5.6 m^2/hour) and sealed together with cement. Model PRB gates were constructed using the same hammer (at 0.6 m/hour) to drive the caissons into position, then excavated using an auger (435 kW at 0.3 m/hour). The gates were then back-filled with sand, ZVI, and soil before the caisson was removed with the vibratory hammer. Though designed as part of the gate, the reactive medium was considered a separate subsystem to investigate the effect of media longevity. ZVI production was modeled as the production of high-iron content cast iron, without additional processing. The exclusion of additional processing may reduce the energy burden associated with the ZVI subsystem, however, the additional processing energy was assumed to be small when compared with the energy demand of the material. The ZVI longevity was assumed to be 10 years for the base case model. Only in the investigation of media longevity effects on potential impacts was the longevity allowed to vary. Following construction, the PRB was assumed to operate for the duration of the medium lifetime without additional inputs. Upon exhaustion of the medium, the gate was to be removed with an auger before major material components were generated, transported, and constructed into a replacement gate. It was assumed that the funnel does not require repair during the 30 year study period.

Pump and Treat System Model

The PTS was modeled with five subsystems: extraction wells, air-stripping unit (ASU), catalytic oxidation unit (COU), granular activated carbon (GAC) unit, and a building to house the treatment units. Model extraction wells were constructed using an eight inch auger (80 kW at 5 m/hour) and were composed of PVC well pipe, filter pack, grout, and a 0.75 kW (1 hp) well pump. The model ASU was composed of an aluminum tower, packed with polyethylene pall ring packing, and a one hp blower. The model

COU was modeled as a fixed bed reactor made out of aluminum and steel, with catalyst, and electric heaters. The model GAC unit was two steel drums each containing 400 pounds of GAC. Model building included a 37.1 m^2, 0.15 m thick structural slab poured from concrete mixing truck (260 kW at 0.14 m^3/hour), 61 m of 0.05 m diameter PVC piping, miscellaneous PVC fittings and valves, and a steel shed. Following construction and assembly, the system was assumed to operate using electricity obtained from the US grid. The only maintenance activity considered for the model PTS was the replacement of GAC filter units every 10 years.

Life-Cycle Assessment

LCA methods were based on ISO 14040 (International Organization for Standardization 1997), government guidelines (Scientific Applications International Corporation 2006), and previously published work (Bayer and Finkel 2006; Diamond et al. 1999). The LCA case study was conducted using SimaPro 7.1 LCA software and associated inventory databases and impact assessment methods (Pre Consultants 2006). Unit processes with inputs or emissions that were not included in the databases were estimated from available literature, calculated using fundamental principles, or omitted. The impact assessment was conducted with characterization factors within the Tool for the Reduction and Assessment of Chemical and other environmental Impacts (TRACI) method (Bare, Gloria, and Norriss 2006) version 2.0. The following environmental impact categories were considered: global warming, acidification, human health, eutrophication, ozone depletion and smog formation. The selection of these impact categories is consistent with previous studies in the literature, as shown in Table 6. The determination of uncertainty was conducted using Monte Carlo simulations with set stop factors available within SimaPro software to generate 95% confidence intervals. System

input data was given an uncertainty value based on our perceived quality of the data. Additional information on assumptions, omitted processes, and uncertainty values are available in Appendix A.

Table 6: Environmental Impact and Resource Consumption Categories Considered in the Literature from (Lemming 2010)

	Diamond et al	Page et al	Bayer and Finkel	Cadotte et al	This Study
Environmental Impacts					
Global Warming	X	X	X	X	X
Ozone Depletion	X			X	X
Photochemical Ozone Formation	X		X	X	X
Acidification	X		X	X	X
Nutrient Enrichment	X			X	X
Ecotoxicity	X		X	X	
Human Toxicity	X	X		X	X
Air pollution					
Land Use	X				
Noise	X				
Resource Consumption					
Fossil Energy	X	X	X		
Clean Groundwater	X	X			
Clean Soil/sand/gravel	X	X			

The goal of the LCA was to model the Dover AFB treatment systems in order to determine the environmentally preferable option and to investigate strategies that would reduce impacts within each system. The assessment was based on a common functional unit: the system-specific requirements (energy, materials) needed to provide effective capture of the contaminant plume and treatment for 30 years. According to design documents, the PRB captures the plume and treats 38 L min^{-1} (10 gpm), while the PTS is designed to operate at a flow rate of 76 L min^{-1} (20 gpm) to meet the same goal (Kim et al. 1994; Gavaskar et al. 2000a). Specifications for both systems incorporated factors of

safety into the designs, which were roughly 1.5 for the PRB and 2 for the PTS (Kim et al. 1994; Gavaskar et al. 2000a), and while the two systems do not have identical safety factors, they are similar and both reflect the need to over design groundwater treatment systems.

The choice of functional unit is important for the comparison of results to existing studies and also to the applicability of results to future remediation projects. A comparison based on equivalent treatment for a particular site is consistent with previous studies (Bayer and Finkel 2006), where the function unit was control of a specified contaminated zone. This allows the direct comparison of two technologies optimized for treatment of the case-study site, but may limit the applicability of results to future projects. Other functional units specified in site remediation case studies include the remediation of a volume of soil or groundwater to a specific target concentration (Diamond et al. 1999; Page et al. 1999; Cadotte, Deschênes, and Samson 2007), which is more in line with the purpose and goal of remediation, but requires additional information related to site characterization and the efficiency of treatment processes. By comparing the PTS and PRB installed and optimized at Dover AFB based on an equivalent treatment functional unit, the implicit assumption is that the systems provide adequate treatment that meets remediation goals with respect to volume of water treated and target concentrations.

The system boundaries, which define the scope of the study and illustrate the processes included, were inclusive of raw materials acquisition, materials production, and use phases. Specific fabrication processes, for example, the fabrication of groundwater pumps or the milling of granular iron were not included in the model, due primarily to

lack of representative data. However, when data existed for intermediate processes, such as the extrusion of PVC pipe or the manufacture of rolled aluminum, those processes were included. System boundaries for the PRB and PTS system are shown in Figure 4 and Figure 5, respectively. Notable omissions include monitoring and end-of-life processes. Monitoring schemes for the two full-scale systems were similar in design documents and anticipated to have a similar annual cost (Gavaskar et al. 2000b; Gavaskar et al. 2000a) so the processes were omitted from the life-cycle comparison. While the inclusion of monitoring processes would change the magnitude of PRB impacts, only a relative comparison of the PRB and PTS was sought in this analysis. The temporal scale of comparison was limited to 30 years of operation, though the contamination, and thus treatment, is expected to extend well beyond this time horizon. Therefore, the case study compares only the first 30 years of operation, and the expectation is that 30 years will not be the end-of-life (EOL) for either technology on-site, allowing EOL processes to be omitted. EOL processes have also been omitted in other LCAs for remediation (Bayer and Finkel 2006). The consideration of EOL processes would likely increase the energy consumption for both technologies, due to demolition and transport from site, but may produce a benefit for the PRB technology if the funnel steel could be recycled or if the ZVI column could remain in the subsurface indefinitely.

Figure 4. Schematic of permeable reactive barrier remediation activities and system boundaries. Abbreviations: ZVI = Zero-Valent Iron.

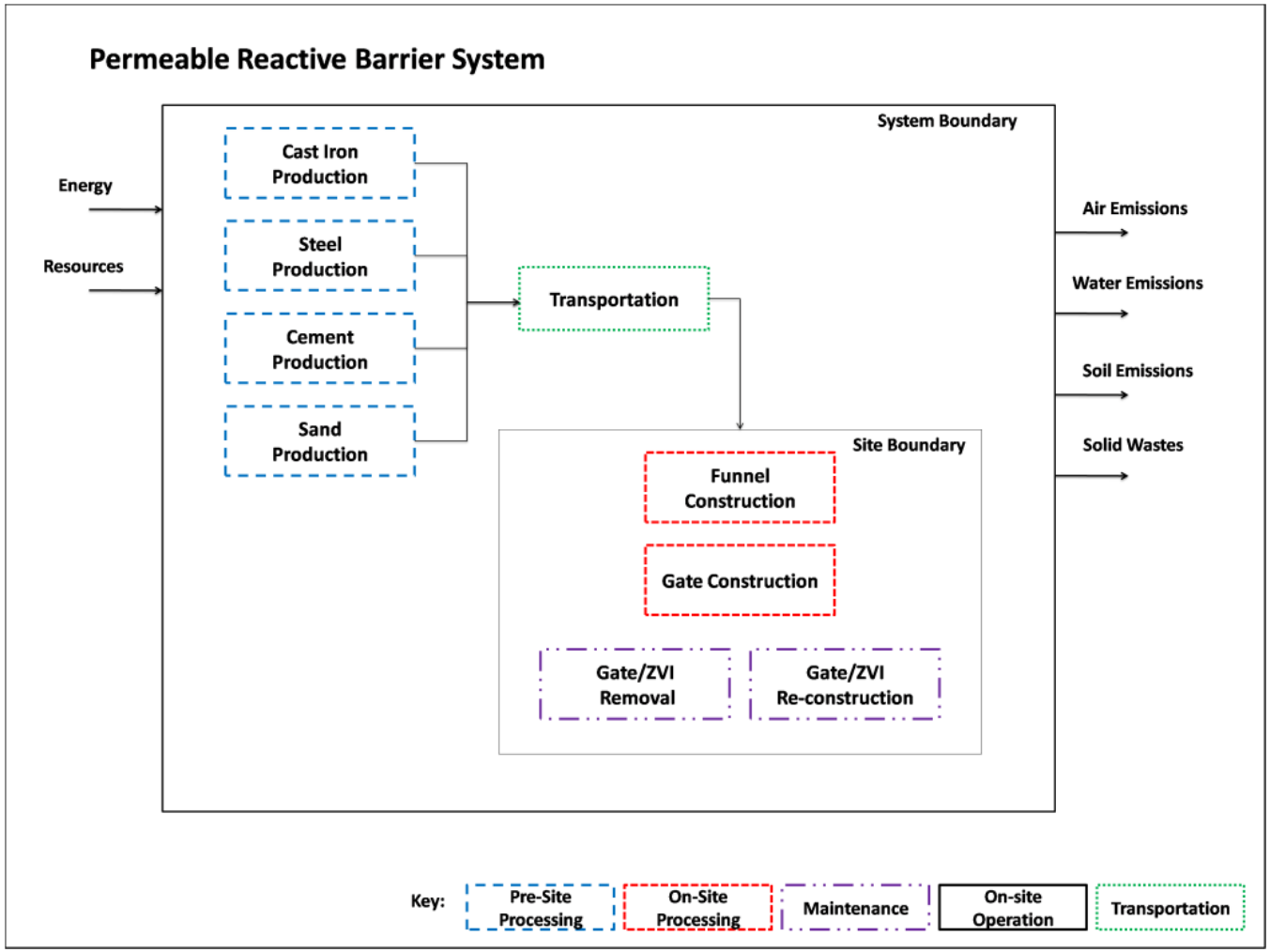

Figure 5. Schematic of pump-and-treat remediation activities and system boundaries. Abbreviations: Al = Aluminum; PVC = Polyvinylchloride; GAC = Granular Activated Carbon; HDPE = High Density Polyethylene; ASU = Air Stripping Unit; COU = Catalytic Oxidation Unit.

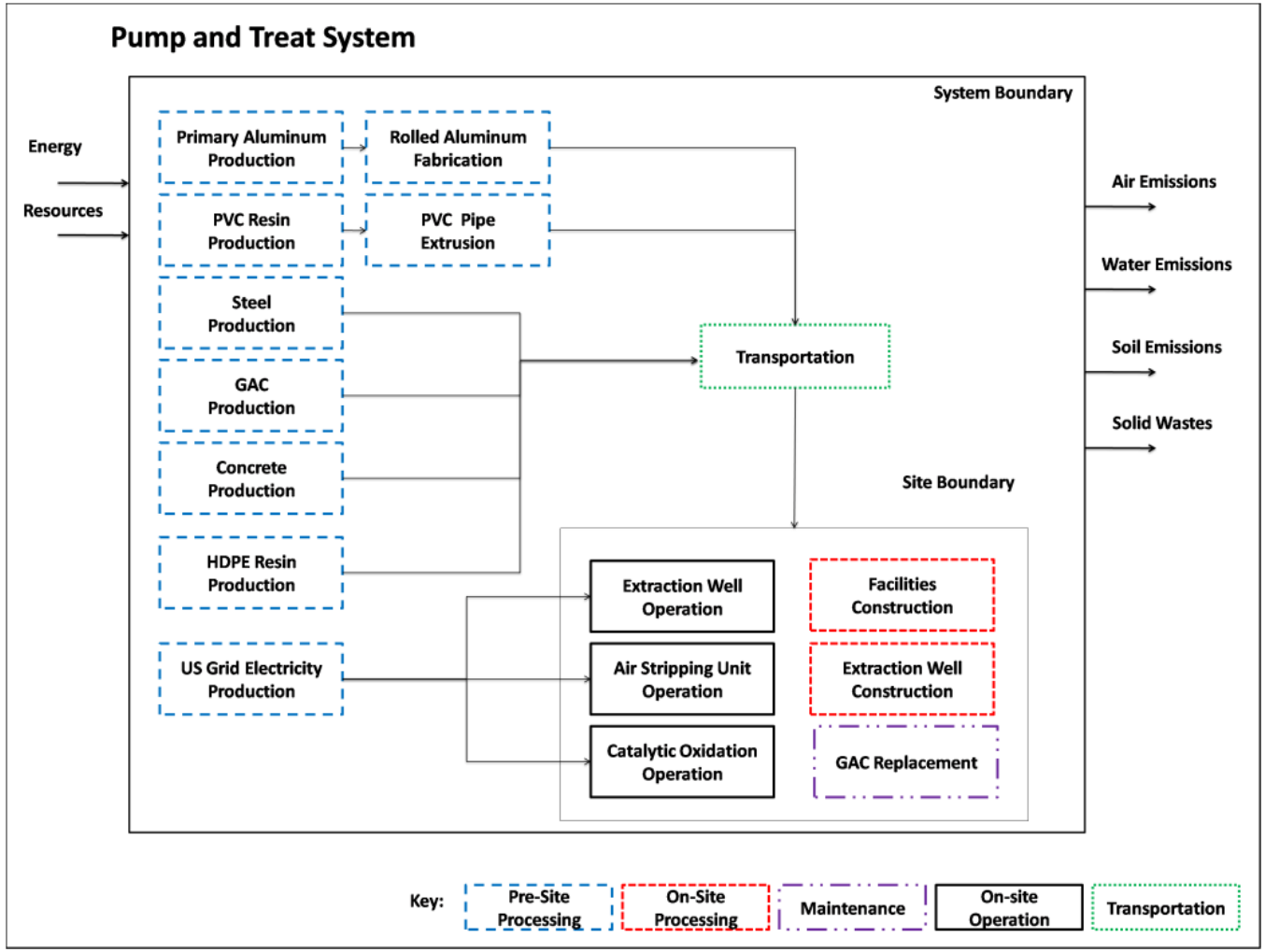

Results and Discussion

Comparison of PRB and PTS Model Systems

Using the life-cycle assessment models developed, the potential impacts of the two alternative technologies were evaluated. The results are compared in Figure 6, normalized to the PTS values in each category. The model PRB with assumed ten year longevity offered significant reductions in acidification and eutrophication compared to the PTS, and even greater reductions in human health and ozone depletion. In the global warming and smog formation categories, however, the normalized results fell within the range of uncertainty in the data. Therefore, while an environmentally preferable option could not be determined within the experimental significance of the case study, the model PRB resulted in fewer environmental impacts. In categories where a statistically significant preferable alternative was not found, the mean impact value of the PRB was within the confidence interval for the PTS, though the confidence interval was uniform across the categories (± 10% for the PRB and ± 28% for the PTS). The overall confidence intervals in Figure 3, however, are similar to those reported in other LCA studies (Bayer and Finkel 2006; Cadotte, Deschênes, and Samson 2007). The comparison illustrates that passive technologies are not inherently more environmentally sustainable than active technologies, and that improvements leading to reductions in the global warming and smog formation impacts of a PRB would most improve its overall environmental favorability relative to PTS. In particular, the result of similar global warming potential, which corresponds to the primary energy required for each technology, suggests that the energy intensity of PRB materials is similar to the operation energy of the PTS. To assess the types of modifications in PRB design, construction, and

operation that could achieve this improvement, the impact contributions due to components of the PRB, materials, energy usage, and longevity of the reactive medium were investigated.

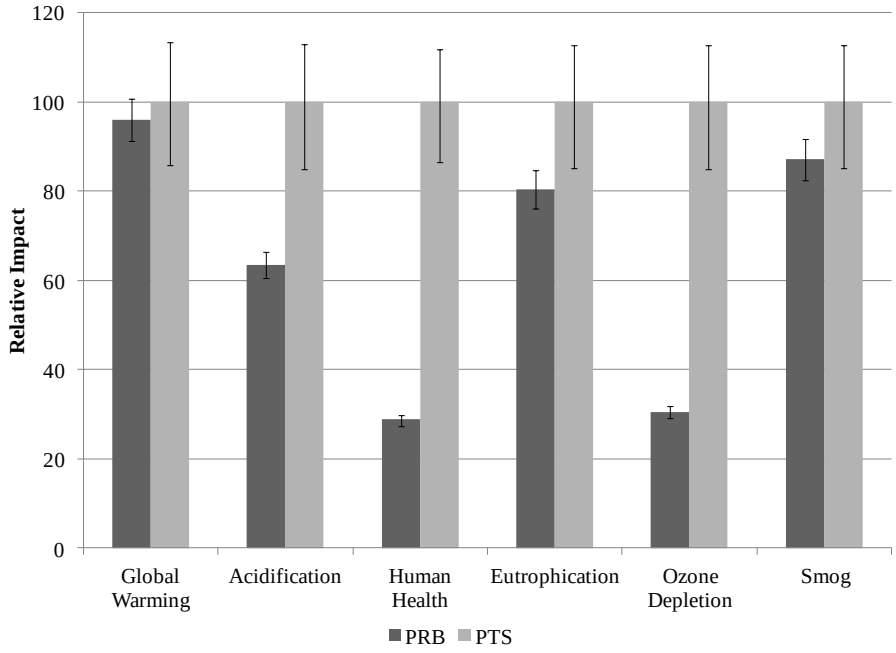

Figure 6. Relative impacts of PRB compared with PTS. Results are normalized by the greatest value in each impact category. Error bars represent 95% confidence intervals as determined by Monte Carlo simulation. Replacement of the gate and ZVI are assumed to occur every 10 years.

Subsystem Contribution to Impact Categories

Life-cycle impacts of the PRB were evaluated in terms of the relative contributions of the reactive media, gate, and funnel subsystems, and the results are presented in Figure 7. Together the gate and reactive medium accounted for more than 80% of impacts, and the reactive medium contributed nearly 50% of the potential impacts for the PRB in all categories. The dominance of the reactive medium in this case study is in contrast to previous studies (Bayer and Finkel 2006), specifically with regard to

potential impacts in acidification, human health, and eutrophication, which were controlled largely by the funnel in their model. The barrier in their study was larger than the barrier installed at Dover AFB, 240 meters long compared to 41.5 m and 17 m deep compared to 12.2 m, and contained 8 gates rather than 4. The larger dimensions and relative length of funnel to length of gate (3.3:1 in this study compared to 12:1 in (Bayer and Finkel 2006)) is likely the reason the funnel has less impact in the presented results. The difference may also be due to the GAC reactive medium used in their PRB, though an influence by GAC was noted in other categories. They explored the use of alternative funnel materials to reduce the environmental impacts of the PRB. However, the relatively small contribution of the funnel subsystem here suggests greater environmental benefits would be gained by considering alternative reactive media or gate construction methods for the model PRB in this study.

A similar characterization and analysis of the PTS provided the relative contributions of the design subsystems, and the results are shown in Figure 8. The extraction, COU, and ASU subsystem contributed 53, 35, and 12 percent of total impacts, respectively. The dominance of the extraction subsystem is in contrast to previous LCA studies (Bayer and Finkel 2006), which may be the result of significant differences in the hydraulic properties in the two studies. The energy demand of the ASU and COU were not as significant as the extraction in the model, though taken together the three electricity-demanding processes accounted for more than 95% of the impacts in every category. The use of cleaner, renewable energy sources would reduce the environmental impacts of the PTS. The importance of energy demand suggests that a PTS with a lower extraction rate may also lower potential impacts of the system. A lower extraction rate,

however, may increase treatment times at many sites, which is not captured in the analysis, and would warrant further investigation.

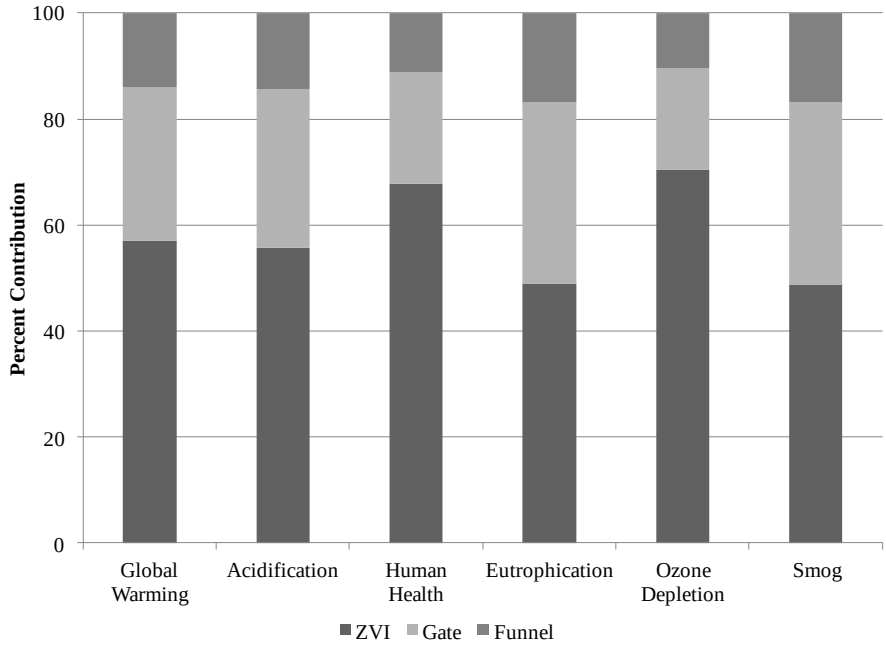

Figure 7. Subsystem contributions to impact categories. Replacement of the gate and ZVI are assumed to occur every 10 years.

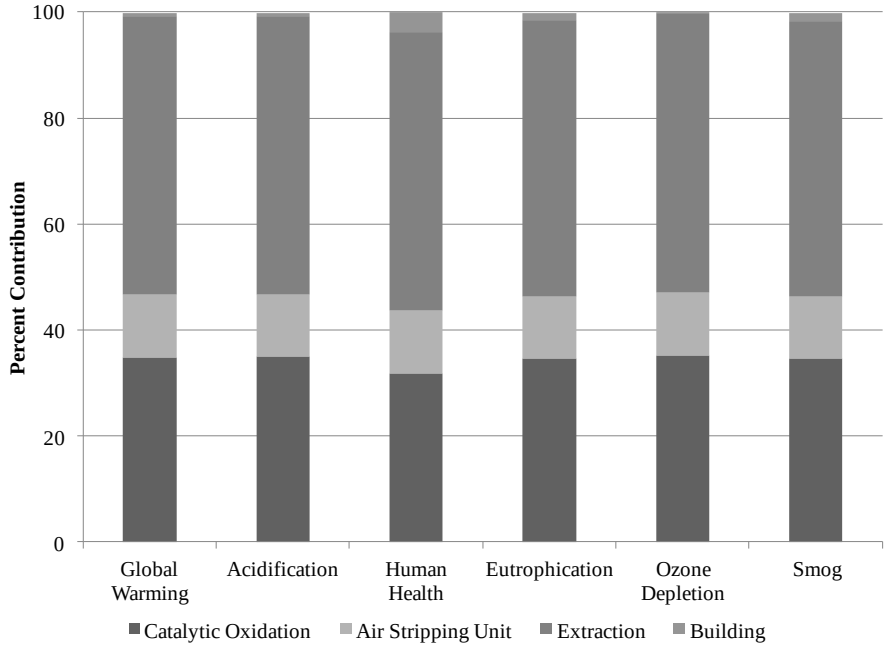

Figure 8. Subsystem contributions to impact categories for the PTS System.

Material Use and Energy Consumption in the Model PRB

Each PRB subsystem was further characterized in terms of material components and energy consumption in construction and transport processes. The results, shown in Figure 9, give the relative contribution of materials, construction, and transport for the model PRB. Materials contributed more than 90% of the potential impacts in the global warming, human health, and ozone depletion categories. Furthermore, ZVI contributed more than 43% of the impacts in each category, and up to 70% in the human health and ozone depletion categories. Together the materials for the gate and funnel subsystem, which both require steel contribute less than 38% of the total impacts across all categories, making the greatest contribution in global warming. The importance of material components was noted in the previous LCA involving a PRB (Bayer and Finkel 2006), where steel was identified as a major cause of impacts. The important contribution of ZVI noted in this study, suggests that alternative reactive media should be considered in order to reduce the environmental impacts of PRBs in categories including global warming.

Construction processes, as illustrated by Figure 9, also contributed 30% of impacts in the eutrophication and smog formation categories and 10% in acidification, and were due to the emissions from diesel combustion by equipment used on site. The construction of the gates on site, distributed in the model between the gate and reactive media subsystems, contributed 20% of the potential impacts, and funnel construction accounted for 10%. The combustion of diesel in equipment or transport vehicles has been noted in other case studies as a main source of potential impacts in site remediation (Suer, Nilsson-Paledal, and Norrman 2004; Cadotte, Deschênes, and Samson 2007), though in those cases it was the major cause of environmental impacts. Although it was

not the cause of a majority of impacts in any category, construction processes significantly contribute to the total potential impact of the PRB, and alternative construction methods, therefore, could produce effective reductions in categories including smog formation. Results of a normalized impact assessment, presented in Appendix A, suggest that the smog formation is less important in the overall impacts when compared with the use of energy or mineral resources.

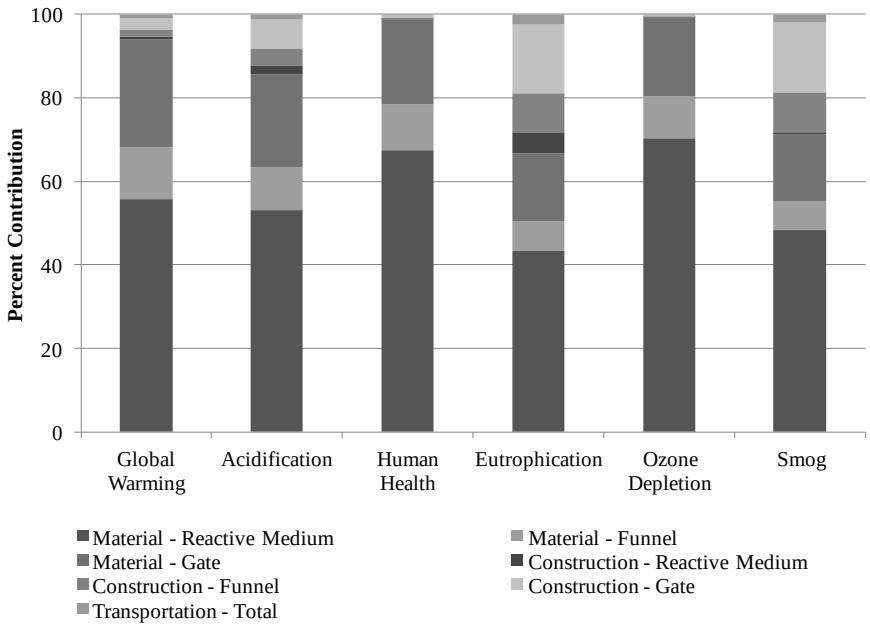

Figure 9. Materials and energy consumption analysis of PRB system. Replacement of the gate and ZVI are assumed to occur every 10 years.

Media Longevity and Potential Impacts of the PRB

The effect of medium longevity on the impacts of the PRB system was investigated by obtaining potential impact values in each category as a function of varying ZVI life. The resulting values, shown in Figure 10, are normalized by the value of the PTS system in each category to facilitate comparisons between the technologies. As the longevity increased from 5 to 30 years, the resulting relative emission in all

categories decreased. Medium longevity had the largest influence on the relative impact in the global warming category, and the smallest influence in human health and ozone depletion. The importance of medium longevity is noted in guidance documents on PRBs as an important factor for the implementation and feasibility of the technology on sites (Gavaskar et al. 2000b). The reactive media longevity also significantly influences the breakeven time and present value of savings when comparing the same PRB and PTS in economic analysis (Gavaskar et al. 2000a), as shown in Table 7. Though medium longevity was not specifically evaluated in the previous LCA with a PRB, replacement of the spent reactive media was noted as a driver of environmental impacts (Bayer and Finkel 2006). This case study establishes reactive medium longevity as a critical parameter that determines the relative favorability of a PRB with respect to its environmental impacts.

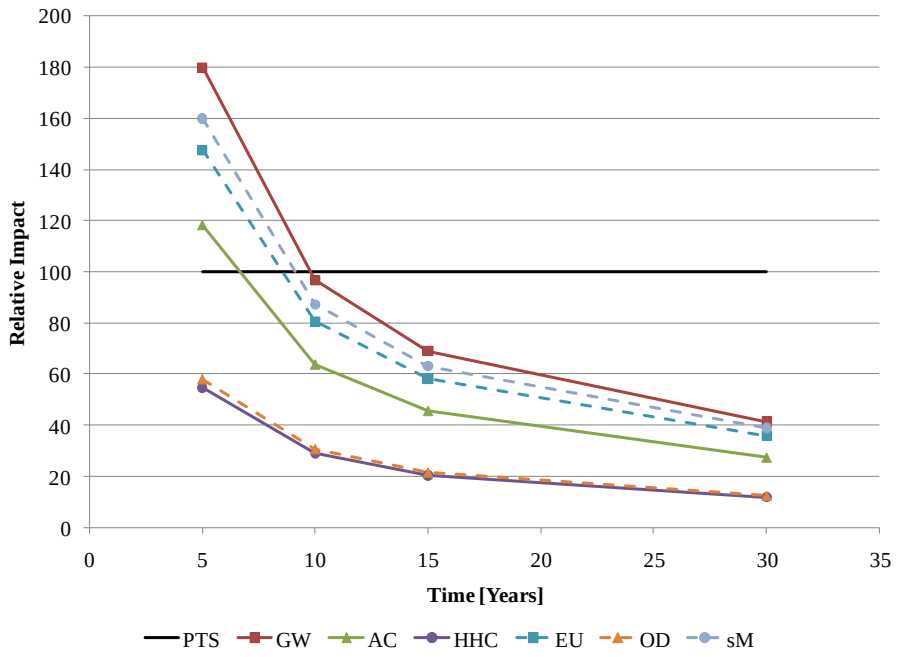

Figure 10. Relative impacts of PRB as a function of medium longevity. Results are normalized by the PTS impact value for each impact category. Lines are used to connect data points. Abbreviations: PTS = Pump-and-Treat System; GW = Global Warming; AC = Acidification; HH = Human Health; EU = Eutrophication; OD = Ozone Depletion; SM = Smog Formation.

For the longest ZVI longevity scenario that was considered, thirty years, substantial benefits in each impact category existed for the PRB, relative to the PTS. PRB installations with thirty years of continuous, successful operation however, have not yet been documented because of the relatively young age of the technology. There are field examples of PRB installations using ZVI for at least ten years (Wilkin and Puls 2003), so the assumption of a ten year longevity is realistic. Lab studies have projected that ZVI may last for thirty or more years (ESTCP 2003), however the extrapolation of lab tests to field performance is not straightforward (Henderson and Demond 2007). If these projections are realistic, the LCA results in this study indicate that the environmental benefits of a ZVI-PRB are substantial.

The minimum longevity for relative PRB environmental benefit at the case study site was determined from the results. The value represents a breakeven point for the implementation of the PRB technology, beyond which the PRB is environmentally preferable. On average, the minimum longevity for environmental benefit falls between five and ten years for impact categories including global warming, smog formation, eutrophication and acidification. Human health and ozone depletion did not have minimum longevity values, since the PRB was more favorable for all scenarios in these categories. Further evaluation revealed that the emission of arsenic and tetrachloromethane in electricity generation required for the operation of the PTS overwhelms the emissions related to human health and ozone depletion for the PRB. Thus, for a ZVI-type PRB to be the environmentally preferable option with respect to the PTS in all impact categories, ZVI longevity must be at least ten years.

Table 7: Break-even Point and Savings by Using a PRB Instead of a PTS at Area 5 (taken from (Gavaskar et al. 2000a))

Assumed Life of Reactive Medium	Break-Even Point	Present Value of Savings at End of 30 years
10 Years	14 Years	$239,000
20 Years	8 Years	$734,000
30 Years	8 Years	$793,000

Implications for Decreasing Environmental Impacts of PRBs

Although the case study results are specific to the Dover AFB, they highlight strategic design considerations for future PRB installations that affect the life-cycle impacts of the technology. First, ZVI was determined to have a significant effect on the potential environmental impacts of the PRB. This suggests that the common use of ZVI

in PRBs may be reducing the environmental benefits of choosing a passive technology, and alternative media should be considered, specifically those that would result in lower life-cycle global warming potential. Potential alternatives might include higher-valent iron minerals or even biological or waste materials, such as mulch, peat, or compost, all of which have been considered for use in PRBs (Scherer et al. 2000). Second, the longevity of reactive media in PRBs will likely control the magnitude of environmental impacts and the relative benefit compared to a PTS. Thus, additional research to better predict and extend the longevity of reactive materials in complex geochemical environments is needed to improve the relative benefit of a PRB compared to other technologies. Third, the construction energy of PRBs will have a significant effect on the environmental impacts in some categories, particularly if reactive media effects are reduced. Reductions in construction energy due to expedited installation could lower potential impacts for the technology, though additional equipment, materials, verification, and monitoring must be considered in the analysis. Installation methods, such as continuous trenching, allow barriers to be installed at a rapid pace with limited equipment (Wilkin, Puls, and Sewell 2003; Gavaskar 1999), and direct injection and hydraulic fracturing methods could be employed at sites unsuited for continuous trenching (McElroy et al. 2003). Overall, the results presented provide a rationale to pursue the development of new reactive materials with extended longevity and new construction methods for PRBs.

This chapter was adapted from: Higgins, M.R. and Olson, T.M. (2009) Life Cycle Case-Study Comparison of Permeable Reactive Barrier versus Pump-and-Treat Remediation. Environmental Science and Technology, 43, 9432–9438.

Chapter 5

Effect of Zero-Valent Iron Nanoparticles on *Escherichia Coli* under Anaerobic Growth Conditions

Introduction

Passive technologies for groundwater remediation rely on a chemical or biological reactive medium to alter geochemical conditions to treat contaminants. Granular ZVI is the most common reactive medium (Scherer et al. 2000) that is applied for the treatment of organic and inorganic compounds, first proposed for groundwater treatment in 1994 (Gillham and O'Hannesin 1994). Recently, ZVI nanoparticles (nZVI) have been investigated as an alternative to granular ZVI (Tratnyek and Johnson 2006). The use of nZVI offers an increased surface area and smaller particle size, which allows nZVI to transform contaminants faster and more efficiently (Zhang 2003). Between 2001 and 2006, there were more than 20 nZVI treatment projects in the United States, and applications are expected to continue (Li, Elliot, and Zhang 2006).

The physical and chemical properties that cause nanoparticles to behave differently from micron-sized particles, including large surface area and small size, also raise concerns about adverse effects on biological systems (Nel et al. 2006). Pure cultures of bacteria can be inactivated, or rendered biologically-inert, upon exposure to nZVI

under a variety of chemical conditions in salt or buffer solutions (Lee et al. 2008; Auffan et al. 2008; Chen et al. 2010; Diao and Yao 2009). The complete review of chemical conditions and adverse effects resulting from exposure are presented in Chapter 2, in Table 2, but those studies conducted under deaerated conditions will be emphasized here. Exposure to 9 mg/L nZVI and 100 mg/L nZVI produced 3.4 (Lee et al. 2008) and greater than 5 log-reduction (Li et al. 2010), respectively, in viable *E. coli* cells under deaerated conditions. The mechanism of toxicity may be related to the disruption of bacterial membranes by both nZVI and Fe(II) (Lee et al. 2008) based on transmission electron microscopy images, or the generation of intercellular reactive oxygen species from the reaction of Fe(II) with intercellular oxygen species (Kim et al. 2010) based on experimental investigation with ROS-quenchers and an oxidative stress assay.

Mixed cultures of microorganisms have shown some tolerance to nZVI in solutions that supports growth, such as simulated river and groundwater solutions (Barnes et al. 2010a; Barnes et al. 2010b; Xiu et al. 2010). (Barnes et al. 2010a; Barnes et al. 2010a)(Barnes et al. 2010a; Barnes et al. 2010a)In a study to assess the feasibility of augmenting bioremediation of TCE with nZVI, it was determined that 1g/L nZVI reduced the rate of bacterial dechlorination by 50%, possibly by disrupting membranes and causing cell death (Xiu et al. 2010). A similar reduction in dechlorination rate was observed when nZVI was exposed to mixed cultures in a groundwater matrix (Barnes et al. 2010a). Examining the effect of nZVI on an indigenous bacterial river community for up to 36 days of exposure indicated that any short-term changes in the number or diversity of bacteria recovered within 3 days (Barnes et al. 2010b).

In aqueous solutions, nZVI participates in chemical reactions that will alter both the reactive surface of nZVI and the bulk solution chemistry, which may also influence the growth or viability of microorganisms. Zero valent iron, whether micro- or nano-sized, is a strong reducing agent capable of lowering the solution electron activity during the corrosion of the metal surface and subsequently reducing many redox-active elements (Scherer et al. 2000). The aerobic or anaerobic corrosion of nZVI will also produce ferrous ions that will interact with available ligands and hydroxide ions that will raise the solution pH. With time in solution, nZVI will "age," where the interactions of nZVI with solution constituents will form mineral coatings of iron oxides or other species on the surface of the nZVI depending on the ions present in solution (Reinsch et al. 2010). All of these chemical changes may influence the interaction of nZVI and bacteria in aqueous solution.

The effect of nZVI on pure cultures of bacteria exposed under anaerobic growth conditions is an interesting case that is missing from the literature, and is the focus of this chapter. This chapter specifically addresses the effect of nZVI on *Escherichia coli* under anaerobic growth conditions, examining the influence of nZVI aging on the adverse effect. It also compares the effect of nZVI with the effect of dissolved ferrous iron, and examines the changes in solution chemistry induced by nZVI through equilibrium speciation modeling.

Results and Discussion

Effect of nZVI on E. coli growth

E. coli growth was reduced in the presence of nZVI relative to the negative control over the entire concentration range tested, 2×10^{-5} M – 5×10^{-3} M (1.59 – 320.28

mg/L) nZVI, as shown in Figure 11. Relative growth showed a bimodal dependence on nZVI concentration above and below 2 x 10^{-4} M nZVI added. A strong adverse effect (no statistically-significant growth) was observed at 2 x 10^{-4} M and 5 x 10^{-3} M nZVI.

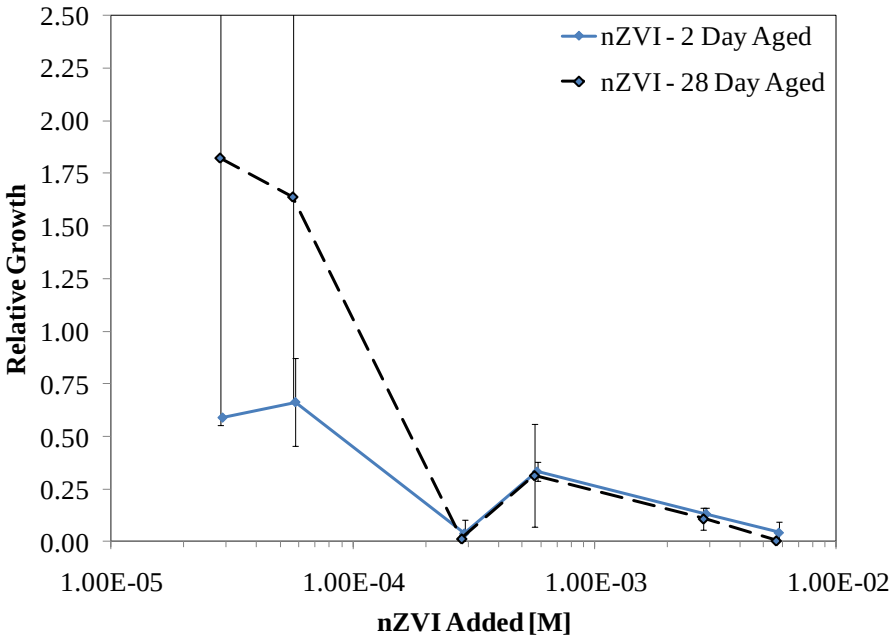

Figure 11. 24 Hour Relative Growth of *E. coli* in the Presence of nZVI as a function of nZVI Added. Error bars are the standard deviation of biological replicates in the same experiment (2-day aged) and standard deviation of biological replicates in the same experiment (28-day aged). See Table 14 and Table 15 for additional details on replication.

The reduced growth in the presence of nZVI at concentrations between 2 x 10^{-5} M to 5 x 10^{-3} M (1.59 – 320.28 mg/L) is consistent with previous studies of nZVI cytotoxicity under deaerated conditions (see Table 2 and Table 3 for literature summary). A 3-log reduction in viable *E. coli* was observed when exposed to 1.61 x 10^{-4} M nZVI (9 mg/L) under deaerated conditions in a 2 mM carbonate buffer solution (Lee et al. 2008), which is consistent with the strong adverse effect observed at 2 x 10^{-4} M nZVI reported here. Similarly, a 5-log reduction in *E. coli* was observed when exposed to 1.79 x 10^{-3} M

(100 mg/L) nZVI in a 5 mM carbonate buffer solution (Li et al. 2010), which is consistent with the strong adverse effect seen at 2 x 10^{-3} M (160.2 mg/L) and 5 x 10^{-3} M (320.28 mg/L) nZVI.

However, the previous investigations of nZVI with *E. coli* examined of the adverse effects on non-growing cells rather of actively-growing cultures. Thus, while the effective concentrations are consistent, the results presented here suggest that *E. coli* continues to grow when exposed to concentrations between 2 x 10^{-4} M and 5 x 10^{-3} M nZVI, though the yield is reduced compared to a biotic control. The ability of *E. coli* to grow in the presence of nZVI is similar to mixed cultures (Barnes et al. 2010a; Barnes et al. 2010b; Xiu et al. 2010), and may be the result of the complex solution chemistry in the presence of nZVI or the ability of the organisms to adapt to stressors. The solution chemistry in the presence of nZVI will be discussed in more detail later in this chapter.

Effect of nZVI Age on E. coli Growth

The effect of aging on growth was observed by comparing 2-day aged and 28-day aged nZVI, as shown in Figure 11. The relative growth of *E. coli* was not significantly reduced in the presence of nZVI age at concentrations below 1 x 10^{-4} M nZVI with the 28-day aged nZVI, while a moderate level of inhibition was observed with the 2-day aged nZVI (~0.5 relative growth). Above 1 x 10^{-4} M nZVI, the relative growth in the presence of both the 2-day and 28-day aged nZVI was similar, including the strong effect observed at 2 x 10^{-4} and 5 x 10^{-3} M nZVI. The convergence of the 2-day and 28-day aged curves at concentrations above 1 x 10^{-4} M nZVI suggests that the observed reduction in growth is not the result of particle-bacteria interactions or that the transformations that occur during nZVI aging effect only a small percentage of the total surface area.

Previous studies found that exposing nZVI to oxygen reduced the adverse effects when *E. coli* were exposed to 9 mg/L (Lee et al. 2008) and 700 mg/L (Auffan et al. 2008). The results presented here examine the aging of nZVI under anaerobic conditions and suggest that the surface may not be fully transformed to an oxidized solid phase, and that nZVI may retain the ability to control solution chemistry at sufficient concentrations. When aged under anaerobic conditions, other nZVI samples have a report half-life of weeks to months (Liu and Lowry 2006; Li et al. 2010) , so it is also possible that the inhibitory effect may be reduced at higher concentrations if longer aging were allowed.

Effect of $FeCl_2$ on E. coli Growth

E. coli growth in the presence of ferrous iron was also investigated, as shown in Figure 12, plotted with the relative growth in the presence of 2-day aged nZVI. Relative growth was not reduced in the presence of $FeCl_2$ at concentrations below 10^{-4} M $FeCl_2$ added, and it is possible that additional ferrous iron enhanced growth at low concentrations. Conversely, when 10^{-3} M $FeCl_2$ was added, no viable cells were present after 24 hours.

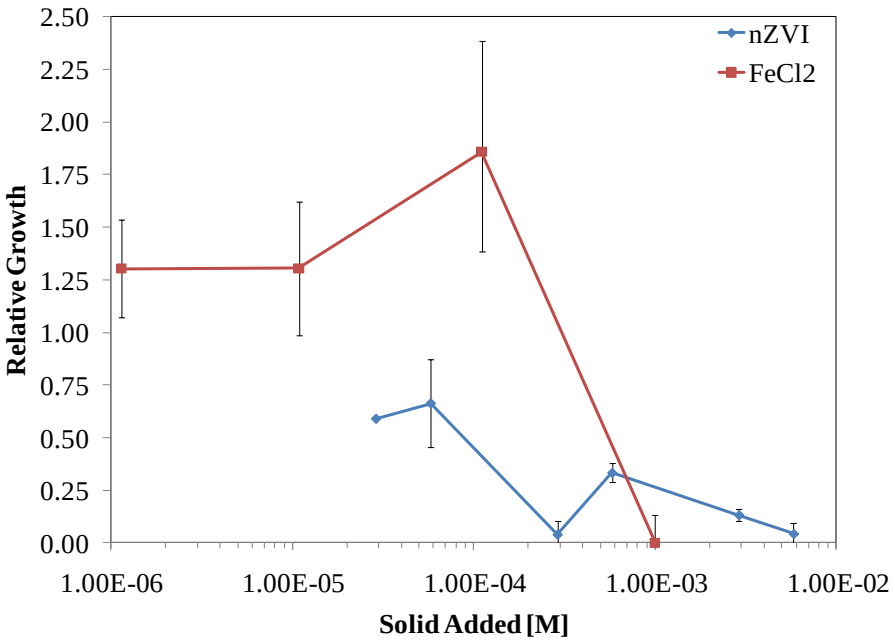

Figure 12. 24 Hour Relative Growth of *E. coli* in the Presence of nZVI and $FeCl_2$ as a function of solid added. Error bars are the standard deviation of biological replicates (*n*=3) in the same experiment (nZVI) and standard deviation of biological replicates (*n*=2) in the two experiments ($FeCl_2$). See Table 14 and Table 16 for additional details on replication.

Comparing the relative growth in the presence of nZVI and $FeCl_2$ may provide insight into the role of ferrous iron in the adverse effect of nZVI. The region of no-effect for $FeCl_2$ overlays the region of effect for nZVI (on a $[Fe]_T$ basis), suggesting that ferrous iron may not be involved in the reduced growth observed in the presence of nZVI below 1×10^{-4} M. However, the similarity in the observed relative growth at higher concentrations suggests that ferrous iron may important when the concentration of nZVI is greater than 1×10^{-4} M nZVI.

A 3-log reduction in *E. coli* was observed when exposed to 10^{-4} M $FeSO_4$ under deaerated conditions in a 2 mM carbonate buffer solution (Lee et al. 2008), an order of magnitude lower than the observed in this study. The generation of intracellular ROS is

suggests as a possible mechanism for Fe (II) inactivation of *E. coli* (Lee et al. 2008), though no experimental evidence was presented to support this assertion. It is possible that the complex solution chemistry of the current system reduces the free-ion concentration necessary produce ROS. Modeling the solution composition in the presence of nZVI and $FeCl_2$ can determine the effect of complexation on the free iron concentration and may provide insight into the species responsible for the observed adverse effect.

Equilibrium Modeling of nZVI and $FeCl_2$ Exposure Systems

The equilibrium speciation in the presence of nZVI and $FeCl_2$ was estimated using PHREEQC modeling software (Parkhurst, Appelo, and Geological Survey (US) 1999). The results of speciation modeling allow some generalization about the effect of increasing nZVI and $FeCl_2$ on the solution chemistry within the microbial growth medium. The model parameters selected for discussion here are based on the hypothesis that the observed reduced growth may be related to electron activity (pe), iron speciation (Fe^{2+} and Fe(EDTA)), or availability of trace metals in solution ($[Me]_T/[Me]_{GM}$).

Model Calibration. The model-predicted solution pH between 6.86 and 8.3 for nZVI and $FeCl_2$ concentrations between 2×10^{-5} and 5×10^{-3} M nZVI and 1×10^{-6} and 1×10^{-3} M $FeCl_2$ is generally consistent with the observed pH experimentally, which was always between 6.3 and 7.5 as measured by pH-paper. The modeling assumption that abiotic reduction of sulfate to sulfide would not take place within 24 hours of nZVI exposure was verified experimentally, as shown in Figure 13. At the highest concentration of nZVI added, 2.83×10^{-3} M nZVI, the reduction in sulfate was only 20%. The speciation model was run without considering the abiotic reduction of sulfate based on these results.

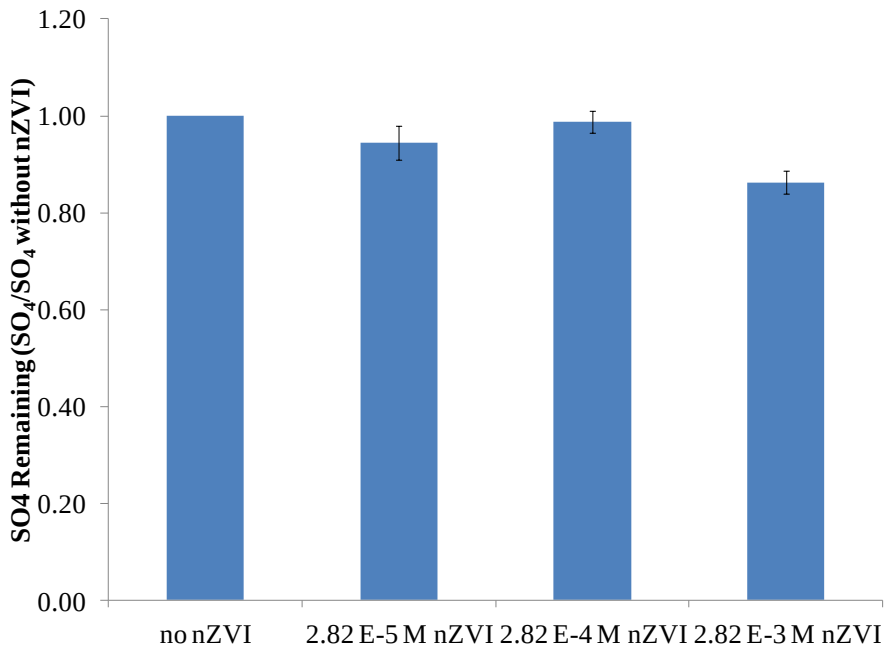

Figure 13. Fraction of sulfate remaining after 24 hours in the presence of nZVI in the microbial growth medium. Error bars represent the standard deviation of experimental replicates (*n*=2).

Electron Activity. The predicted value of the electron activity (pe) in the microbial growth solution as a function of nZVI or $FeCl_2$ added is shown in Figure 14 in open symbols and plotted on the secondary y-axis, with relative growth also plotted in close symbols on the primary y-axis for comparison. In the presence of nZVI, pe is below -6 (E_h = -354 mV) and falls to -9 (E_h = -531 mV) at the highest concentrations. The pe in the presence of nZVI is controlled by the corrosion of Fe^0. In the presence of $FeCl_2$, the pe is higher through the entire region studied, but does fall from -2.9 (E_h = -171 mV) to -5.5 (E_h = -324 mV), coinciding with the reduction in relative growth. The pe in the $FeCl_2$ model is controlled by the precipitation of solid phases, specifically $CoFe_2O_4$, that control the total Fe(II) and Fe(III) in the system. The precipitation of solid phases is discussed in greater detail later in this chapter.

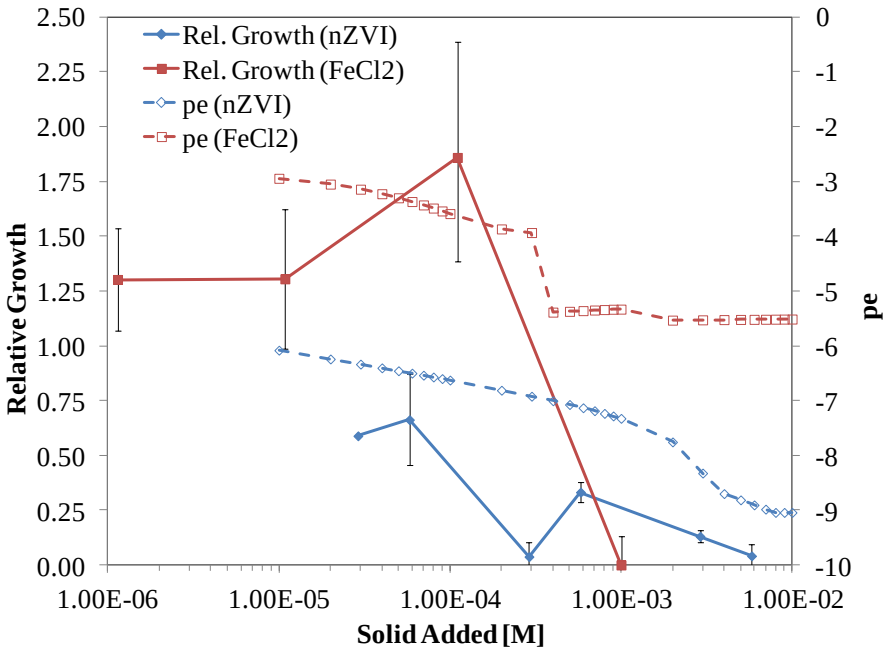

Figure 14. Equilibrium redox potential as predicted by PHREEQ Model in the presence of nZVI and $FeCl_2$.

Decreasing solution pe can change the structure and function of cytoplasmic membranes or the metabolism of *E. coli*. The permeability of protons within the cytoplasmic membrane, which can modify the internal pH and the ΔpH of the membrane, is sensitive to electron activity (Riondet et al. 1999). The ratio of fermentation produces in *E. coli* fermentating glucose is also affected by electron activity, and electron activity also regulates enzyme activity and acetyl-CoA affecting energy generation and biomass synthesis (Riondet et al. 2000). *E. coli* growth under glucose fermentation conditions may reduce the pe to -10.1 (E_h = -600 mV) alone, suggesting that the magnitude of electron activity induced by nZVI or $FeCl_2$ may not be the cause of reduced growth as much as the presence of a redox-regulating phase (Bagramyan and Trchounian 1997; Bagramyan, Galstyan, and Trchounian 2000).

Iron Speciation. The predicted concentration of iron (II) associated with specific ligands in the microbial growth solution as a function of nZVI or $FeCl_2$ added is shown in Figure 15 and Figure 16, respectively. Fe(II)-EDTA complexes are predicted to be the dominant form of Fe(II) below 2 x 10^{-3} M nZVI or $FeCl_2$ added. In both systems, Fe^{2+} becomes the dominant species at $[Fe]_{added} > 3 \times 10^{-3}$ M, when the EDTA in the growth medium is fully-complexed. The concentration of Fe(II) in complexes with phosphate in solution is very similar to the concentration of ferrous iron until the 10^{-3} M nZVI or $FeCl_2$ added when vivianite ($FePO_4$) is predicted to precipitate from solution.

Increasing concentrations of iron in solution may upset the iron homeostasis within cells, causing a number of biological and chemical reactions to occur. High concentrations of ferrous iron within the cells can lead to ferrous iron-mediated generation of reactive oxygen species (ROS), even under anaerobic conditions ()(Duesterberg, Cooper, and Waite 2005). The generation of ROS has been suggested in the literature as a possible mechanism of nZVI cytotoxicity (Lee et al. 2008; Auffan et al. 2008; Kim et al. 2010). Previous studies suggest that the production of intracellular oxidants including hydroxyl radicals (·OH) or ferryl ions (Fe(IV)) produced by the reaction of Fe^{2+} with hydrogen peroxide may be responsible for inactivation and inhibition (Kim et al. 2010).

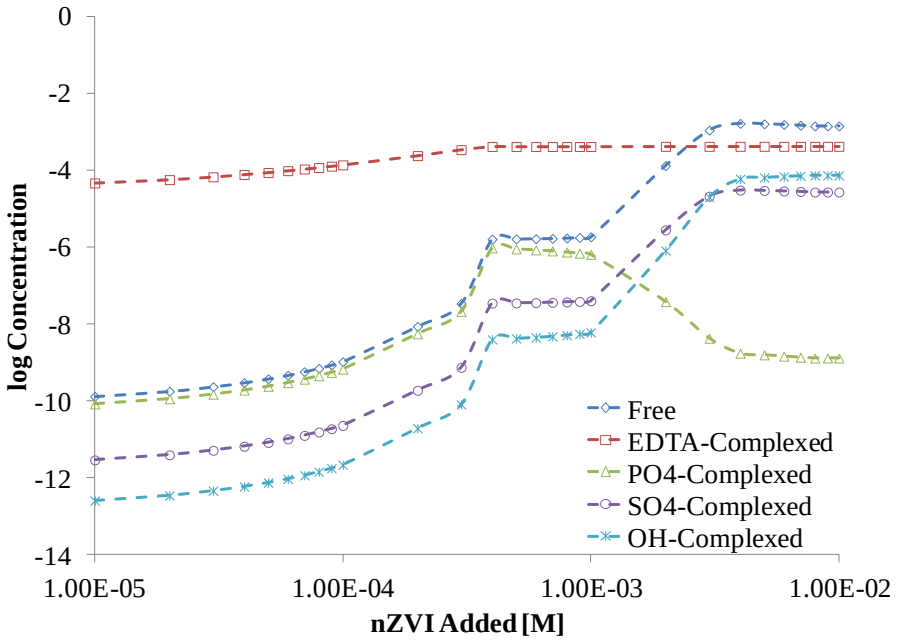

Figure 15. Predicted association of Fe(II) with ligands in the microbial growth medium as a function of nZVI added.

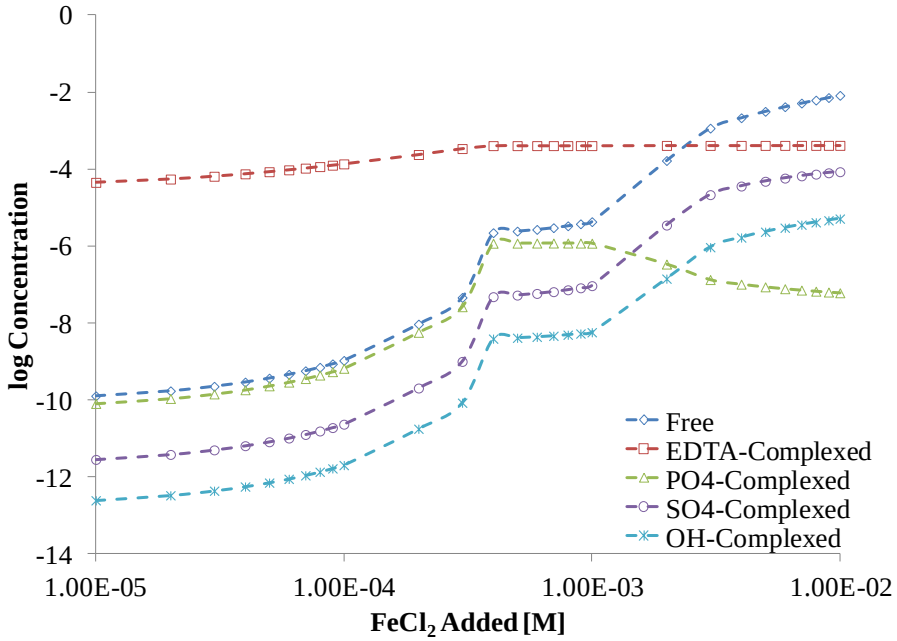

Figure 16. Predicted association of Fe(II) with ligandsin the microbial growth medium as a function of $FeCl_2$ added.

Availability of Trace Metals. The saturation indices for select solid phases are presented in Figure 17 and Figure 18, with the saturation index plotted as function of nZVI or $FeCl_2$ added, respectively. The saturation index, defined as the the logarithm of the dissolution reaction constant for a solid phase, describes the saturation relative to equilibrium with a SI < 0 indicating undersaturation and SI = 0 indicating that the solution is in equilibrium with that solid phase. In the both systems, the model predicts the precipitation of $MnHPO_4$, $CoFe_2O_4$, hydroxylapatite $Ca_5(PO_4)_3OH$ and vivianite $Fe_3(PO_4)_2$ from solution as a function of nZVI or $FeCl_2$ added. In both systems, the formation of $MnHPO_4$ is predicted, until total iron concentrations in the system exceed the solubility for vivianite, at which point Mn(II) is returned to solution. The different behavior in the two systems at high concentration is due to a slightly different pH trend; nZVI tends to increase the pH (final pH = 8.46) while $FeCl_2$ tends to decrease the pH (final pH 6.65). The saturation indices suggest that manganese concentration in solution varies with the addition of nZVI and could be related reduction in growth observed in toxicity experiments.

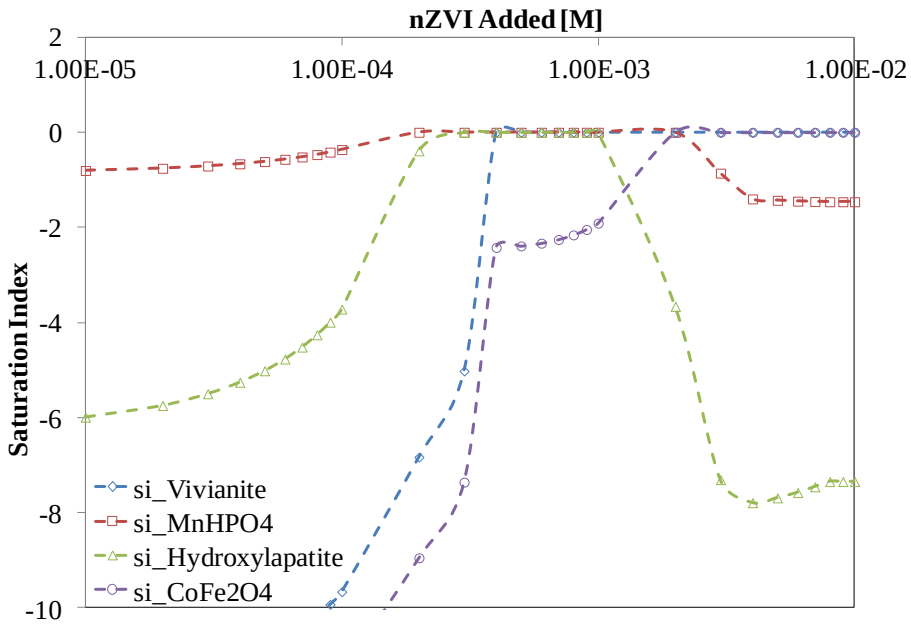

Figure 17 Predicted saturation indices in the microbial growth medium as a function of nZVI added.

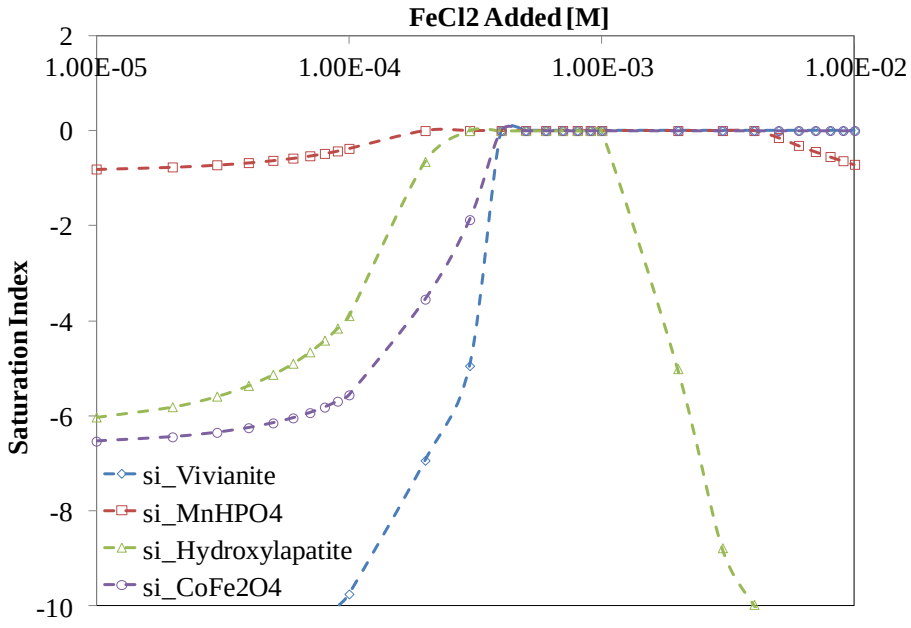

Figure 18 Predicted saturation indices in the microbial growth medium as a function of $FeCl_2$ added.

The predicted dissolved fraction of added manganese in the microbial growth solution as a function of nZVI or $FeCl_2$ added is shown in Figure 19 in open symbols and plotted on the secondary y-axis, with relative growth also plotted on the primary y-axis. The fraction of available manganese in solution goes to 0.01 at 4 x 10^{-4} M nZVI or $FeCl_2$ added but returns to solution beginning at 2 x 10^{-3} M nZVI or $FeCl_2$ added. The speciation model predicts the formation $MnHPO_{4(s)}$ and reduction of manganese in the presence of both nZVI and $FeCl_2$ at concentrations where relative growth also decreased, possibly indicating the importance of manganese in *E. coli* growth.

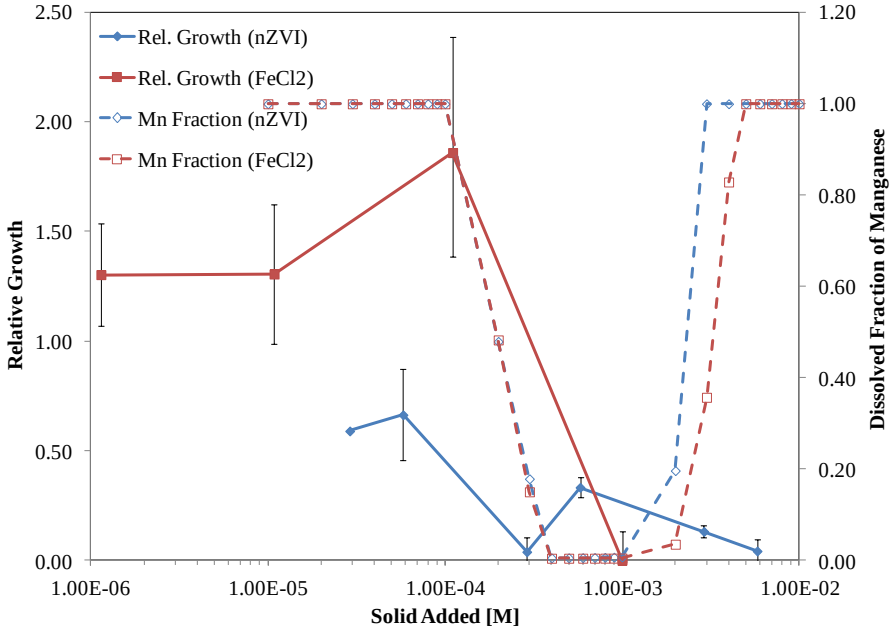

Figure 19. Predicted dissolved fraction of manganese in the microbial growth medium as a function of nZVI or $FeCl_2$ added plotted with the 24 hour relative growth of E. coli in the present od nZVI or $FeCl_2$.

Manganese plays an important role in cellular processes including defenses against oxidative stress (Schiavone and Hassan 1988; Horsburgh et al. 2002). Manganese superoxide dismutase (MnSOD) is one of three superoxide dismutase enzymes in *E. coli*

and though production is generally repressed under anaerobic growth conditions, it is possible that external oxidants or the oxidation of ferrous iron may induce biosynthesis (Schiavone and Hassan 1988). There is also some evidence that *E. coli* and other bacteria may accumulate manganese for an alternative catalytic scavenging of superoxide or hydrogen peroxide (Horsburgh et al. 2002).

Implications for the Use nZVI for Environmental Remediation

The results presented in this chapter show that exposure to nZVI under anaerobic conditions reduced the growth of *E. coli* and that increasing nZVI in solution will likely reduce the electron activity, increase the concentration of ferrous iron, and change the availability of metals. Though the microbial growth medium used in this study is more complex than a typical groundwater, it highlights some important considerations when applying nZVI for groundwater remediation. First, the effect of nZVI on growing organisms seems to be less severe than the effect on organisms in a non-growth state. This has been previously reported with mixed cultures (Barnes et al. 2010a; Barnes et al. 2010b), but appears to also be true for pure cultures. Though soil bacteria are not growing in a rich growth medium, there may be resistance to nanoparticles that is not obtained in non-growth studies. Second, it is likely that the presence of redox-sensitive elements in the groundwater solution and the changing chemistry downstream of an installed nZVI barrier will be the dominant concern for ecotoxicity, rather than the direct interactions between nZVI and microorganisms.

Chapter 6

Effect of Iron Sulfide Nanoparticles on *Escherichia Coli* under Anaerobic Growth Conditions

Introduction

Iron sulfide minerals occur naturally, some in nanoparticulate phases, in anoxic environments including deep-ocean hydrothermal vents (Rickard and Luther 2007) . Iron sulfide minerals have been identified as reaction products in zero-valent iron permeable reactive barriers (Wilkin et al. 2005), and have an affinity for many common groundwater contaminants including trichloroethylene and tetrachloroethylene (Butler and Hayes 1999) and arsenic (Gallegos, Hyun, and Hayes 2007), which led to the development of mackinawite, iron (II) monosulfide, as a reactive medium for groundwater remediation (Han et al. 2011). FeS can be synthesized in the laboratory as a nanocrystalline solid with particle dimensions in the nanometer range (Jeong, Lee, and Hayes 2008) and can be applied as a coating to sand grains to form granular reactive media for emplacement into the subsurface (Han et al. 2011). After emplacement in the subsurface, the reactive medium may cause local environmental impacts associated with the release of nanoparticles or dissolution products into the surrounding environment.

Under naturally-occurring solution conditions, FeS nanoparticles are known to form stable suspensions with a primary particle size in the nanometer range (Lee 2009). FeS is also known to dissolve at low- to medium-ionic strength conditions and near-neatural pH to release ferrous ions and bisulfide ions into solution (Rickard 2006). Both the presence of stable nanoparticle solutions and the release of ferrous and bisulfide ions raises questions about the potential toxicity of FeS reactive medium under the anaerobic conditions found in subsurface barriers.

The potential toxicity of nanoparticles has been under investigation for the last few years using a variety of model organisms and nanoparticles in laboratory and environmental matrices. *Escherichia coli* is often used in bacterial toxicity studies as a model gram-negative microorganism (Klaine et al. 2008). *E.coli* toxicity to a variety of nanoparticles has been investigated including metal oxides (Zhang et al. 2007; Thill et al. 2006; Adams, Lyon, and Alvarez 2006), nano-silver (Sondi and Salopek-Sondi 2004; Morones et al. 2005; Fabrega et al. 2009), zero-valent iron (Han et al. 2011), and quantum dots (Mahendra et al. 2008; Dumas et al. 2010). These studies have shown that *E. coli* is inactivated and/or inhibited by a variety of nanomaterials at different concentrations. The general mechanisms of nanoparticle toxicity that are suggested in the literature include adsorption/membrane disruption, generation of reactive oxygen species, and production of toxic ions (Klaine et al. 2008). The specific mechanism may be dependent on the size of nanoparticles, the solution chemistry, the duration or exposure, and the number of bacteria exposed.

Though the toxicity of iron sulfide nanoparticles has not been studied, the toxicity of zero-valent iron nanoparticles (nZVI) and other reduced iron-containing has been

evaluated in the literature (Lee et al. 2008; Auffan et al. 2008; Li et al. 2010) and in the previous chapter of this dissertation. The results suggest that nZVI is toxic to *E. coli*, under deaerated and aerobic conditions at concentrations around 10 mg/L (1.8E-4 M) under deaerated conditions and around 100 mg/L (1.8E-03 M) under aerobic conditions(Lee et al. 2008; Auffan et al. 2008; Li et al. 2010) . The most likely mechanism of toxicity is the release of ferrous ions to solution and acute oxidative stress (Lee et al. 2008), supported by the lack of toxicity observed with higher-valent iron solid phases (Auffan et al. 2008). The likely reason for greater toxicity under deaerated conditions is a lack of oxygen to passivate the nZVI surface during exposure. Reports on the toxicity of nZVI to actively growing mixed communities suggest that the toxicity may be less if microorganisms are in a growth state (Barnes et al. 2010a; Barnes et al. 2010b). Evidence from the study of nZVI toxicity suggests that FeS may have a negative effect on *E. coli*, and may release of ferrous ions and lower the electron activity in solution.

The objective of this chapter was to understand the effect of iron sulfide (FeS) nanoparticles on the growth of *E. coli* under anaerobic growth conditions. The stability of iron sulfide nanoparticles in the growth medium was examined as a function of particle concentration, to understand the potential effect of nanoparticle aggregation or dissolution. The effect of FeS nanoparticles was compared with the effect of Na_2S and $FeCl_2$ under the same conditions to investigate potential toxicity of dissolution ions. The results are also interpreted relative to nZVI toxicity experiments conducted under similar conditions to investigate a possible environmental advantage for groundwater remediation using FeS nanoparticles. These results could be used in combination with

information on the particle mobility in the subsurface to determine the potential for adverse effects from nanoparticle emplacement for permeable reactive barriers.

Results and Discussion

FeS Dissolution and Solubility in Microbial Growth Medium

The dissolution of FeS in the microbial growth medium over twenty four hours is presented in Figure 20. The fraction of FeS added, calculated as the difference of the iron before and after centrifugation is plotted as a function of time. The solid phase concentrations did not change after 3 hours of reaction in microbial growth medium for all concentrations tested. FeS added at concentrations of 2×10^{-4} and 2×10^{-5} M did not result in measurable particulate FeS after 24 hours in the microbial growth medium. However, when 2.0×10^{-3} M FeS was added, there was 83% particulate FeS remaining after 24 hours.

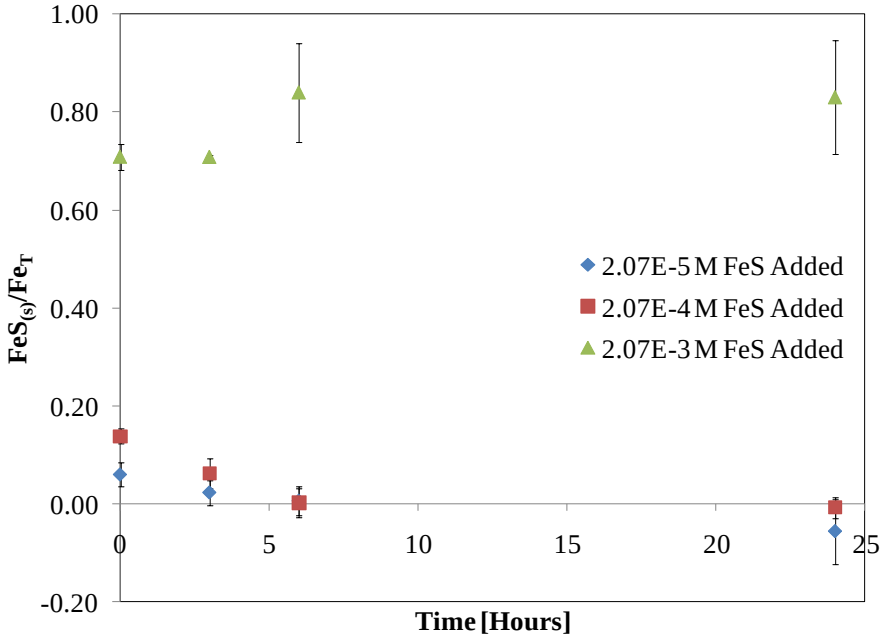

Figure 20. Dissolution of FeS in the microbial growth medium, plotted as solid fraction as a function of time. Error bars represent the standard deviation of replicates (*n*=2).

To further evaluate the thermodynamic solubility of FeS in the microbial growth medium, the 24-hour solubility was determined as a function of FeS added. The dissolved Fe concentration is plotted as a function of FeS added in Figure 21. The experimental results were compared with PHREEQC equilibrium speciation model results for the same concentrations of FeS added, shown as the dashed line. FeS solubility in the microbial growth medium is 6.0×10^{-4} M FeS as determined by the average of experimental values. The PHREEQC speciation model prediction is very similar to experimentally obtained value, with solubility predicted as 4.1×10^{-4} M FeS. The experimental values may over-predict solubility because of difficulty separating particulate iron from dissolved iron, especially as the nanoparticles partially dissolve and become even smaller.

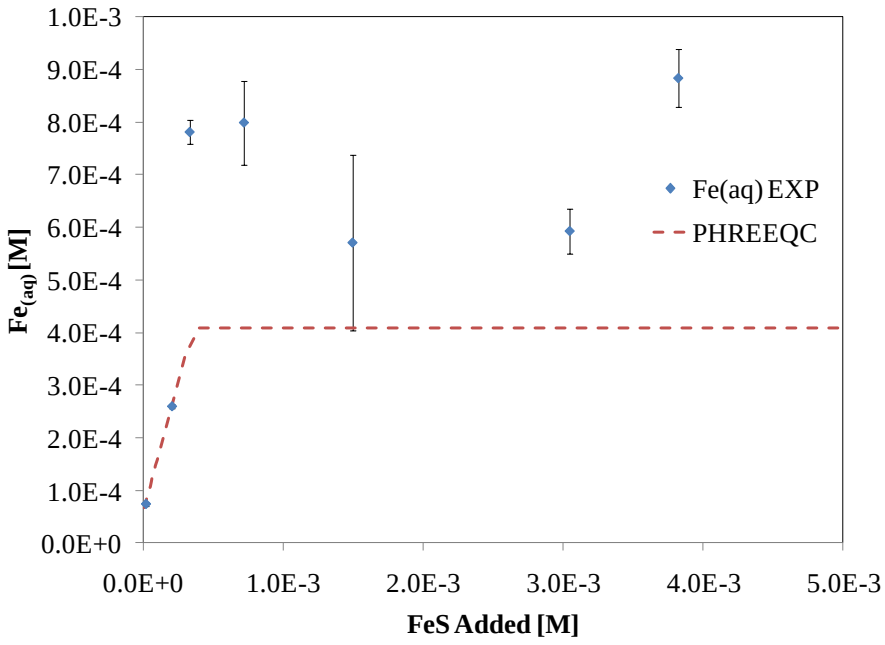

Figure 21. Solubility of FeS in the microbial growth medium. $[Fe]_T$ as a function of FeS added. Error bars represent the standard deviation of replicates (n=2).

The dissolution of FeS in the microbial growth medium reduced the exposure concentrations of FeS and introduced ferrous iron and sulfide ions to the solution. The aqueous concentrations were nearly constant within three hours and therefore the chemistry of the system was likely stable during 24 hour inhibition experiments. The solubility of FeS in the microbial growth medium allowed for the effect of particle presence to be tested within the range of 6 $x10^{-4}$ M to 10^{-3} M FeS added, and the effect of dissolution products below 6 $x10^{-4}$ M FeS. Finally, the agreement of experimental data and PHREEQC model suggests that the equilibrium model is appropriate for the description of the solution chemistry in this system.

Effect of FeS and Na_2S on E. coli Growth

The growth of *E. coli* was reduced in the presence of 2.7 x 10^{-5} M – 5.3 x 10^{-3} M (2.3 – 463 mg/L) FeS, as shown in Figure 22. The growth in the presence of FeS relative to the growth in a negative control reported as a fraction is presented as a function of FeS added. There was no significant difference in relative growth above or below FeS solubility (6 x 10^{-4} M FeS indicated with a dashed line). Furthermore, relative growth did not decrease above solubility, though concentration of FeS in solution increases by an order of magnitude.

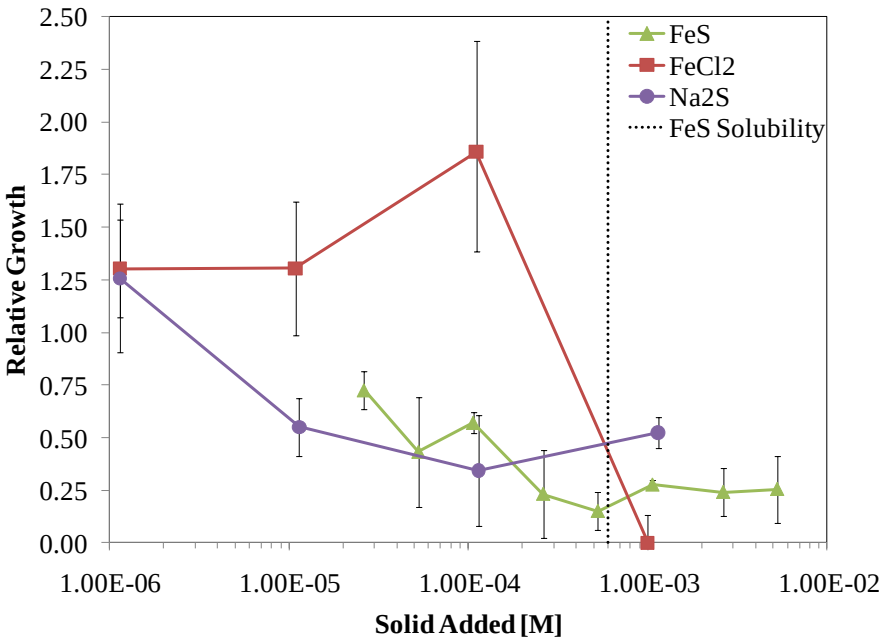

Figure 22. Comparison of the 24 hour relative *E. coli* growth in the presence of FeS, Na_2S and $FeCl_2$. Error bars represent the standard deviation of biological replicates (*n*=3) in two experiment (FeS), the standard deviation of biological replicates (*n*=2) in three experiments (Na_2S), and the standard deviation of biological replicates (*n*=2) in two experiments ($FeCl_2$). See Table 17, Table 18, and Table 16 for additional details on replication.

E. coli growth in the presence of Na_2S is also shown in Figure 22. Relative growth was reduced at concentrations greater than 10^{-6} M Na_2S added. The adverse effect observed did not vary with concentration from 10^{-5} M to 10^{-3} M Na_2S added. The growth of *E. coli* in the presence of Na_2S and FeS was similar below the FeS solubility, which suggests that the presence of dissolved sulfide may be responsible for the observed effect on growth. Above solubility, FeS had slightly stronger effect, possibly due to the concentrations of sulfide and iron that are predicted to be in equilibrium with FeS. The relative growth in the presence of FeS above solubility was between the relative growth observed in the presence of Na_2S and $FeCl_2$. FeS may have a lower adverse effect when

compared with Fe(II) on an equimolar basis because FeS controls the concentrations of Fe(II) and S(II) in solution.

Though FeS toxicity to microorganisms has not been previously tested the effect of nZVI, Fe(II)-solids, and sulfide have been reported. Under deaerated conditions nZVI significantly inactivates *E. coli*, up to 5 log-reduction during 60 minutes of exposure to 100 mg/L (Li et al. 2010), and can reduce growth of mixed cultures in natural samples (Barnes et al. 2010a). The effect of Fe_2O_3 on *E. coli* depends on the exposure concentration and conditions, with no effect of 9 mg/L under deaerated conditions (Lee et al. 2008) and up to 80% inactivation under aerobic conditions at 700 mg/L (Auffan et al. 2008). An important consideration in whether a solid can induce ROS is the coordination and structure of Fe, and reports suggest that the FeS structure may support the generation of ROS (Berglin and Carlsson 1985). The presence of sulfide and interactions with trace metals may also be important in the presence of FeS (Caffrey and Voordouw 2010).

Equilibrium Modeling of FeS and Na_2S Exposure Systems

The equilibrium speciation in the FeS and Na_2S exposure systems was determined using PHREEQC modeling software. Similar to the previous chapter, the parameters selected for discussion were based on hypothesis that mechanism may be related to redox potential (pe), iron speciation ($[Fe^{2+}]$ and [Fe(EDTA)]), or availability of trace metals in solution ($[Me]_T/[Me]_{GM}$).

Electron Activity. The predicted value of the electron activity (pe) in the microbial growth solution as a function of FeS or Na_2S added is shown in Figure 23 in open symbols on the secondary y-axis with the inhibition data plotted in closed symbols on the primary axis. In the FeS system, reducing conditions prevail throughout the range of FeS-added studied staying in the range of with the pe = -3.7 (E_h = -218 mV). The pe

in the presence of FeS is controlled by the S(II)/S(VI) couple with S(II) from FeS and S(VI) from the microbial growth medium. In the presence of Na_2S, the pe is higher below 10^{-5} M Na_2S but falls to -3.7 (E_h = -218 mV) around 10^{-5} M Na_2S. The pe in the presence of Na_2S is also controlled by the S(II)/S(VI) couple. The similarity in predicted pe may be the reason for the similarity in relative growth over the concentration range from 10^{-5} to 10^{-3} M FeS or Na_2S added (on a $[S]_T$ basis).

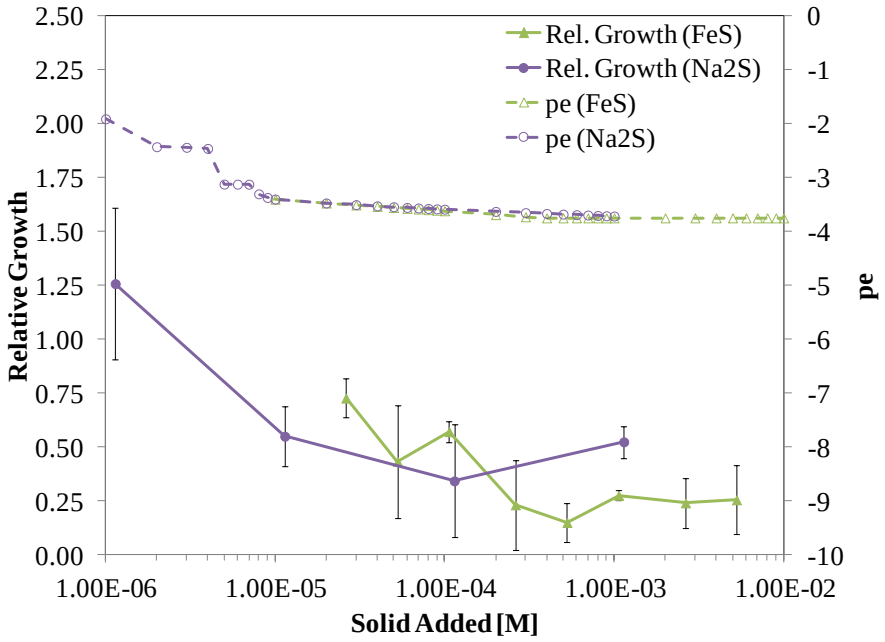

Figure 23. Predicted pe as a function of FeS or Na_2S added plotted with 24 hour relative growth of E. coli in the presence of FeS and Na_2S.

Availability of Trace Metals. The speciation model run in the presence of both the FeS and Na_2S predicts the formation of metal sulfide phases that will reduce the concentration of trace nutrients in the microbial growth solution. The dissolved metal fraction as a function of Na_2S added is shown in Figure 24. As the sulfide concentration increases, the nearly all trace metal nutrients are predicted to precipitation as sulfide

solids. Copper and molybdenum are removed at total sulfide concentrations below 10^{-5} M, suggesting that they are not of primary concern in the inhibition of *E. coli*. Zinc and cobalt are removed between 10^{-5} M S(-II) and 10^{-3} M S(-II), suggesting that they are related to the observed inhibition. It is not clear what specific function zinc and cobalt may serve in the metabolism of E. coli under glucose fermentation conditions, but as the trace metals with the highest concentration in the growth medium they may be providing addition micronutrients that are necessary for growth.

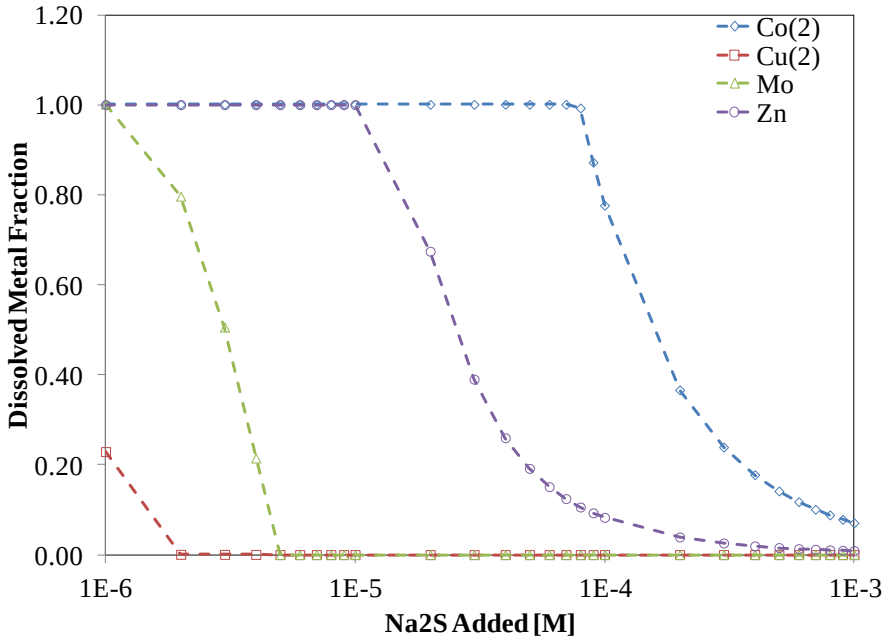

Figure 24. Predicted dissolved metal fraction as a function of Na_2S added to the microbial growth medium.

Comparison of FeS and nZVI Exposure under Anaerobic Growth Conditions

Comparing the relative growth of *E. coli* exposed to nZVI and FeS under anaerobic growth conditions can provide insights into whether the environmental impact on the soil microbial population could be reduced by using FeS reactive media for *in situ*

remediation. The growth of *E. coli* in the presence of nZVI or FeS is presented in Figure 25 as the relative growth as a function of solid added on a molar basis. Relative growth is similar over the range of molar concentrations studied, 2 x 10^{-5} M to 5 x 10^{-3} M $[Fe]_T$. The molar volumes of FeS (21.4 cm^3/mol) (Wolthers, Van der Gaast, and Rickard 2003) and nZVI (8.33 cm^3/mol) (Tratnyek and Johnson 2006) suggest that for equimolar concentrations of FeS and nZVI, the volume of FeS in solution will be 2.6 times greater than nZVI. The bimodal trend as function of nZVI added is not present in the FeS data, as the relative growth in the presence of FeS shows a single trend, leveling off above the solubility in the microbial growth medium. The lack of strong adverse effect in the FeS exposure may be due to lower dissolved ferrous iron concentrations in the presence of FeS.

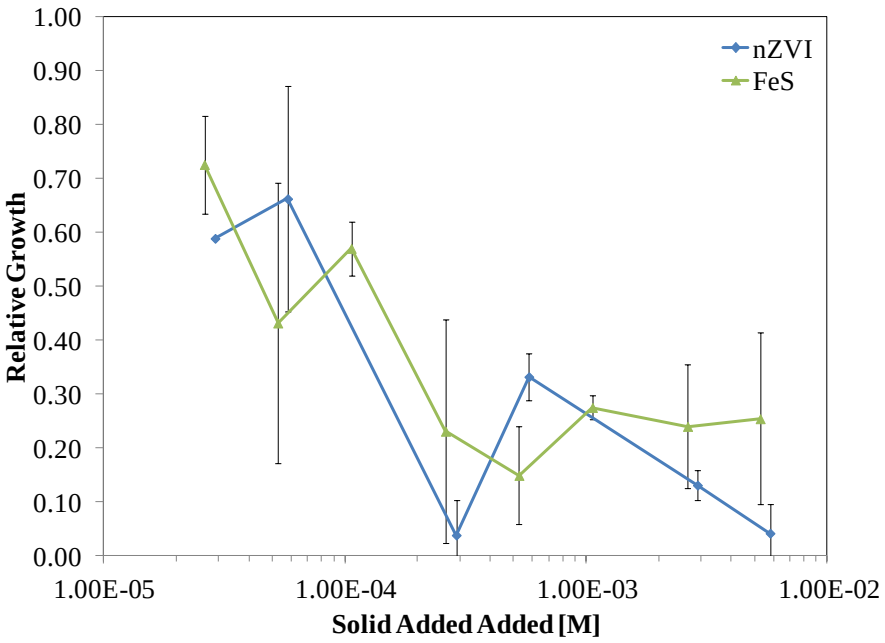

Figure 25. Comparison of 24 hour relative growth of *E. coli* in the presence of nZVI and FeS as a function of solid added.

The effect of nZVI and FeS on the solution chemistry can provide some insight into the possible advantages of FeS in remediation applications. First, the electron activity is significantly lower in the nZVI system when compared with the FeS system, consistent with the more reduced state of nZVI, suggesting that any effect of the electron activity on *E. coli* growth is expected to be greater in the nZVI system than in the FeS system. Second, the ferrous iron concentration is significantly higher in the nZVI system when compared with the FeS system, such that any effect of the ferrous iron concentration on *E. coli* growth will be greater under nZVI exposure than FeS exposure, because FeS solubility reduces the ferrous iron concentration to below the EDTA-complexable concentration. Finally, the prediction of reduced trace nutrient availability is similar in the two systems, with reduced available manganese in the presence of nZVI and reduced trace nutrient availability in the presence of FeS.

Chapter 7

Conclusions

Introduction

This dissertation was aimed at understanding the global and local environmental impacts of *in situ* groundwater remediation with reduced iron reactive media. In particular, the research conducted emphasized the importance of the geochemistry of reduced iron reactive media, as it relates to environmental performance and impacts. The major conclusions from this research are summarized in this chapter.

Contributions of this Dissertation

Life-Cycle Case Study Comparison

In situ groundwater remediation with permeable reactive barriers has been in use for more nearly twenty year (Wilkin, Puls, and Sewell 2003), treating a variety of contaminants. These systems operate without the addition of energy during the use phase, which is an environmental benefit to choosing an *in situ*, passive technology. However, energy demand during use phase was not adequate to characterize the environmental performance of the technology relative to alternatives due to the high material demand during construction. This dissertation compared a pump-and-treat

system with a permeable reactive barrier in a life cycle assessment case study. Assuming a 10 year reactive media longevity, there was a significant environmental advantage for the PRB in the acidification, human health, and ozone depletion impact categories. Though the mean value was lower than the PTS, there was no significant advantage of the PRB in the global warming, eutrophication, or smog formation categories. Zero-valent iron reactive media contributed nearly 50% of the environmental impacts in every category for the PRB and electricity represented 90% of the PTS impacts. It was determined that the minimum longevity for the PRB to have a lower relative environmental benefit was ten years. This breakeven point provides a benchmark for the design and operation of PRBs with regard to environmental sustainability. These results suggest that further improvements in the design and construction of PRBs are necessary, and highlight the importance of the geochemistry of reduced iron media and longevity to environmental performance.

Effect of Zero-Valent Iron Nanoparticles on Bacterial Growth

Zero-valent iron nanoparticles can significantly enhance the reactivity when compared with granular zero valent iron (Zhang 2003), but may pose a threat to microorganisms in the subsurface or natural water bodies (Tratnyek and Johnson 2006). The toxicity of nZVI to microorganisms under aerobic and deaerated conditions has been reported when organisms are not in a growth state (Lee et al. 2008; Auffan et al. 2008; Li et al. 2010). However the effect of nZVI on pure cultures under anaerobic growth conditions was unknown. This dissertation presents the results of *E. coli* growth in the presence of nZVI under anaerobic conditions. *E. coli* growth was reduced in the presence of 2×10^{-5} M to 5×10^{-3} M nZVI with a bimodal distribution above and below 2

x 10^{-4} M nZVI. The comparison of 2- and 28-day aged nZVI suggests that the oxidation after 28-days was insufficient to passivate the nZVI surface such that the particle could not control solution composition at concentrations above 2 x 10^{-4} M nZVI. In both the 2- and 28-day aged experiments the bimodal distribution as a function of nZVI concentrations was obtained, suggesting that multiple mechanisms may be involved. The effect of $FeCl_2$ on *E. coli* growth under the same conditions showed no effect at concentrations below 10^{-3} M, while no growth was observed at 10^{-3} M $FeCl_2$.

Equilibrium speciation modeling was used to predict the solution chemistry in the presence of nZVI and $FeCl_2$, including solution pH, pe, iron speciation, and metal speciation. The pe was predicted to be below -5.5 in the presence of both nZVI and $FeCl_2$.The concentration of ferrous iron in solution increased in the presence of nZVI and $FeCl_2$, after full complexation of the EDTA in the microbial growth medium, Finally, the predicted concentration of manganese in solution varied as a function of nZVI added.

Inhibitory Effect of Iron Sulfide Nanoparticles

Iron sulfide nanoparticle based reactive media has been proposed for the remediation of arsenic-contaminated groundwater (Han et al. 2011). Iron sulfide coated sand may be generated in batch mode or nanoparticles may be introduced into an aquifer as a slurry and deposited on natural aquifer grains (Lee 2009). In either emplacement method, there is the possibility for particle release and the possible toxicity of FeS nanoparticles was unknown. This dissertation evaluated the growth of *E. coli* exposed to of FeS nanoparticles under anaerobic conditions. *E. coli* growth was reduced in the presence of 2 x 10^{-5} M FeS to 5 x 10^{-3} M FeS. The solubility of FeS in the microbial growth medium was determined to be 6 x 10^{-4} M FeS, indicating that the toxicity

experiments were conducted at concentrations where FeS was present as well as at concentrations where FeS completely dissolved to form ferrous iron and sulfide species in solution. No significant difference in the relative growth occurs as the solubility of FeS is exceeded, suggesting specific particle-*E. coli* interactions are not the cause of reduced growth. *E. coli* growth was also reduced in the presence of Na_2S at concentrations greater than 10^{-5} M Na_2S, with the magnitude of relative growth similar to the growth in the presence of FeS.

Equilibrium speciation modeling was used to predict solution chemistry in the presence of FeS and Na_2S, similar to previously described analysis with nZVI. The predicted electron activity (pe) in the presence of FeS or Na_2S was -3.7, controlled by the sulfate/sulfide redox couple. As a function of increasing sulfide concentration from 1 x 10^{-6} to 1 x 10^{-3} M Na_2S, the precipitation of copper, molybdenum, cobalt, and zinc sulfides are predicted, significantly reducing the availability of trace metals in the growth medium.

Comparing the effect of nZVI and FeS reveals that the pe was lower in nZVI systems (pe -3.7 compared to pe -6 to -9), suggesting that any adverse effects caused by the electron activity will likely be more severe in nZVI systems. The nZVI system also had higher concentrations of ferrous iron, which has been implicated in previous toxicity assessments. The availability of trace metals, for growth or cellular defenses, however is predicted in the presence of nZVI and FeS.

Recommendations for Future Work

This dissertation provides initial information on the global and local environmental impacts of *in situ* remediation with reduced iron reactive media. Recommendations for future work that would build on the conclusions here include:

1. **Examine the global environmental impacts of remediation using an FeS-coated sand permeable reactive barrier**. A model for the production of FeS-coated sand could be developed, and the use of FeS versus nZVI could be compared to investigate potential energy savings by using a less-reduced form of iron as reactive media.
2. **Examine the inhibitory effect of FeS and nZVI to natural soil microorganism in simulated groundwater matrix.** The most relevant inhibition experiment for understanding the effect of nanoparticulate reactive media is one with natural soil microorganism in natural or simulated groundwater solution. Such experiments would identify organisms sensitive to the inhibitory effects and better quantify the ecotoxicity of reduced iron reactive media.
3. **Examine the inhibitory effect of surface-modified FeS and nZVI to microorganisms.** Inhibitory effects based on specific particle-bacterium interactions can only occur in suspensions where nanoparticles are sufficiently stable. Comparing the results presented here with inhibition in the presence of stable particle suspensions may indicate the importance of nanoparticle-bacterium interactions.

Appendix A

Supplementary Material for Life-Cycle Case Study Comparison of Permeable Reactive Barrier versus Pump-and-Treat Remediation

Case Study Description

The aquifer underlying Dover AFB consists of approximately 36 to 38 feet of unconfined silty sand material above a silty clay aquitard (Kim et al. 1994; Gavaskar et al. 2000a). The hydraulic conductivity and gradient are low, resulting in a groundwater flow of 0.06 to 0.3 ft/day (Gavaskar et al. 2000a).

The life cycle assessment case study was conducted using design documents available from pilot-scale testing performed on-site (Kim et al. 1994; Gavaskar et al. 2000b; Gavaskar et al. 2000a). Design components were investigated to determine their material requirements and operating energy demand. These values were used to define design inventories for the treatment systems. Design inventories for the permeable reactive barrier (PRB) system and pump-and-treat system (PTS) are given in Table 8and Table 9, respectively. The quality of design inventory data was evaluated qualitatively and assigned a quality index, which was used in uncertainty analysis as described below. The design inventories were used as the input to the SimaPro LCA modeling software,

and the program created system inventories for the materials and energy necessary for each design.

Table 8: Design Inventory for Permeable Reactive Barrier System.

System Element	Quantity	Units	Quality Index
Gate Steel	9300	kg/gate	A
Gate Sand	37900	kg/gate	B
Gate Soil	21400	kg/gate	B
Gate Construction Energy	140	GJ/gate	C
Gray Cast Iron	24500	kg/gate	A
ZVI Construction Energy	42.7	GJ/gate	C
Funnel Steel	47800	kg	B
Funnel Cement	10300	kg	A
Funnel Construction Energy	241	GJ	C

Table 9: Design Inventory for Pump-and-Treat System.

System Element	Quantity	Units	Quality Index
Extraction Well PVC Pipe	40	kg/well	B
Extraction Well Cement	2000	kg/well	B
Extraction Well Gravel	330	kg/well	B
Extraction Well Steel (Pump)	50	kg/well	N/A
Extraction Well Construction Energy	2.3	GJ/well	C
Extraction Well Operation Energy	35.3	GJ/year-well	C
Catalytic Oxidation Unit Aluminum	50	kg	D
Catalytic Oxidation Unit Steel	50	kg	D
Catalytic Oxidation Unit Operating Energy	70.5	GJ/year	C
Air Stripping Unit Aluminum	110	kg	D
Air Stripping Unit HDPE	330	kg	C
Air Stripping Unit Steel (Blower)	50	kg	N/A
Air Stripping Unit Operating Energy	23.6	GJ/year	C
GAC Unit Steel	50	kg	A
GAC Unit GAC	180	kg	A
Treatment Facilities PVC Pipe	80	kg	B
Treatment Facilities Concrete	12100	kg	C
Treatment Facilities Steel	450	kg	D
Treatment Facilities Construction Energy	37.5	GJ	C

Life Cycle Assessment Methods and Assumptions

Life Cycle Assessment Assumptions. Throughout the assessment, assumptions were made to maintain focus on desired goals and limit time-consuming data collection, while providing transparency and clarity in results. Major assumptions or omissions and justification are presented in Table 10.

Table 10: Major Assumptions in Life Cycle Assessment.

Omission/Assumption	Justification
Life Cycle Framework	
The time horizon was set equal to 30 years.	Time horizons of 20, 30, and 50 years were evaluated and resulting trends were similar.
End-of-Life (EOL) processes were neglected.	The treatment on site, and the life of the treatment technology, is expected to continue beyond the 30 year study period. Generally, EOL activities for PRBs are very uncertain, due to limited information on long-term use or removal. EOL activities for the PTS would likely be minimal due to low materials influence.
The functional unit was set to treatment of 10 gallons per minute (gpm) for PRB and 20 gpm for PTS.	This unit has been used in economic comparisons of the technology and was the basis for full-scale designs.
Monitoring processes were neglected.	Monitoring activities were expected to be very similar for the two technologies. Optimization of monitoring strategy was outside scope of the study.
Permeable Reactive Barrier System Scope	
ZVI was modeled as gray cast iron.	Process-level inventory data for gray cast iron was readily available. The manufacturing processes for cast iron and ZVI are similar.
Steel caisson is regenerated and transported to the site for gate replacement.	The assumption represents a worst-case scenario.
Distance of transport between materials manufacturing and site was set equal to 100 miles.	Distances of 50, 100, and 200 miles were evaluated and resulting trends were similar.
Mode of transport was tractor-trailer truck.	The assumption represents a worst-case scenario.
Pump-and-Treat System Scope	
Reactor fabrication processes were neglected.	Significant uncertainty in process energy and material requirements exists. Based on the contribution of reactors to cost of 30-year operation (1) it was expected to have minimal contribution to system impacts.
High Density Polyethylene (HDEP) Pall-Ring packing manufacture was neglected.	Significant uncertainty in process energy and material requirements exists. Based on the contribution of air-stripping unit materials to cost of 30-year operation (1) it was expected to have minimal contribution to system impacts.
The catalyst production energy was set equal to 1000 kilowatt-hours (kWh) per installation.	The assumption represents a worst-case scenario. There was limited information on catalyst manufacturing due to proprietary concerns.
The pumps and blowers were modeled as 50 kilograms of steel.	Similar to Bayer and Finkel (4), this simplification expected to capture major impacts of these complicated design components.
The operating energy was assumed to be entirely electrical and was supplied by US electricity grid.	According to design documents, more than 99% of operating power was supplied by electricity (1).
Distance of transport between materials manufacturing and site was set equal to 100 miles.	Assumption was made to coordinate with PRB system assumption.
Mode of transport was tractor-trailer truck.	Assumption was made to coordinate with PRB system assumption.

TRACI Life Cycle Impact Assessment. Life cycle impact assessment was conducted using characterization factors from the United States Environmental Protection Agency's Tool for the Reduction and Assessment of Chemical and Other Environmental Impacts (TRACI). The impact categories used in the case study, associated units, and relevant TRACI characterization factors are presented in Table 11. The human health (HH) category for the case study used the characterization factors and units from the TRACI impact category for human health related to cancer.

Table 11: Impact Assessment Categories, Units, and TRACI Characterization Factors.

Impact Category	Units*	Characterization Factors
Global Warming (GW)	CO_2 eq.	Carbon dioxide=1; dinitrogen monoxide=3.0E+2; hexafluoroethane=1.2E+4; methane=23; dichloromethane=10; tetrachloromethane=1.4E+3; tetrafluoromethane=5.3E+3
Acidification (AC)	H+ eq.	Ammonia=95; Hydrogen chloride=45; Hydrogen Fluoride=82; Sulfur dioxide=51; Sulfur oxides=51;
Human Health (HH)	Benzene eq.	Arsenic=8.4E+3; Arsenic ion(W) =2.81E+2; Benzene=1; Beryllium=12; Cadmium=25; Cadmium Ion(W)=5.4E-49; Chromium=70; Chromium(W)=5.6E-46; Dioxins=3.1E+8; Dioxins(W)=2.3E+7; Fomaldehyde=3.6E-3; Lead=58; tetrachloromethane=9.0; Nickel=1.5
Eutrophication (EU)	N eq.	Ammonia-1.2E-1; Ammonium ion(W)=7.8E-1; BOD5(W)=5.0E-2; COD(W)=5.0E-2; Nitrate(W)=2.4E-1; Nitrogen oxides=6.9E-2; Phosphate (W)= 2.4;
Ozone Depletion (OD)	CFC-11 eq.	Tetrachloromethane=7.3E-1
Smog Formation (SF)	NOx eq.	Carbon monoxide=1.3E-2; Dichloromethane=1.9E-2; Formaldehyde=1.8; Methane=3.0E-3; Nitrogen Oxides=1; VOC=7.8E-1

*CO_2 = Carbon Dioxide; H+ = proton; N = Nitrogen; CFC-11 = trichlorofluoromethane ; NOx = Nitrogen Oxides.

IMPACT 2002 Life Cycle Impact Assessment. A second impact assessment method was used to examine the comparison of model PRB and PTS, and the IMPACT 2002+ model (Jolliet 2003) was specifically chosen because of the availability of normalization factors. Normalization allows the results of the impact assessment to be quantified such that the relative importance of each impact category can be determined.

The impact categories for the IMPACT 2002+ model are described in Table 12. There are a number of categories that are similar to TRACI, and some categories which are not included in the TRACI model, such as land occupation and ionizing radiation.

Table 12: Impact Categories for the Impact 2002+ Model

Category	Units
Carcinogens	kg C_2H_3Cl
Non-Carcinogens	kg C_2H_3Cl
Respiratory inorganics	kg $PM_{2.5}$
Ionizing radiation	Bq C-14
Ozone layer depletion	kg CFC-11
Respiratory organics	kg ethylene
Aquatic ecotoxicity	kg TEG water
Terrestrial ecotoxicity	kg TEG soil
Terrestrial acid/nutri	kg SO_2
Land occupation	m2org.arable
Aquatic acidification	kg SO_2
Aquatic eutrophication	kg PO_4 P-lim
Global warming	kg CO_2
Non-renewable energy	MJ primary
Mineral extraction	MJ surplus

The results of the impact assessment, shown in Figure 26, show the same general trend as the TRACI assessment for most categories, but the PRB has much greater impacts in the respiratory organics and mineral extraction categories. As a point of comparison, the results in the global warming category are very similar for the two impact assessment models.

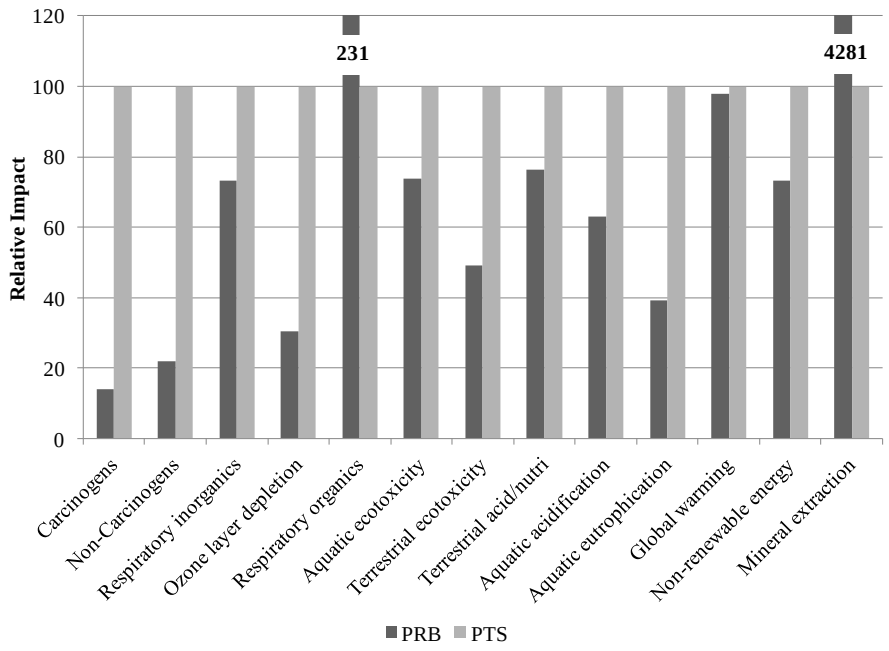

Figure 26. Comparison of PTS and PRB with IMPACT 2002+ impact assessment model.

The normalized results of the comparison, shown in Figure 27, reveal that the most important damage category is the resources category, which describes the depletion of non-renewable energy and mineral resources. The results of the normalized comparison reveal the importance of the non-renewable energy resources, because the final weighting shows that the PRB has greater normalized impacts when compared with the PRB. The normalized impact assessment suggests that the reduction in mineral resources is more important than reducing the smog formation potential through alternative construction methods.

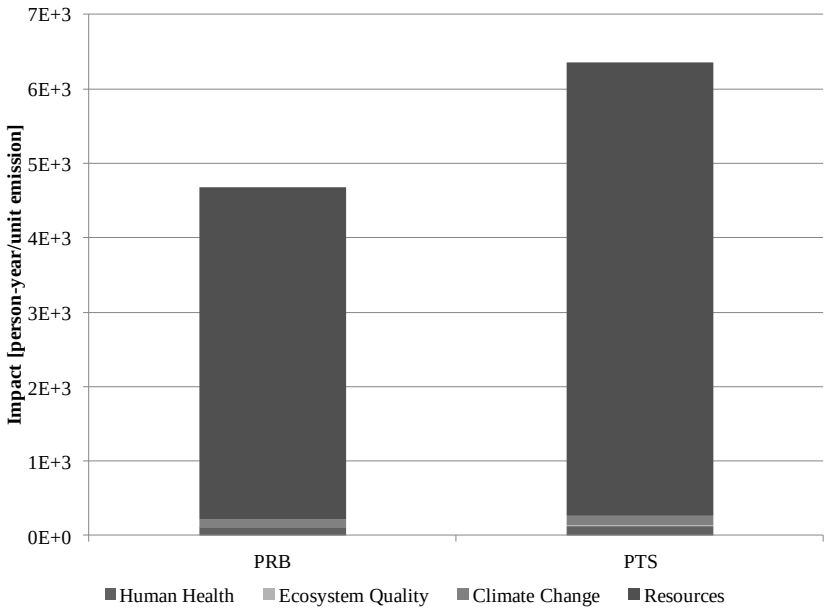

Figure 27. Normalized comparison of PTS and PRB with IMPACT 2002+ impact assessment model.

Uncertainty Analysis. Uncertainty analysis was carried out to determine the statistical significance of PRB and PTS comparison results. LCI data was assigned uncertainty value based on the origin of the information: US data was accepted as reported (no uncertainty) while data adapted from other regions was assigned lognormal distribution with 15% uncertainty. Lognormal distributions were assigned to system inventory data with uncertainty values and squared-geometric standard deviations (SGSD) assigned based on the quality index, and the scale provided in Table 13. Transportation distance was included in the uncertainty analysis with a 50% uncertainty.

Table 13: Uncertainty Analysis Scale

Qualitative Descriptor	Quality Index	Uncertainty	Squared Geometric Standard Deviation
Exact	N/A	0%	1.00
Excellent	A	5%	1.05
Good	B	15%	1.15
Satisfactory	C	25%	1.25
Poor	D	50%	1.50

Appendix B

Toxicity Test Data Tables

Table 14: 2-day aged nZVI Exposure Toxicity Test Data

Count	nZVI Exposure	Exposure Stdev	Relative Growth	Positive Error	Negative Error
1	2.90E-05		0.59		
3	5.80E-05	0.00E+00	0.66	0.21	0.21
3	2.90E-04	0.00E+00	0.04	0.07	0.07
3	5.80E-04	0.00E+00	0.33	0.04	0.04
3	2.90E-03	0.00E+00	0.13	0.03	0.03
3	5.80E-03	0.00E+00	0.04	0.05	0.05

Table 15: 28-day aged nZVI Exposure Toxicity Test Data

Count	nZVI Exposure	Exposure Stdev	Relative Growth	Positive Error	Negative Error
2	2.82E-05	0.00E+00	1.82	1.27	1.27
2	5.64E-05	0.00E+00	1.64	0.98	0.98
2	2.82E-04	0.00E+00	0.01	0.02	0.02
2	5.64E-04	0.00E+00	0.31	0.24	0.24
2	2.82E-03	0.00E+00	0.11	0.05	0.05
2	5.64E-03	0.00E+00	0.00	0.01	0.01

Table 16: $FeCl_2$ Exposure Toxicity Test Data

Count (*n*)	$FeCl_2$ Exposure	Exposure Stdev	Relative Growth	Positive Error	Negative Error
3	1.14E-06	0.00E+00	1.30	0.23	0.23
5	1.08E-05	7.67E-07	1.31	0.32	0.32
4	1.11E-04	7.00E-06	1.86	0.53	0.47
2	1.00E-03	0.00E+00	0.00	0.13	0.00

Table 17: FeS Exposure Toxicity Test Data

Count (*n*)	FeS Exposure	Exposure Stdev	Relative Growth	Positive Error	Negative Error
2	2.62E-05	0	0.73	0.09	0.09
4	5.27E-05	4.83E-07	0.43	0.26	0.26
2	1.06E-04	0	0.57	0.05	0.05
2	2.62E-04	0	0.23	0.21	0.21
4	5.27E-04	4.83E-06	0.15	0.09	0.09
2	1.06E-03	0	0.27	0.02	0.02
4	2.64E-03	2.41E-05	0.24	0.12	0.12
4	5.27E-03	4.83E-05	0.25	0.16	0.16

Table 18: Na_2S Exposure Toxicity Test Data

Count (*n*)	Na_2S Exposure	Exposure Stdev	Relative Growth	Positive Error	Negative Error
4	1.14E-06	0.00E+00	1.26	0.35	0.35
6	1.14E-05	0.00E+00	0.55	0.14	0.14
4	1.14E-04	0.00E+00	0.34	0.26	0.26
2	1.14E-03	0.00E+00	0.52	0.07	0.07

Appendix C

nZVI Equilibrium Speciation Code

```
# Speciation in the Microbial Growth Media
# Monica R. Higgins
# 5/21/2011
# For use with nZVI Toxicity Experiments

#Add nZVI phase as iron metal.  log K from Stumm and Morgan 1996
PHASES
        Fe(metal)
        Fe(s) = Fe+2 + 2e-
        log_k   14.9

SOLUTION_MASTER_SPECIES
                Mops   Mops-    0.0     Mops            208.255
SOLUTION_SPECIES
            #Primary Master Species
                Mops- = Mops-
            log_k         0.0
                #Secondary Species
                Mops- + H+ = H(Mops)
            log_k         7.200
            delta_h       0 kcal

                #Stop SO4 from reducing to HS-
                SO4-2 + 9H+ + 8e- = HS- + 4H2O #this equation from database
                log_k   -200            #database log K 33.66

Solution 1 Pure Water
      units mol/L
                pH  7.0
                density 1
      temp    22.0
SAVE Solution 1
```

```
END

Solution 2 MOPS Buffer
      units mol/L
                  pH  7.0
                  density 1
      temp    22.0

Mops   0.1

SAVE Solution 2
END

Solution 3 MEDIA Stock
      units mol/L
                  pH  7.0
                  density 1
      temp    22.0

Na      0.00690386
K       0.00433000
N(-3)   0.03784000 as NH4
Mg      0.00088447
Ca      0.00037341
Co(2)   0.00000948
Cu(2)   0.00000517
Zn      0.00002280
Mn(2)   0.00003975
Fe(2)   0.000088
P       0.00250000
S(6)    0.00092422
Cl      0.03883788
B       0.00000503
Mo      0.00000381
Edta    0.00103562
Mops    0.01250000
# Glucose       0.013876775

SAVE Solution 3
END

MIX 1 MOPS_Solution (1x)
1 0.95  # Water
2 0.05  # MOPS Buffer

SAVE Solution 4
```

```
END

MIX 2
3 0.4    # Media Stock
4 0.6   # 1x MOPS Buffer

SAVE Solution 5 #1x Media and MOPS
END


USE Solution 5

EQUILIBRIUM_PHASES

Fe(metal)   0   0.00001
Mackinawite 0   0
Chalcocite      0       0
Djurleite       0       0
Chalcopyrite    0       0
Anilite 0       0
MoS2    0       0
CoFe2O4         0       0
BlaubleiII      0       0
BlaubleiI       0       0
Cuprousferrite  0       0
Covellite       0       0
Vivianite       0       0
MnHPO4          0       0
Sphalerite      0       0
Hydroxylapatite         0       0
CoS(beta)       0       0
Fe(OH)2.7Cl.3           0       0
ZnS(am)         0       0
FeMoO4          0       0
CaHPO4          0       0
CoS(alpha)      0       0
CaHPO4:2H2O             0       0
Cuprite0        0
SAVE Solution 6
END
```

Appendix D

$FeCl_2$ Equilibrium Speciation Code

```
# Speciation in the Microbial Growth Media
# Monica R. Higgins
# 5/21/2011
# For use with FeCl2 Toxicity Experiments

SOLUTION_MASTER_SPECIES
        Mops   Mops-    0.0     Mops            208.255
SOLUTION_SPECIES
    #Primary Master Species
        Mops- = Mops-
    log_k       0.0
        #Secondary Species
        Mops- + H+ = H(Mops)
    log_k       7.200
    delta_h     0 kcal

        #Stop SO4 from reducing to HS-
        SO4-2 + 9H+ + 8e- = HS- + 4H2O #this equation from database
        log_k   -200            #database log K 33.66

Solution 1 Pure Water
    units mol/L
        pH  7.0
        density 1
    temp    22.0
SAVE Solution 1
END

Solution 2 MOPS Buffer
    units mol/L
        pH  7.0
        density 1
```

```
    temp    22.0

Mops   0.1

SAVE Solution 2
END

Solution 3 MEDIA Stock
    units mol/L
            pH  7.0
            density 1
    temp    22.0

Na      0.00690386
K       0.00433000
N(-3)   0.03784000 as NH4
Mg      0.00088447
Ca      0.00037341
Co(2)   0.00000948
Cu(2)   0.00000517
Zn      0.00002280
Mn(2)   0.00003975
Fe(2)   0.000088
P       0.00250000
S(6)    0.00092422
Cl      0.03883788
B       0.00000503
Mo      0.00000381
Edta    0.00103562
Mops    0.01250000
# Glucose      0.013876775

SAVE Solution 3
END

MIX 1 MOPS_Solution (1x)
1 0.95  # Water
2 0.05  # MOPS Buffer

SAVE Solution 4
END

Solution 5 Ferrous Chloride Stock
    units mol/L
            pH  7.0
            density 1
```

```
      temp    22.0
Cl 0.2
Fe(2) 0.1 # 1E-1 M Fe(2)
Mops   0.005

SAVE Solution 5
END

MIX 2
3 0.4
4 0.5999
5 0.0001

EQUILIBRIUM_PHASES
Mackinawite 0   0
Chalcocite      0       0
Djurleite       0       0
Chalcopyrite    0       0
Anilite 0       0
MoS2    0       0
CoFe2O4         0       0
BlaubleiII      0       0
BlaubleiI       0       0
Cuprousferrite  0       0
Covellite       0       0
Vivianite       0       0
MnHPO4          0       0
Sphalerite      0       0
Hydroxylapatite         0       0
CoS(beta)       0       0
Fe(OH)2.7Cl.3           0       0
ZnS(am)         0       0
FeMoO4          0       0
CaHPO4          0       0
CoS(alpha)      0       0
CaHPO4:2H2O             0       0
Cuprite0        0
SAVE Solution 6
END
```

Appendix E

FeS Equilibrium Speciation Code

```
# Speciation in the Microbial Growth Media
# Monica R. Higgins
# 5/21/2011
# For use with FeS Toxicity Experiments

#Add MOPS Buffer
SOLUTION_MASTER_SPECIES
        Mops   Mops-    0.0     Mops            208.255
SOLUTION_SPECIES
    #Primary Master Species
        Mops- = Mops-
    log_k       0.0
        #Secondary Species
        Mops- + H+ = H(Mops)
    log_k       7.200
    delta_h     0 kcal

PHASES
        Fix_pe
        e-=e-
        log_k 0

Solution 1 Pure Water
    units mol/L
        pH  7.0
        density 1
    temp    22.0
SAVE Solution 1
END

Solution 2 MOPS Buffer
    units mol/L
```

```
                pH  7.0
                density 1
        temp    22.0

Mops    0.1

SAVE Solution 2
END

Solution 3 MEDIA Stock
        units mol/L
                pH  7.0
                density 1
        temp    22.0

Na      0.00690386
K       0.00433000
N(-3)   0.03784000 as NH4
Mg      0.00088447
Ca      0.00037341
Co(2)   0.00000948
Cu(2)   0.00000517
Zn      0.00002280
Mn(2)   0.00003975
Fe(2)   0.000088
P       0.00250000
S(6)    0.00092422
Cl      0.03883788
B       0.00000503
Mo      0.00000381
Edta    0.00103562
Mops    0.01250000
# Glucose       0.013876775

SAVE Solution 3
END

MIX 1 MOPS_Solution (1x)
1 0.95  # Water
2 0.05  # MOPS Buffer

SAVE Solution 4
END

MIX 2
3 0.4   # Media Stock
```

```
4 0.6   # 1x MOPS Buffer

SAVE Solution 5 #1x Media and MOPS
END

USE Solution 5
EQUILIBRIUM_PHASES
Mackinawite   0   0.00001
Chalcocite    0     0
Djurleite     0     0
Chalcopyrite  0     0
Anilite 0     0
MoS2  0       0
CoFe2O4       0     0
BlaubleiII    0     0
BlaubleiI     0     0
Cuprousferrite 0    0
Covellite     0     0
Vivianite     0     0
MnHPO4        0     0
Sphalerite    0     0
Hydroxylapatite       0     0
CoS(beta)     0     0
Fe(OH)2.7Cl.3         0     0
ZnS(am)       0     0
FeMoO4        0     0
CaHPO4        0     0
CoS(alpha)    0     0
CaHPO4:2H2O           0     0
Cuprite0      0
SAVE Solution 6
END
```

Appendix F

Na_2S Equilibrium Speciation Code

```
# Speciation in the Microbial Growth Media
# Monica R. Higgins
# 5/21/2011
# For use with Na2S Toxicity Experiments

SOLUTION_MASTER_SPECIES
        Mops   Mops-   0.0    Mops          208.255
SOLUTION_SPECIES
    #Primary Master Species
        Mops- = Mops-
    log_k       0.0
        #Secondary Species
        Mops- + H+ = H(Mops)
    log_k       7.200
    delta_h     0 kcal

PHASES
        Fix_pe
        e-=e-
        log_k 0

Solution 1 Pure Water
    units mol/L
        pH  7.0
        density 1
    temp    22.0
SAVE Solution 1
END

Solution 2 MOPS Buffer
    units mol/L
        pH  7.0
```

```
                density 1
        temp    22.0

Mops    0.1

SAVE Solution 2
END

Solution 3 MEDIA Stock
        units mol/L
                pH  7.0
                density 1
        temp    22.0

Na      0.00690386
K       0.00433000
N(-3)   0.03784000 as NH4
Mg      0.00088447
Ca      0.00037341
Co(2)   0.00000948
Cu(2)   0.00000517
Zn      0.00002280
Mn(2)   0.00003975
Fe(2)   0.000088
P       0.00250000
S(6)    0.00092422
Cl      0.03883788
B       0.00000503
Mo      0.00000381
Edta    0.00103562
Mops    0.01250000
# Glucose      0.013876775

SAVE Solution 3
END

MIX 1 MOPS_Solution (1x)
1 0.95  # Water
2 0.05  # MOPS Buffer

SAVE Solution 4
END

Solution 5 Sodium Sulfide Stock
        units mol/L
                pH  7.0
```

```
                density 1
    temp    22.0
Na 0.02
S(-2) 0.01 # 1E-2 M S(-2)
Mops   0.005

SAVE Solution 5

END

MIX 2
3 0.4
4 0.5999
5 0.0001 #1 E-6 M S(-2)

EQUILIBRIUM_PHASES
Mackinawite 0   0
Chalcocite      0       0
Djurleite       0       0
Chalcopyrite    0       0
Anilite 0       0
MoS2    0       0
CoFe2O4         0       0
BlaubleiII      0       0
BlaubleiI       0       0
Cuprousferrite  0       0
Covellite       0       0
Vivianite       0       0
MnHPO4          0       0
Sphalerite      0       0
Hydroxylapatite         0       0
CoS(beta)       0       0
Fe(OH)2.7Cl.3           0       0
ZnS(am)         0       0
FeMoO4          0       0
CaHPO4          0       0
CoS(alpha)      0       0
CaHPO4:2H2O             0       0
Cuprite0        0
SAVE Solution 6
END
```

Appendix G

Selected Values from Minteq.v4 Thermodynamic Database

The Minteq.v4 database was used in this dissertation. The full database is available within PHREEQC for Windows Version 2.1701, and is available in the literature (HydroGeoLogic. and Allison Geoscience Consultant 1998). The following tables give the thermodynamic information from the database that was accessed to complete speciation of the nZVI, FeS, $FeCl_2$ and Na_2S exposure systems.

Table 19: Elements included in PHREEQC Modeling

Elements	Species	Alkalinity	Formula	Formula Weight
B	H3BO3	0	B	10.81
Ca	Ca+2	0	Ca	40.078
Cl	Cl-	0	Cl	35.453
Co	Co+3	-1	Co	58.9332
Cu	Cu+2	0	Cu	63.546
Edta	Edta-4	2	Edta	288.214
Fe	Fe+3	-2	Fe	55.847
H	H+	-1	H	1.0079
K	K+	0	K	39.0983
Mg	Mg+2	0	Mg	24.305
Mn	Mn+3	0	Mn	54.938
Mo	MoO4-2	0	Mo	95.94
Mops	Mops-	0	Mops	208.255
N	NO3-	0	N	14.0067
Na	Na+	0	Na	22.9898
P	PO4-3	2	P	30.9738
S	SO4-2	0	SO4	32.066
Zn	Zn+2	0	Zn	65.39

Table 20: Thermodynamic information for aqueous species in PHREEQC modeling

Species	Equation	log K	delta h
Ca(Edta)-2	Ca+2 + Edta-4 = Ca(Edta)-2	12.420	-25.52
Ca(NH3)2+2	Ca+2 + 2NH4+ = Ca(NH3)2+2 + 2H+	-18.788	0.00
Ca+2	Ca+2 = Ca+2	0.000	
CaH(Edta)-	Ca+2 + Edta-4 + H+ = CaH(Edta)-	15.900	0.00
CaH2BO3+	Ca+2 + H3BO3 = CaH2BO3+ + H+	-7.476	17.00
CaH2PO4+	Ca+2 + 2H+ + PO4-3 = CaH2PO4+	20.923	-6.00
CaHPO4	Ca+2 + H+ + PO4-3 = CaHPO4	15.035	-3.00
CaNH3+2	Ca+2 + NH4+ = CaNH3+2 + H+	-9.144	0.00
CaNO3+	Ca+2 + NO3- = CaNO3+	0.500	-5.40
CaOH+	Ca+2 + H2O = CaOH+ + H+	-12.697	64.11
CaPO4-	Ca+2 + PO4-3 = CaPO4-	6.360	12.97
CaSO4	Ca+2 + SO4-2 = CaSO4	2.360	7.10
Cl-	Cl- = Cl-	0.000	
Co(Edta)-	Co+3 + Edta-4 = Co(Edta)-	43.974	0.00
Co(Edta)-2	Co+2 + Edta-4 = Co(Edta)-2	18.166	-15.00
Co(NH3)+2	Co+2 + NH4+ = Co(NH3)+2 + H+	-7.164	-65.00
Co(NH3)2+2	Co+2 + 2NH4+ = Co(NH3)2+2 + 2H+	-14.778	0.00
Co(NH3)3+2	Co+2 + 3NH4+ = Co(NH3)3+2 + 3H+	-22.922	0.00
Co(NH3)4+2	Co+2 + 4NH4+ = Co(NH3)4+2 + 4H+	-31.446	0.00
Co(NH3)5+2	Co+2 + 5NH4+ = Co(NH3)5+2 + 5H+	-40.470	0.00
Co(NH3)5Cl+2	Co+3 + 5NH4+ + Cl- = Co(NH3)5Cl+2 + 5H+	-17.958	113.38
Co(NH3)6Cl+2	Co+3 + 6NH4+ + Cl- = Co(NH3)6Cl+2 + 6H+	-33.918	104.34
Co(NH3)6OH+2	Co+3 + 6NH4+ + H2O = Co(NH3)6OH+2 + 7H+	-43.715	0
Co(NH3)6SO4+	Co+3 + 6NH4+ + SO4-2 = Co(NH3)6SO4+ + 6H+	-28.993	124.5
Co(NO3)2	Co+2 + 2NO3- = Co(NO3)2	0.509	0
Co(OH)2	Co+2 + 2H2O = Co(OH)2 + 2H+	-18.794	0
Co(OH)3-	Co+2 + 3H2O = Co(OH)3- + 3H+	-31.491	0
Co(OH)4-2	Co+2 + 4H2O = Co(OH)4-2 + 4H+	-46.288	0
Co+2	Co+3 + e- = Co+2	32.400	0
Co+3	Co+3 = Co+3	0.000	

Species	Equation	log K	delta h
Co2OH+3	2Co+2 + H2O = Co2OH+3 + H+	-10.997	0.00
Co4(OH)4+4	4Co+2 + 4H2O = Co4(OH)4+4 + 4H+	-30.488	0.00
CoCl+	Co+2 + Cl- = CoCl+	0.539	2.00
CoCl+2	Co+3 + Cl- = CoCl+2	2.309	16.00
CoH(Edta)	Co+3 + Edta-4 + H+ = CoH(Edta)	47.168	0.00
CoH(Edta)-	Co+2 + Edta-4 + H+ = CoH(Edta)-	21.595	-22.90
CoH2(Edta)	Co+2 + Edta-4 + 2H+ = CoH2(Edta)	23.499	0.00
CoHPO4	Co+2 + H+ + PO4-3 = CoHPO4	15.413	0.00
CoNO2+	Co+2 + NO2- = CoNO2+	0.848	0.00
CoNO3+	Co+2 + NO3- = CoNO3+	0.200	0.00
CoOH+	Co+2 + H2O = CoOH+ + H+	-9.697	0.00
CoOH+2	Co+3 + H2O = CoOH+2 + H+	-1.291	0.00
CoOOH-	Co+2 + 2H2O = CoOOH- + 3H+	-32.092	260.45
CoSO4	Co+2 + SO4-2 = CoSO4	2.300	6.20
Cu(Edta)-2	Cu+2 + Edta-4 = Cu(Edta)-2	20.500	-34.73
Cu(HS)3-	Cu+2 + 3HS- = Cu(HS)3-	25.899	0.00
Cu(NO2)2	Cu+2 + 2NO2- = Cu(NO2)2	3.030	0.00
Cu(NO3)2	Cu+2 + 2NO3- = Cu(NO3)2	-0.400	0.00
Cu(OH)2	Cu+2 + 2H2O = Cu(OH)2 + 2H+	-16.194	0.00
Cu(OH)3-	Cu+2 + 3H2O = Cu(OH)3- + 3H+	-26.879	0.00
Cu(OH)4-2	Cu+2 + 4H2O = Cu(OH)4-2 + 4H+	-39.980	0.00
Cu(S4)2-3	Cu+ + 2HS- = Cu(S4)2-3 + 2H+	3.390	0.00
Cu+	Cu+2 + e- = Cu+	2.690	6.90
Cu+2	Cu+2 = Cu+2	0.000	
Cu2(OH)2+2	2Cu+2 + 2H2O = Cu2(OH)2+2 + 2H+	-10.594	76.62
CuCl	Cu+ + Cl- = CuCl	3.100	0.00
CuCl+	Cu+2 + Cl- = CuCl+	0.200	8.30
CuCl2	Cu+2 + 2Cl- = CuCl2	-0.260	44.18
CuCl2-	Cu+ + 2Cl- = CuCl2-	5.420	-1.76
CuCl3-	Cu+2 + 3Cl- = CuCl3-	-2.290	57.28
CuCl3-2	Cu+ + 3Cl- = CuCl3-2	4.750	1.09
CuCl4-2	Cu+2 + 4Cl- = CuCl4-2	-4.590	32.55

Species	Equation	log K	delta h
CuH(Edta)-	Cu+2 + Edta-4 + H+ = CuH(Edta)-	24.000	-43.10
CuH2(Edta)	Cu+2 + Edta-4 + 2H+ = CuH2(Edta)	26.200	0.00
CuNH3+2	Cu+2 + NH4+ = CuNH3+2 + H+	-5.234	-72.00
CuNO2+	Co+2 + NO2- = CoNO2+	0.848	0.00
CuNO3+	Cu+2 + NO3- = CuNO3+	0.500	-4.10
CuOH(Edta)-3	Cu+2 + Edta-4 + H2O = CuOH(Edta)-3 + H+	8.500	0.00
CuOH+	Cu+2 + H2O = CuOH+ + H+	-7.497	35.81
CuS4S5-3	Cu+ + 2HS- = CuS4S5-3 + 2H+	2.660	0.00
CuSO4	Cu+2 + SO4-2 = CuSO4	2.360	8.70
Edta-4	Edta-4 = Edta-4	0.000	
Fe(Edta)-	Fe+3 + Edta-4 = Fe(Edta)-	27.700	-11.30
Fe(Edta)-2	Fe+2 + Edta-4 = Fe(Edta)-2	16.000	-16.74
Fe(HS)2	Fe+2 + 2HS- = Fe(HS)2	8.950	0.00
Fe(HS)3-	Fe+2 + 3HS- = Fe(HS)3-	10.987	0.00
Fe(OH)2	Fe+2 + 2H2O = Fe(OH)2 + 2H+	-20.494	119.62
Fe(OH)2(Edta)-3	Fe+2 + Edta-4 + H2O = FeOH(Edta)-3 + H+	6.500	0.00
Fe(OH)2(Edta)-4	Fe+2 + Edta-4 + 2H2O = Fe(OH)2(Edta)-4 + 2H+	-4.000	0.00
Fe(OH)2+	Fe+3 + 2H2O = Fe(OH)2+ + 2H+	-4.594	0.00
Fe(OH)3	Fe+3 + 3H2O = Fe(OH)3 + 3H+	-12.560	103.80
Fe(OH)3-	Fe+2 + 3H2O = Fe(OH)3- + 3H+	-28.991	126.43
Fe(OH)4-	Fe+3 + 4H2O = Fe(OH)4- + 4H+	-21.588	0.00
Fe(SO4)2-	Fe+3 + 2SO4-2 = Fe(SO4)2-	5.380	19.20
Fe+2	Fe+3 + e- = Fe+2	13.032	-42.70
Fe+3	Fe+3 = Fe3+	0.000	
Fe2(OH)2+4	2Fe+3 + 2H2O = Fe2(OH)2+4 + 2H+	-2.854	57.62
Fe3(OH)4+5	3Fe+3 + 4H2O = Fe3(OH)4+5 + 4H+	-6.288	65.24
FeCl+2	Fe+3 + Cl- = FeCl+2	1.480	23.00
FeCl2+	Fe+3 + 2Cl- = FeCl2+	2.130	0.00
FeCl3	Fe+3 + 3Cl- = FeCl3	1.130	0.00
FeH(Edta)	Fe+3 + Edta-4 + H+ = FeH(Edta)	29.200	-11.72
FeH(Edta)-	Fe+2 + Edta-4 + H+ = FeH(Edta)-	19.060	-27.61
FeH2PO4+	Fe+2 + 2H+ + PO4-3 = FeH2PO4+	22.273	0.00

Species	Equation	log K	delta h
FeH2PO4+2	Fe+3 + 2H+ + PO4-3 = FeH2PO4+2	23.852	0.00
FeHPO4	Fe+2 + H+ + PO4-3 = FeHPO4	15.975	0.00
FeHPO4+	Fe+3 + H+ + PO4-3 = FeHPO4+	22.292	-30.54
FeNO3+2	Fe+3 + NO3- = FeNO3+2	1.000	-37.00
FeOH(Edta)-2	Fe+3 + Edta-4 + H2O = FeOH(Edta)-2 + H+	19.900	0.00
FeOH(Edta)-3	Fe+3 + Edta-4 + 2H2O = Fe(OH)2(Edta)-3 + 2H+	9.850	0.00
FeOH+	Fe+2 + H2O = FeOH+ + H+	-9397.000	55.81
FeOH+2	Fe+3 + H2O = FeOH+2 + H+	-2.187	41.81
FeSO4	Fe+2 + SO4-2 = FeSO4	2.390	8.00
FeSO4+	Fe+3 + SO4-2 = FeSO4+	4.050	25.00
H(Edta)-3	H+ + Edta-4 = H(Edta)-3	10.948	-23.43
H(Mops)	Mops- + H+ = H(Mops)	7.200	0.00
H+	H+ = H+	0.000	
H2	2 H+ + 2 e- = H2	-3.150	
H2(Edta)-2	2H+ + Edta-4 = H2(Edta)-2	17.221	-41.00
H2BO3-	H3BO3 = H2BO3- + H+	-9.236	13.00
H2Mo7O24-4	7MoO4-2 + 10H+ = H2Mo7O24-4 + 4H2O	64.159	-215.00
H2MoO4	MoO4-2 + 2H+ = H2MoO4	8.164	-26.00
H2O	H2O = H2O	0.000	
H2PO4-	2H+ + PO4-3 = H2PO4-	19.574	-18.00
H2S	H+ + HS- = H2S	7.020	-22.00
H3(Edta)-	3H+ + Edta-4 = H3(Edta)-	20.340	-35.56
H3BO3	H3BO3 = H3BO3	0.000	
H3Mo7O24-3	7MoO4-2 + 11H+ = H3Mo7O24-3 + 4H2O	67.405	-217.00
H3PO4	3H+ + PO4-3 = H3PO4	21.721	-10.10
H4(Edta)	4H+ + Edta-4 = H4(Edta)	22.500	-34.31
H5(BO3)2-	2H3BO3 = H5(BO3)2- + H+	-9.306	8.40
H5(Edta)+	5H+ + Edta-4 = H5(Edta)+	24.000	-32.22
H8(BO3)3-	3H3BO3 = H8(BO3)3- + H+	-7.306	29.40
HMo7O24-5	7MoO4-2 + 9H+ = HMo7O24-5 + 4H2O	59.377	-218.00
HMoO4-	MoO4-2 + H+ = HMoO4-	4.299	20.00
HPO4-2	H+ + PO4-3 = HPO4-2	12.375	-15.00

Species	Equation	log K	delta h
HS-	SO4-2 + 9H+ + 8e- = HS- + 4H2O	33.660	-60.14
HSO4-	H+ + SO4-2 = HSO4-	1.990	22.00
K(Edta)-3	K+ + Edta-4 = K(Edta)-3	1.700	0.00
K+	K+ = K+	0.000	
KHPO4-	K+ + H+ + PO4-3 = KHPO4-	13.255	0.00
KSO4-	K+ + SO4-2 = KSO4-	0.850	4.10
Mg(Edta)-2	Mg+2 + Edta-4 = Mg(Edta)-2	10.570	13.81
Mg+2	Mg+2 = Mg+2	0.000	
MgH(Edta)-	Mg+2 + Edta-4 + H+ = MgH(Edta)-	14.970	0.00
MgH2BO3+	Mg+2 + H3BO3 = MgH2BO3+ + H+	-7.696	13.00
MgH2PO4+	Mg+2 + 2H+ + PO4-3 = MgH2PO4+	21.256	-4.69
MgHPO4	Mg+2 + H+ + PO4-3 = MgHPO4	15.175	-3.00
MgOH+	Mg+2 + H2O = MgOH+ + H+	-11.397	67.81
MgPO4-	Mg+2 + PO4-3 = MgPO4-	4.654	12.97
MgSO4	Mg+2 + SO4-2 = MgSO4	2.260	5.80
Mn(Edta)-2	Mn+2 + Edta-4 = Mn(Edta)-2	15.600	-19.25
Mn(NO3)2	Mn+2 + 2NO3- = Mn(NO3)2	0.600	-1.66
Mn(OH)3-	Mn+2 + 3H2O = Mn(OH)3- + 3H+	-34.800	0.00
Mn(OH)4-2	Mn+2 + 4H2O = Mn(OH)4-2 + 4H+	-48.288	0.00
Mn+2	e- + Mn+3 = Mn+2	25.350	-107.80
Mn+3	Mn+3 = Mn+3	0.000	
MnCl+	Mn+2 + Cl- = MnCl+	0.100	0.00
MnCl2	Mn+2 + 2Cl- = MnCl2	0.250	0.00
MnCl3-	Mn+2 + 3Cl- = MnCl3-	-0.310	0.00
MnH(Edta)-	Mn+2 + Edta-4 + H+ = MnH(Edta)-	19.100	-24.27
MnNO3+	Mn+2 + NO3- = MnNO3+	0.200	0.00
MnO4-	Mn+2 + 4H2O = MnO4- + 8H+ + 5e-	-127.794	822.67
MnO4-2	Mn+2 + 4H2O = MnO4-2 + 8H+ + 4e-	-118.422	711.07
MnOH+	Mn+2 + H2O = MnOH+ + H+	-10.597	55.81
MnSO4	Mn+2 + SO4-2 = MnSO4	2.250	8.70
Mo7O24-6	7MoO4-2 + 8H+ = Mo7O24-6 + 4H2O	52.990	-228.00
MoO4-2	MoO4-2 = MoO4-2	0.000	

Species	Equation	log K	delta h
Mops-	Mops- = Mops-	0.000	
Na(Edta)-3	Na+ + Edta-4 = Na(Edta)-3	2.700	-5.86
Na+	Na+ = Na+	0.000	
NaH2BO3	Na+ + H3BO3 = NaH2BO3 + H+	-9.036	0.00
NaHPO4-	Na+ + H+ + PO4-3 = NaHPO4-	13.445	0.00
NaSO4-	Na+ + SO4-2 = NaSO4-	0.730	1.00
NH3	NH4+ = NH3 + H+	-9.244	-52.00
NH4+	NO3- + 10 H+ + 8 e- = NH4+ + 3 H2O	119.077	-187.06
NH4SO4-	NH4+ + SO4-2 = NH4SO4-	1.030	0.00
NO2-	NO3- + 2 H+ + 2 e- = NO2- + H2O	28.570	-43.76
NO3-	NO3- = NO3-	0.000	
O2	2H2O = O2 + 4H+ + 4e-	-85.995	
OH-	H2O = OH- + H+	-13.997	55.81
PO4-3	PO4-3 = PO4-3	0.000	
S-2	HS- = S-2 + H+	-17.300	49.40
S2-2	HS- = S2-2 + H+	-11.783	46.40
S3-2	HS- = S3-2 + H+	-10.767	42.20
S4-2	HS- = S4-2 + H+	-9.961	39.30
S5-2	HS- = S5-2 + H+	-9.365	37.60
S6-2	HS- = S6-2 + H+	-9.881	0.00
SO4-2	SO4-2 = SO4-2	0.000	
Zn(Edta)-2	Zn+2 + Edta-4 = Zn(Edta)-2	18.000	-19.25
Zn(HS)2	Zn+2 + 2HS- = Zn(HS)2	12.820	0.00
Zn(HS)3-	Zn+2 + 3HS- = Zn(HS)3-	16.100	0.00
Zn(HS)4-2	Zn+2 + 2HS- + 2HS- = Zn(HS)4-2	14.640	0.00
Zn(NO3)2	Zn+2 + 2NO3- = Zn(NO3)2	-0.300	0.00
Zn(OH)2	Zn+2 + 2H2O = Zn(OH)2 + 2H+	-17.794	0.00
Zn(OH)3-	Zn+2 + 3H2O = Zn(OH)3- + 3H+	-28.091	0.00
Zn(OH)4-2	Zn+2 + 4H2O = Zn(OH)4-2 + 4H+	-40.488	0.00
Zn(SO4)2-2	Zn+2 + 2SO4-2 = Zn(SO4)2-2	3.280	0.00
Zn+2	Zn+2 = Zn+2	0.000	
ZnCl+	Zn+2 + Cl- = ZnCl+	0.400	5.40

Species	Equation	log K	delta h
ZnCl2	Zn+2 + 2Cl- = ZnCl2	0.600	37.00
ZnCl3-	Zn+2 + 3Cl- = ZnCl3-	0.500	40.00
ZnCl4-2	Zn+2 + 4Cl- = ZnCl4-2	0.199	45.86
ZnH(Edta)-	Zn+2 + Edta-4 + H+ = ZnH(Edta)-	21.400	-28.45
ZnNO3+	Zn+2 + NO3- = ZnNO3+	0.400	-4.60
ZnOH(Edta)-3	Zn+2 + Edta-4 + H2O = ZnOH(Edta)-3 + H+	5.800	0.00
ZnOH+	Zn+2 + H2O = ZnOH+ + H+	-8.997	55.81
ZnOHCl	Zn+2 + H2O + Cl- = ZnOHCl + H+	-7.480	0.00
ZnS(HS)-	Zn+2 + 2HS- = ZnS(HS)- + H+	6.810	0.00
ZnS(HS)2-2	Zn+2 + 3HS- = ZnS(HS)2-2 + H+	6.120	0.00
ZnSO4	Zn+2 + SO4-2 = ZnSO4	2.340	6.20

Table 21: Thermodynamic information for phases in PHREEQC modeling

Phase	Formula	Equation	log K	delta H
(Co(NH3)5Cl)(NO3)2	(Co(NH3)5Cl)(NO3)2	(Co(NH3)5Cl)(NO3)2 + 5H+ = Co+3 + 5NH4+ + Cl- + 2NO3-	6.2887	6.4199
(Co(NH3)5Cl)Cl2	(Co(NH3)5Cl)Cl2	(Co(NH3)5Cl)Cl2 + 5H+ = Co+3 + 5NH4+ + 3Cl-	4.5102	-10.74
(Co(NH3)5OH2)Cl3	(Co(NH3)5OH2)Cl3	(Co(NH3)5OH2)Cl3 + 5H+ = Co+3 + 5NH4+ + 3Cl- + H2O	11.7351	-25.37
(Co(NH3)6)(NO3)3	(Co(NH3)6)(NO3)3	(Co(NH3)6)(NO3)3 + 6H+ = Co+3 + 6NH4+ + 3NO3-	17.9343	1.59
(Co(NH3)6)Cl3	(Co(NH3)6)Cl3	(Co(NH3)6)Cl3 + 6H+ = Co+3 + 6NH4+ + 3Cl-	20.0317	-33.1
Anhydrite	CaSO4	CaSO4 = Ca+2 + SO4-2	-4.36	-7.2
Anilite	Cu0.25Cu1.5S	Cu0.25Cu1.5S + H+ = 0.25Cu+2 + 1.5Cu+ + HS-	-31.878	182.15
Antlerite	Cu3(OH)4SO4	Cu3(OH)4SO4 + 4H+ = 3Cu+2 + 4H2O + SO4-2	8.788	0
Atacamite	Cu2(OH)3Cl	Cu2(OH)3Cl + 3H+ = 2Cu+2 + 3H2O + Cl-	7.391	-93.43
Bianchite	ZnSO4:6H2O	ZnSO4:6H2O = Zn+2 + SO4-2 + 6H2O	-1.765	-0.6694
Birnessite	MnO2	MnO2 + 4H+ + e- = Mn+3 + 2H2O	18.091	0
Bixbyite	Mn2O3	Mn2O3 + 6H+ = 2Mn+3 + 3H2O	-0.6445	-124.49
BlaubleiI	Cu0.9Cu0.2S	Cu0.9Cu0.2S + H+ = 0.9Cu+2 + 0.2Cu+ + HS-	-24.162	0
BlaubleiII	Cu0.6Cu0.8S	Cu0.6Cu0.8S + H+ = 0.6Cu+2 + 0.8Cu+ + HS-	-27.279	0
Brochantite	Cu4(OH)6SO4	Cu4(OH)6SO4 + 6H+ = 4Cu+2 + 6H2O + SO4-2	15.222	-202.86
Brucite	Mg(OH)2	Mg(OH)2 + 2H+ = Mg+2 + 2H2O	16.844	113.996
Ca3(PO4)2(beta)	Ca3(PO4)2	Ca3(PO4)2 = 3Ca+2 + 2PO4-3	-28.92	54
Ca4H(PO4)3:3H2O	Ca4H(PO4)3:3H2O	Ca4H(PO4)3:3H2O = 4Ca+2 + H+ + 3PO4-3 + 3H2O	-47.08	0
CaHPO4	CaHPO4	CaHPO4 = Ca+2 + H+ + PO4-3	-19.275	0
CaHPO4:2H2O	CaHPO4:2H2O	CaHPO4:2H2O = Ca+2 + H+	-18.995	23

		+ PO4-3 + 2H2O		
CaMoO4	CaMoO4	CaMoO4 = Ca+2 + MoO4-2	-7.95	-2
Chalcanthite	CuSO4:5H2O	CuSO4:5H2O = Cu+2 + SO4-2 + 5H2O	-2.64	6.025
Chalcocite	Cu2S	Cu2S + H+ = 2Cu+ + HS-	-34.92	168
Chalcopyrite	CuFeS2	CuFeS2 + 2H+ = Cu+2 + Fe+2 + 2HS-	-35.27	148.448
Co(BO2)2	Co(BO2)2	Co(BO2)2 + 2H2O + 2H+ = Co+2 + 2H3BO3	27.0703	0
Co(OH)2	Co(OH)2	Co(OH)2 + 2H+ = Co+2 + 2H2O	13.094	0
Co(OH)3	Co(OH)3	Co(OH)3 + 3H+ = Co+3 + 3H2O	-2.309	-92.43
Phase	Formula	Equation	log K	delta H
Co3(PO4)2	Co3(PO4)2	Co3(PO4)2 = 3Co+2 + 2PO4-3	-34.6877	0
Co3O4	Co3O4	Co3O4 + 8H+ = Co+2 + 2Co+3 + 4H2O	-10.4956	-107.5
CoCl2	CoCl2	CoCl2 = Co+2 + 2Cl-	8.2672	-79.815
CoCl2:6H2O	CoCl2:6H2O	CoCl2:6H2O = Co+2 + 2Cl- + 6H2O	2.5365	8.0598
CoFe2O4	CoFe2O4	CoFe2O4 + 8H+ = Co+2 + 2Fe+3 + 4H2O	-3.5281	-158.82
CoHPO4	CoHPO4	CoHPO4 = Co+2 + PO4-3 + H+	19.0607	0
CoMoO4	CoMoO4	CoMoO4 = MoO4-2 + Co+2	-7.7609	-23.3999
CoO	CoO	CoO + 2H+ = Co+2 + H2O	12.5864	-106.295
CoS(alpha)	CoS	CoS + H+ = Co+2 + HS-	-7.44	0
CoS(beta)	CoS	CoS + H+ = Co+2 + HS-	-11.07	0
CoSO4	CoSO4	CuSO4 = Cu+2 + SO4-2	2.9395	-73.04
CoSO4:6H2O	CoSO4:6H2O	CoSO4:6H2O = Co+2 + SO4-2 + 6H2O	-2.4726	1.0801
Covellite	CuS	CuS + H+ = Cu+2 + HS-	-22.3	97
Cu(OH)2	Cu(OH)2	Cu(OH)2 + 2H+ = Cu+2 + 2H2O	8.764	-56.42
Cu2(OH)3NO3	Cu2(OH)3NO3	Cu2(OH)3NO3 + 3H+ = 2Cu+2 + 3H2O + NO3-	9.251	-72.5924
Cu2SO4	Cu2SO4	Cu2SO4 = 2Cu+ + SO4-2	-1.95	-19.079
Cu3(PO4)2	Cu3(PO4)2	Cu3(PO4)2 = 3Cu+2 + 2PO4-3	-36.85	0
Cu3(PO4)2:3H2O	Cu3(PO4)2:3H2O	Cu3(PO4)2:3H2O = 3Cu+2 + 2PO4-3 + 3H2O	-35.12	0
Cumetal	Cu	Cu = Cu+ + e-	-8.756	71.67

CuMoO4	CuMoO4	CuMoO4 = MoO4-2 + Cu+2	-13.0762	12.2
CuOCuSO4	CuOCuSO4	CuOCuSO4 + 2H+ = 2Cu+2 + H2O + SO4-2	10.3032	-137.777
Cupricferrite	CuFe2O4	CuFe2O4 + 8H+ = Cu+2 + 2Fe+3 + 4H2O	5.9882	-201.21
Cuprite	Cu2O	Cu2O + 2H+ = 2Cu+ + H2O	-1.406	-124.02
Cuprousferrite	CuFeO2	CuFeO2 + 4H+ = Cu+ + Fe+3 + 2H2O	-8.9171	-15.89
CuSO4	CuSO4	CuSO4 = Cu+2 + SO4-2	2.9395	-73.04
Djurleite	Cu0.066Cu1.868S	Cu0.066Cu1.868S + H+ = 0.066Cu+2 + 1.868Cu+ + HS-	-33.92	200.334
Epsomite	MgSO4:7H2O	MgSO4:7H2O = Mg+2 + SO4-2 + 7H2O	-2.1265	11.5601
Fe(metal)	Fe(s)	Fe(s) = Fe+2 + 2e-	14.9	
Fe(OH)2	Fe(OH)2	Fe(OH)2 + 2H+ = Fe+2 + 2H2O	13.564	0
Phase	Formula	Equation	log K	delta H
Fe(OH)2.7Cl.3	Fe(OH)2.7Cl.3	Fe(OH)2.7Cl.3 + 2.7H+ = Fe+3 + 2.7H2O + 0.3Cl-	-3.04	0
Fe2(SO4)3	Fe2(SO4)3	Fe2(SO4)3 = 2Fe+3 + 3SO4-2	-3.7343	-242.028
Fe3(OH)8	Fe3(OH)8	Fe3(OH)8 + 8H+ = 2Fe+3 + Fe+2 + 8H2O	20.222	0
FeMoO4	FeMoO4	FeMoO4 = MoO4-2 + Fe+2	10.091	-11.1
Ferrihydrite	Fe(OH)3	Fe(OH)3 + 3H+ = Fe+3 + 3H2O	2.191	-73.374
FeS(ppt)	FeS	FeS + H+ = Fe+2 + HS-	-2.95	-11
Goethite	FeOOH	FeOOH + 3H+ = Fe+3 + 2H2O	0.491	-60.5843
Goslarite	ZnSO4:7H2O	ZnSO4:7H2O = Zn+2 + SO4-2 + 7H2O	-2.0112	14.21
Greigite	Fe3S4	Fe3S4 + 4H+ = 2Fe+3 + Fe+2 + 4HS-	-45.035	0
Gypsum	CaSO4:2H2O	CaSO4:2H2O = Ca+2 + SO4-2 + 2H2O	-4.61	1
H-Jarosite	(H3O)Fe3(SO4)2(OH)6	(H3O)Fe3(SO4)2(OH)6 + 5H+ = 3Fe+3 + 2SO4-2 + 7H2O	-12.1	-230.748
H2MoO4	H2MoO4	H2MoO4 = MoO4-2 + 2H+	-12.8765	49
H2S(g)	H2S	H2S = H+ + HS-	-8.01	0
Halite	NaCl	NaCl = Na+ + Cl-	1.6025	3.7
Hausmannite	Mn3O4	Mn3O4 + 8H+ + 2e- =	61.03	-421

		3Mn+2 + 4H2O		
Hematite	Fe2O3	Fe2O3 + 6H+ = 2Fe+3 + 3H2O	-1.418	-128.987
Hydroxylapatite	Ca5(PO4)3OH	Ca5(PO4)3OH + H+ = 5Ca+2 + 3PO4-3 + H2O	-44.333	0
K-Jarosite	KFe3(SO4)2(OH)6	KFe3(SO4)2(OH)6 + 6H+ = K+ + 3Fe+3 + 2SO4-2 + 6H2O	-14.8	-130.875
K2MoO4	K2MoO4	K2MoO4 = MoO4-2 + 2K+	3.2619	-3.38
Langite	Cu4(OH)6SO4:H2O	Cu4(OH)6SO4:H2O + 6H+ = 4Cu+2 + 7H2O + SO4-2	17.4886	-165.55
Lepidocrocite	FeOOH	FeOOH + 3H+ = Fe+3 + 2H2O	1.371	0
Lime	CaO	CaO + 2H+ = Ca+2 + H2O	32.6993	-193.91
Mackinawite	FeS	FeS + H+ = Fe+2 + HS-	-3.6	0
Maghemite	Fe2O3	Fe2O3 + 6H+ = 2Fe+3 + 3H2O	6.386	0
Magnesioferrite	Fe2MgO4	Fe2MgO4 + 8H+ = Mg+2 + 2Fe+3 + 4H2O	16.8597	-278.92
Magnetite	Fe3O4	Fe3O4 + 8H+ = 2Fe+3 + Fe+2 + 4H2O	3.4028	-208.526
Manganite	MnOOH	MnOOH + 3H+ + e- = Mn+2 + 2H2O	25.34	0
Melanothallite	CuCl2	CuCl2 = Cu+2 + 2Cl-	6.2572	-63.407
Melanterite	FeSO4:7H2O	FeSO4:7H2O = Fe+2 + SO4-2 + 7H2O	-2.209	20.5
Phase	Formula	Equation	log K	delta H
Mg(OH)2(active)	Mg(OH)2	Mg(OH)2 + 2H+ = Mg+2 + 2H2O	18.794	0
Mg3(PO4)2	Mg3(PO4)2	Mg3(PO4)2 = 3Mg+2 + 2PO4-3	-23.28	0
MgHPO4:3H2O	MgHPO4:3H2O	MgHPO4:3H2O = Mg+2 + H+ + PO4-3 + 3H2O	-18.175	0
MgMoO4	MgMoO4	MgMoO4 = Mg+2 + MoO4-2	-1.85	0
Mirabilite	Na2SO4:10H2O	Na2SO4:10H2O = 2Na+ + SO4-2 + 10H2O	-1.114	79.4416
Mn2(SO4)3	Mn2(SO4)3	Mn2(SO4)3 = 2Mn+3 + 3SO4-2	-5.711	-163.427
Mn3(PO4)2	Mn3(PO4)2	Mn3(PO4)2 = 3Mn+2 + 2PO4-3	-23.827	8.8701
MnCl2:4H2O	MnCl2:4H2O	MnCl2:4H2O = Mn+2 + 2Cl- + 4H2O	2.7151	-10.83
MnHPO4	MnHPO4	MnHPO4 = Mn+2 + PO4-3 +	-25.4	0

		H+		
MnS(grn)	MnS	MnS + H+ = Mn+2 + HS-	0.17	-32
MnS(pnk)	MnS	MnS + H+ = Mn+2 + HS-	3.34	0
MnSO4	MnSO4	MnSO4 = Mn+2 + SO4-2	2.5831	-64.8401
MoO3	MoO3	MoO3 + H2O = MoO4-2 + 2H+	-8	0
MoS2	MoS2	MoS2 + 4H2O = MoO4-2 + 6H+ + 2HS- + 2e-	-70.2596	389.02
Na-Jarosite	NaFe3(SO4)2(OH)6	NaFe3(SO4)2(OH)6 + 6H+ = Na+ + 3Fe+3 + 2SO4-2 + 6H2O	-11.2	-151.377
Na2Mo2O7	Na2Mo2O7	Na2Mo2O7 + H2O = 2MoO4-2 + 2Na+ + 2H	-16.5966	56.2502
Na2MoO4	Na2MoO4	Na2MoO4 = MoO4-2 + 2Na+	1.4901	-9.98
Na2MoO4:2H2O	Na2MoO4:2H2O	Na2MoO4:2H2O = MoO4-2 + 2Na+ + 2H2O	1.224	0
Nantokite	CuCl	CuCl = Cu+ + Cl-	-6.73	42.662
Nsutite	MnO2	MnO2 + 4H+ + e- = Mn+3 + 2H2O	17.504	0
O2(g)	O2	O2 + 4H+ + 4e- = 2H2O	83.0894	-571.66
Periclase	MgO	MgO + 2H+ = Mg+2 + H2O	21.5841	-151.23
Portlandite	Ca(OH)2	Ca(OH)2 + 2H+ = Ca+2 + 2H2O	22.804	-128.62
Pyrite	FeS2	FeS2 + 2H+ + 2e- = Fe+2 + 2HS-	-18.5082	49.844
Pyrochroite	Mn(OH)2	Mn(OH)2 + 2H+ = Mn+2 + 2H2O	15.194	-97.0099
Pyrolusite	MnO2	MnO2 + 4H+ + 2e- = Mn+2 + 2H2O	41.38	-272
Sphalerite	ZnS	ZnS + H+ = Zn+2 + HS-	-11.45	30
Strengite	FePO4:2H2O	FePO4:2H2O = Fe+3 + PO4-3 + 2H2O	-26.4	-9.3601
Sulfur	S	S + H+ + 2e- = HS-	-2.1449	-16.3
Phase	Formula	Equation	log K	delta H
Tenorite	CuO	CuO + 2H+ = Cu+2 + H2O	7.644	-64.867
Thenardite	Na2SO4	Na2SO4 = 2Na+ + SO4-2	0.3217	-9.121
Vivianite	Fe3(PO4)2:8H2O	Fe3(PO4)2:8H2O = 3Fe+2 + 2PO4-3 + 8H2O	-36	0
Wurtzite	ZnS	ZnS + H+ = Zn+2 + HS-	-8.95	21.171
Zincite	ZnO	ZnO + 2H+ = Zn+2 + H2O	11.34	-89.62
Zincosite	ZnSO4	ZnSO4 = Zn+2 + SO4-2	3.9297	-82.586
Zn(BO2)2	Zn(BO2)2	Zn(BO2)2 + 2H2O + 2H+ = Zn+2 + 2H3BO3	8.29	0

Zn(NO3)2:6H2O	Zn(NO3)2:6H2O	Zn(NO3)2:6H2O = Zn+2 + 2NO3- + 6H2O	3.3153	24.5698
Zn(OH)2	Zn(OH)2	Zn(OH)2 + 2H+ = Zn+2 + 2H2O	12.2	0
Zn(OH)2(am)	Zn(OH)2	Zn(OH)2 + 2H+ = Zn+2 + 2H2O	12.474	-80.62
Zn(OH)2(beta)	Zn(OH)2	Zn(OH)2 + 2H+ = Zn+2 + 2H2O	11.754	-83.14
Zn(OH)2(epsilon)	Zn(OH)2	Zn(OH)2 + 2H+ = Zn+2 + 2H2O	11.534	-81.8
Zn(OH)2(gamma)	Zn(OH)2	Zn(OH)2 + 2H+ = Zn+2 + 2H2O	11.734	0
Zn2(OH)2SO4	Zn2(OH)2SO4	Zn2(OH)2SO4 + 2H+ = 2Zn+2 + 2H2O + SO4-2	7.5	0
Zn2(OH)3Cl	Zn2(OH)3Cl	Zn2(OH)3Cl + 3H+ = 2Zn+2 + 3H2O + Cl-	15.191	0
Zn3(PO4)2:4H2O	Zn3(PO4)2:4H2O	Zn3(PO4)2:4H2O = 3Zn+2 + 2PO4-3 + 4H2O	-35.42	0
Zn3O(SO4)2	Zn3O(SO4)2	Zn3O(SO4)2 + 2H+ = 3Zn+2 + 2SO4-2 + H2O	18.9135	-258.08
Zn4(OH)6SO4	Zn4(OH)6SO4	Zn4(OH)6SO4 + 6H+ = 4Zn+2 + 6H2O + SO4-2	28.4	0
Zn5(OH)8Cl2	Zn5(OH)8Cl2	Zn5(OH)8Cl2 + 8H+ = 5Zn+2 + 8H2O + 2Cl-	38.5	0
ZnCl2	ZnCl2	ZnCl2 = Zn+2 + 2Cl-	7.05	-72.5
Znmetal	Zn	Zn = Zn+2 + 2e-	25.7886	-153.39
ZnMoO4	ZnMoO4	ZnMoO4 = MoO4-2 + Zn+2	-10.1254	-10.6901
ZnO(active)	ZnO	ZnO + 2H+ = Zn+2 + H2O	11.1884	-88.76
ZnS(am)	ZnS	ZnS + H+ = Zn+2 + HS-	-9.052	15.3553
ZnSO4:1H2O	ZnSO4:1H2O	ZnSO4:1H2O = Zn+2 + SO4-2 + H2O	-0.638	-44.0699

Appendix H

nZVI Exposure Modeling with the Inclusion of Magnetite

Introduction

A common mineral found on the surface of aged nZVI is magnetite, Fe_3O_4 (Liu and Lowry 2006). In modeling the solution chemistry in the presence of nZVI, the formation of magnetite was suppressed, based on the assumption that significant amount of passivating phase would not form during the 24 hour exposure of toxicity tests. This Appendix presents the results of modeling if magnetite.

Modeling Results

Solution pe. The solution pe is greater above 2×10^{-3} M nZVI added if magnetite is allowed to precipitate, as shown in Figure 28. The formation of magnetite controls the pe at these concentrations by fixing the aqueous concentrations of both Fe(II) and Fe(III) in solution. However, the pe is still lower in the presence of magnetite than in the presence of FeS, $FeCl_2$, or Na_2S. This suggests that the formation of magnetite will not change the interpretation of solution pe results, though the magnitude may change.

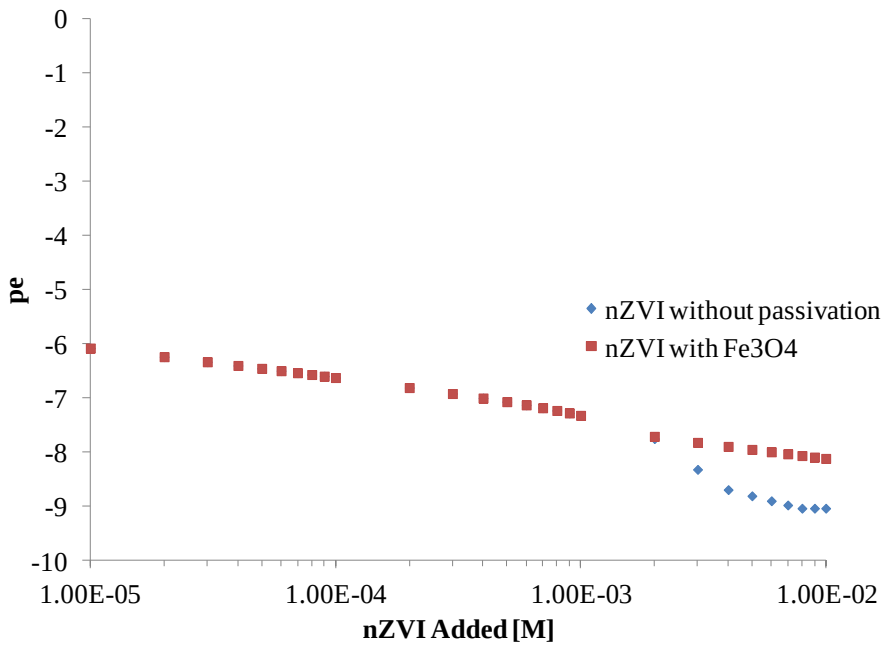

Figure 28. Predicted solution pe with and without Fe_3O_4 considered in the model.

Iron (II) Speciation. Similar to the solution pe, allowing the precipitation of magnetite changes the total iron concentration and the iron speciation above 2 x 10^{-3} M nZVI added. The total concentration of Fe(II) is lower if magnetite is allowed to precipitate, because additional iron added results in additional magnetite formed above 2 x 10^{-3} M nZVI added. If magnetite is allowed to precipitate, the concentration of ferrous iron never exceeds the concentration of EDTA-complexed iron, as shown in Figure 29. The concentrations of phosphate- and hydroxide-complexed iron also change when magnetite is allowed to form, likely because of the pH and pe of the solution in the presence of magnetite. In the absence of magnetite, the ferrous iron concentration exceeds the EDTA-complexed concentration, and was implicated in the observed reduced growth at high concentrations of nZVI. The results of modeling with magnetite show

that in the presence of significant oxide phases the concentrations of ferrous iron may be lower. This is potentially significant for permeable reactive barrier applications, where appreciable passivation may occur over time and reduce the ferrous iron concentrations to which microbes are exposed.

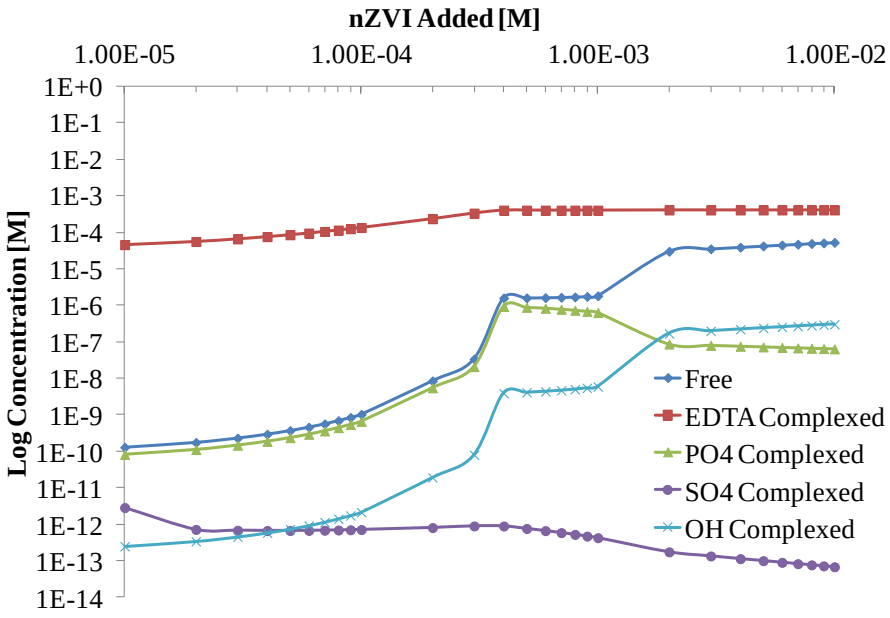

Figure 29. Predicted concentrations of iron associated with ligands in the growth medium as a function of nZVI added if magnetite is allowed to precipitate.

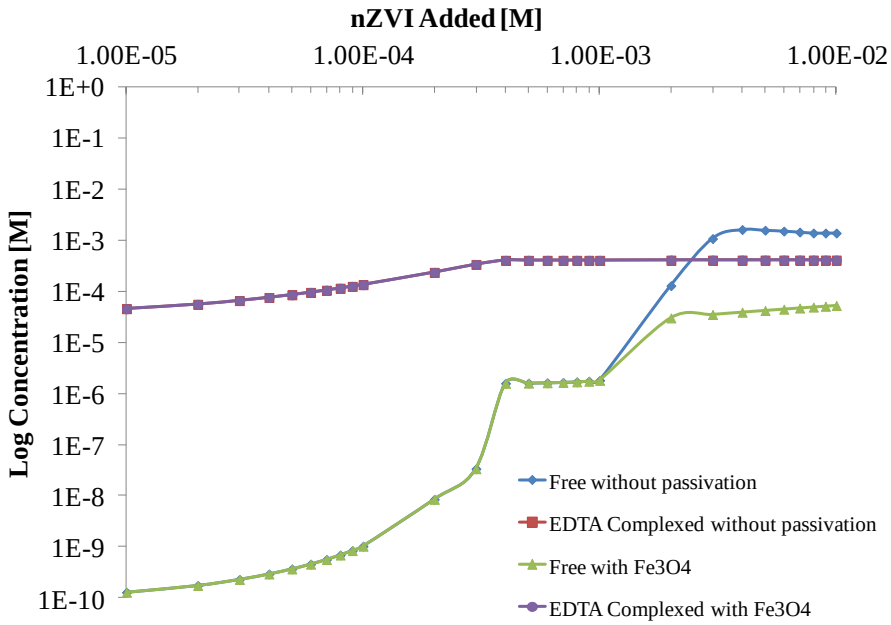

Figure 30. Predicted concentrations of free and EDTA complexed Fe(II) with and without Fe_3O_4 considered in the model.

Manganese Concentration. The precipitation of magnetite reduces the manganese in solution when nZVI added exceeds 2 x 10^{-3} M. The formation of magnetite reduces the iron available for the formation of vivianite such that magnetite coexists with $MnHPO_4$ at high concentrations of nZVI added. The predicted removal of manganese from solution was suggested to be related to the observed reduced growth in the presence of nZVI, possibly because of the importance of manganese to cellular defenses against oxidative stress. Reduced manganese above 2 x 10^{-3} M nZVI added does not contradict such an interpretation, though the effect of reduced manganese may be involved in the observed reduced growth when *E. coli* are exposed to concentrations of nZVI greater than 2 x 10^{-4} M nZVI if passivation is considered.

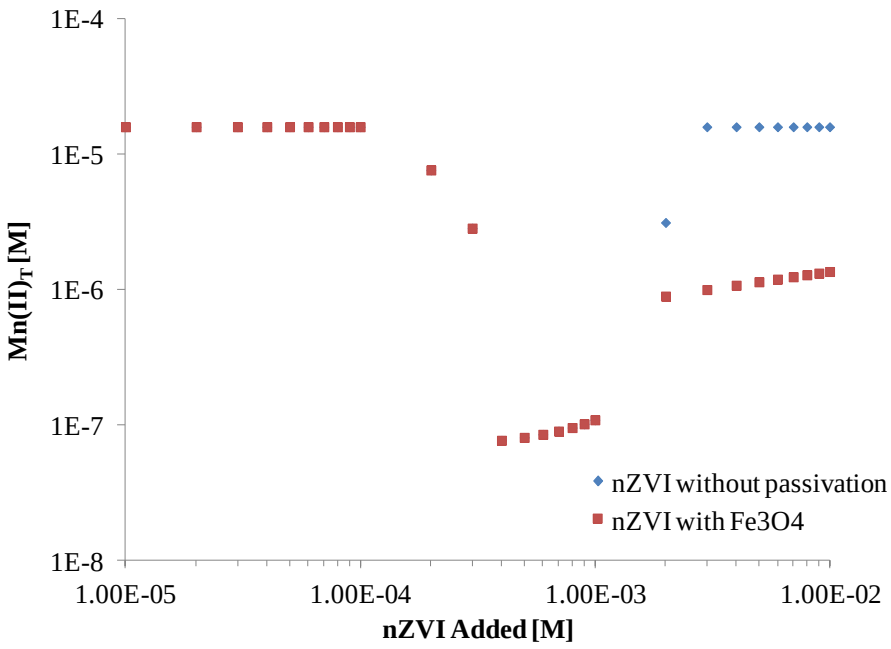

Figure 31. Predicted concentration of Mn(II) with and without Fe_3O_4 considered in the model.

Summary. The inclusion of magnetite as a solid phase considered within the equilibrium speciation model changes the solution chemistry at concentrations above 2×10^{-3} M nZVI added. The precipitation of magnetite generates lower solution pH and higher solution pe when compared with the model excluding magnetite. The speciation of ferrous iron changed in the presence of magnetite such that the concentration of ferrous iron does not exceed the concentration of EDTA-complexed iron, suggesting that if significant passivation is expected the ferrous ion-mediated oxidative stress or redox imbalance may not be as important in understanding nZVI-microbe interactions. The formation of magnetite also reduces the predicated concentration of manganese is solution, due to the coexistence of magnetite and $MnHPO_4$.

References

Adams, L. K., D. Y. Lyon, and P. J. J. Alvarez. 2006. Comparative eco-toxicity of nanoscale TiO2, SiO2, and ZnO water suspensions. *Water Research* 40, (19): 3527-32.

Andrews, S. C., A. K. Robinson, and F. Rodriguez-Quinones. 2003. Bacterial iron homeostasis. *FEMS Microbiology Reviews* 27, (2-3) (JUN): 215-37.

, D. T. Waite, A. Masion, J. C. Woicik, M. R. Wiesner, and J. Y. Bottero. 2008. Relation between the redox state of iron-based nanoparticles and their cytotoxicity toward escherichia coli. *Environmental Science & Technology* 42, (17): 6730-5.

Bagramyan, K., A. Galstyan, and A. Trchounian. 2000. Redox potential is a determinant in the escherichia coli anaerobic fermentative growth and survival: Effects of impermeable oxidant. *Bioelectrochemistry* 51, (2): 151-6.

Bagramyan, K., and A. Trchounian. 1997. Decrease of redox potential in the anaerobic growing E-coli suspension and proton-potassium exchange. *Bioelectrochemistry and Bioenergetics* 43, (1) (JUN): 129-34.

Bare, J., T. Gloria, and G. Norriss. 2006. Development of the method and US normalization database for life cycle impact assessment and sustainability metrics. *Environmental Science and Technology* 40, (16): 5108-15.

Bare, Jane C., Gregory A. Norris, David W. Pennington, and Thomas McKone. 2003. TRACI: The tool for the reduction and assessment of chemical and other environmental impacts. *Journal of Industrial Ecology* 6, (3-4): 49-78.

Barnes, R. J., O. Riba, M. N. Gardner, A. C. Singer, S. A. Jackman, and I. P. Thompson. 2010a. Inhibition of biological TCE and sulphate reduction in the presence of iron nanoparticles. *Chemosphere* 80, (5): 554-62.

Barnes, R. J., C. J. van der Gast, O. Riba, L. E. Lehtovirta, J. I. Prosser, P. J. Dobson, and I. P. Thompson. 2010b. The impact of zero-valent iron nanoparticles on a river water bacterial community. *Journal of Hazardous Materials*.

Bayer, Peter, Michael Finekel, and Georg Teutsch. 2005. Cost-optimal contaminant plume management with a combination of pump-and-treat and physical barrier systems. *Ground Water Monitoring & Remediation* 25, (2): 96-106.

Bayer, Peter, and Michael Finkel. 2006. Life cycle assessment of active and passive groundwater remediation technologies. *Journal of Contaminant Hydrology,* 83, (3-4) (2/10): 171-99.

Bear, J., and Y. Sun. 1998. Optimization of pump-treat-inject (PTI) design for the remediation of a contaminated aquifer: Multi-stage design with chance constraints. *Journal of Contaminant Hydrology* 29, (3): 225-44.

Benning, Liane G., Rick T. Wilkin, and H. L. Barnes. 2000. Reaction pathways in the fe-S system below 100 C. *Chemical Geology* 167, : 25-51.

Berglin, EH, and J. Carlsson. 1985. Potentiation by sulfide of hydrogen peroxide-induced killing of escherichia coli. *Infection and Immunity* 49, (3): 538.

Berner, R. A. 1964. Iron sulfides formed from aqueous solution at low temperatures and atmospheric pressure. *The Journal of Geology* 72, (3): 293-306.

Bradley, M. M. D. 2007. Effects of fis on escherichia coli gene expression during different growth stages. *Microbiology (Society for General Microbiology)* 153, (9) (-09): 2922-40.

Braun, V., and M. Braun. 2002. Iron transport and signaling in escherichia coli. *FEBS Letters* 529, (1): 78-85.

Brayner, R., R. Ferrari-Iliou, N. Brivois, S. Djediat, M. F. Benedetti, and F. Fievet. 2006. Toxicological impact studies based on escherichia coli bacteria in ultrafine ZnO nanoparticles colloidal medium. *Nano Letters* 6, (4): 866-70.

Brunet, L., D. Y. Lyon, E. M. Hotze, P. J. J. Alvarez, and M. R. Wiesner. 2009. Comparative photoactivity and antibacterial properties of C60 fullerenes and titanium dioxide nanoparticles. *Environmental Science & Technology* 43, (12): 4355-60.

Butler, E. C., and K. F. Hayes. 1999. Kinetics of the transformation of trichloroethylene and tetrachloroethylene by iron sulfide. *Environmental Science & Technology* 33, (12): 2021-7.

———. 1998. Effects of solution composition and pH on the reductive dechlorination of hexachloroethane by iron sulfide. *Environmental Science & Technology* 32, (9): 1276-84.

Cadotte, M., L. Deschênes, and R. Samson. 2007. Selection of a remediation scenario for a diesel-contaminated site using LCA. *The International Journal of Life Cycle Assessment* 12, (4): 239-51.

Caffrey, S. M., and G. Voordouw. 2010. Effect of sulfide on growth physiology and gene expression of desulfovibrio vulgaris hildenborough. *Antonie Van Leeuwenhoek* 97, (1): 11-20.

Cantrell, Kirk J., Daniel I. Kaplan, and Thomas W. Wietsma. 1995/7. Zero-valent iron for the in situ remediation of selected metals in groundwater. *Journal of Hazardous Materials* 42, (2): 201-12.

Chen, J., Z. Xiu, G. V. Lowry, and P. J. J. Alvarez. 2010. Effect of natural organic matter on toxicity and reactivity of nano-scale zero-valent iron. *Water Research*.

Cohen, Robert M., Jamers W. Mercer, Robert M. Greenwald, and Milovan S. Beljin. 1997. *Design guidelines for conventional pump-and-treat systems.* EPA-540-S-97-504.

Crichton, R. R., and R. J. Ward. 1995. Iron species in iron homeostasis and toxicity. *Analyst* 120, (3): 693-7.

Davison, W. 1991. The solubility of iron sulphides in synthetic and natural waters at ambient temperature. *Aquatic Sciences* 53, (4): 309-29.

Day, Steven R., Stephanie F. O'Hannesin, and Lloyd Marsden. 1999. Geotechnical techniques for the construction of reactive barriers. *Journal of Hazardous Materials,* 67, (3) (6/30): 285-97.

Demple, B. 1991. Regulation of bacterial oxidative stress genes. *Annual Review of Genetics* 25, (1): 315-37.

Denich, T. J., L. A. Beaudette, H. Lee, and J. T. Trevors. 2003. Effect of selected environmental and physico-chemical factors on bacterial cytoplasmic membranes. *Journal of Microbiological Methods* 52, (2) (FEB): 149-82.

Diamond, M. L., C. A. Page, M. Campbell, S. McKenna, and R. Lall. 1999. Life cycle framework for assessment of site remediation options: Method and generic survey. *Environmental Toxicology and Chemistry* 18, (4): 788-800.

Diao, MingHui, and MaoSheng Yao. 2009. Use of zero-valent iron nanoparticles in inactivating microbes. *Water Research (Oxford)* 43, (20): 5243-51.

Duesterberg, C. K., W. J. Cooper, and T. D. Waite. 2005. Fenton-mediated oxidation in the presence and absence of oxygen. *Environmental Science & Technology* 39, (13): 5052-8.

Duffus, John H., Monica Nordberg, and Douglas M. Templeton. 2007. Glossary of terms used in toxicology, 2nd edition. *Pure and Applied Chemistry* 79, (7): 1153-344.

Dumas, E., C. Gao, D. Suffern, S. E. Bradforth, N. M. Dimitrijevic, and J. L. Nadeau. 2010. Interfacial charge transfer between CdTe quantum dots and gram negative vs gram positive bacteria. *Environmental Science & Technology* 44, (4): 1464-70.

ESTCP. 2003. *Evaluating the longevity and hydraulic performance of permeable reactive barriers at department of defense sites.* US Department of Defense, Environmental Security Technology Certification Program, #CU-9907.

Fabrega, J., S. R. Fawcett, J. C. Renshaw, and J. R. Lead. 2009. Silver nanoparticle impact on bacterial growth: Effect of pH, concentration, and organic matter. *Environ.Sci.Technol* 43, (19): 7285-90.

Focazio, Michael J., Alan H. Welch, Sharon A. Watkins, Dennis R. Helsel, and Marilee A. Morn. 2000. *A retrospective analysis on the occurrence of arsenic in ground-water resources of the united states and limitations in drinking-water-supply characterizations.* U.S. Geological Survey, Water-Resources Investigations Report 99-4279.

Franson, M. A. H., and American Public Health Association. 1985. *Standard methods: For the examination of water and wastewater*. Vol. 1015American Public Health Association Washington DC.

Gallegos, T. J., S. P. Hyun, and K. F. Hayes. 2007. Spectroscopic investigation of the uptake of arsenite from solution by synthetic mackinawite. *Environmental Science and Technology* 41, : 7781.

Gallegos, Tanya Janell. 2007. Sequestration of arsenic(III) by synthetic mackinawite under anoxic conditions. Ph.D., University of Michigan.

Gavaskar, A. R., N. Gupta, B. Sass, W. S. Yoon, R. Janosy, E. H. Drescher, and J. Hicks. 2000a. *Design, construction, and monitoring of the permeable reactive barrier in area 5 at dover air force base.* AFRL-ML-TY-TR-2000-4546.

Gavaskar, Arun, Neeraj Gupta, Bruce Sass, Robert Janosy, and James Hicks. 2000b. *Design guidance for application of permeable reactive barriers for groundwater remediation.*

Gavaskar, Arun R. 1999. Design and construction techniques for permeable reactive barriers. *Journal of Hazardous Materials*, 68, (1-2) (8/12): 41-71.

GeoChemTec. Zero-valent iron, iron hydroxide and iron oxide. Available from http://www.geochemtec.eu/Tutorials/iron%20oxide%20hydroxide.html (accessed 8/14/2011).

Gillham, Robert W., and Stephanie F. O'Hannesin. 1994. Enhanced degradation of halogenated aliphatics by zero-valent iron. *Ground Water* 32, (6).

Goderniaux, , Brouyere, Fowler, Blenkinsop, Therrien, and Orban. 2009. Large scale surface-subsurface hydrological model to assess climate change impacts on groundwater reserves. *Journal of Hydrology* 373, (1-2): 122.

Guan, J., and MM Aral. 1999. Optimal remediation with well locations and pumping rates selected as continuous decision variables. *Journal of Hydrology* 221, (1-2): 20-42.

Haase, Dagmar. 2009. Effects of urbanisation on the water balance - A long-term trajectory. *Environmental Impact Assessment Review* 29, (4): 211.

Han, Young-Soo, Tanya J. Gallegos, Avery H. Demond, and Kim F. Hayes. 2011. FeS-coated sand for removal of arsenic(III) under anaerobic conditions in permeable reactive barriers. *Water Research* 45, (2) (JAN): 593-604.

Henderson, Andrew D., and Avery H. Demond. 2007. Long-term performance of zero-valent iron permeable reactive barriers: A critical review. *Environmental Engineering Science* 24, (4): 401-23.

Hochella, Michael F. Jr, and Andrew S. Madden. 2005. Earth's nano-compartment for toxic metals. *Elements* 1, (4).

Horsburgh, M. J., S. J. Wharton, M. Karavolos, and S. J. Foster. 2002. Manganese: Elemental defence for a life with oxygen. *Trends in Microbiology* 10, (11): 496-501.

Hunger, Stefan, and Liane G. Benning. 2007. Greigite: A true intermediate on the polysulfide pathway to pyrite. *Geochemical Transactions* 8, (1).

Hutson, Susan S., Nancy L. Barber, Joan F. Kenny, Kristin S. Linsey, Deborah S. Lumia, and Molly A. Maupin. 2004. *Estimated use of water in the united states in 2000.* Reston, VA: US Geological Survey Circular 1268.

HydroGeoLogic., and Allison Geoscience Consultant. 1998. *MINTEQA2/PRODEFA2, A geochemical assessment model for environmental systems: User manual supplement for version 4.0.*

Imlay, J. A. 2008. Cellular defenses against superoxide and hydrogen peroxide. *Annual Review of Biochemistry* 77, : 755.

International Organization for Standardization. 1997. *ISO 14040: Environmental management - life cycle assessment - principles and framework*International Organization for Standardization.

Jeen, S. W., R. W. Gillham, and D. W. Blowes. 2006. Effects of carbonate precipitates on long-term performance of granular iron for reductive dechlorination of TCE. *Environmental Science & Technology* 40, (20): 6432-7.

Jeong, Hoon Y., Jun H. Lee, and Kim F. Hayes. 2008. Characterization of synthetic nanocrystalline mackinawite: Crystal structure, particle size, and specific surface area. *Geochimica Et Cosmochimica Acta,* 72, (2) (1/15): 493-505.

Jolliet, Olivier O. 2003. IMPACT 2002 : A new life cycle impact assessment methodology. *The International Journal of Life Cycle Assessment* 8, (6) (-11): 324-30.

Kamolpornwijit, W., L. Liang, OR West, GR Moline, and AB Sullivan. 2003. Preferential flow path development and its influence on long-term PRB performance: Column study. *Journal of Contaminant Hydrology* 66, (3-4): 161-78.

Kenny, J. F., N. L. Barber, S. S. Hutson, K. S. Linsey, J. K. Lovelace, and M. A. Maupin. 2009. *Estimated use of water in the united states in 2005.* US Geological Survey Circular 1344.

Kim, B. C., A. R. Gavaskar, S. K. Ong, S. H. Rosansky, C. A. Cummings, C. L. Criner, A. J. Pollack, and E. H. Drescher. 1994. *Crossflow air stripping with catalytic oxidation.* AL/EQ-TR-1994-0041.

Kim, Jee Yeon, Hee-Jin Park, Changha Lee, Kara L. Nelson, David L. Sedlak, and Jeyong Yoon. 2010. Inactivation of escherichia coli by nanoparticulate zerovalent iron and ferrous ion. *Applied and Environmental Microbiology* 76, (22) (NOV): 7668-70.

Klaine, S. J., P. J. Alvarez, G. E. Batley, T. F. Fernandes, R. D. Handy, D. Y. Lyon, S. Mahendra, M. J. McLaughlin, and J. R. Lead. 2008. Nanomaterials in the environment: Behavior, fate, bioavailability, and effects. *Environmental Toxicology and Chemistry / SETAC* 27, (9) (Sep): 1825-51.

Korte, N. E. 2000. US Department of Energy, ORNL/TM-2000/345.

Kuo, C. H., AN Michel, and WG Gray. 1992. Design of optimal pump-and-treat strategies for contamined groundwater remediation using the simulated annealing algorithm. *Advances in Water Resources* 15, (2): 95-105.

Lee, C., J. Y. Kim, W. I. Lee, K. L. Nelson, J. Yoon, and D. L. Sedlak. 2008. Bactericidal effect of zero-valent iron nanoparticles on escherichia coli. *Environ.Sci.Technol* 42, (13): 4927-33.

Lee, Jun Hee. 2009. Chemical optimization of in situ emplacement of nano-particulate iron sulfide in porous media. Ph.D., University of Michigan.

Lemming, Gitte G. 2010. Life cycle assessment of soil and groundwater remediation technologies: Literature review. *The International Journal of Life Cycle Assessment* 15, (1) (-01): 115-27.

Li, Xiao-Qin, Daniel W. Elliot, and Wei-xan Zhang. 2006. Zero-valent iron nanoparticles for abatement of environmental pollutants: Materials and engineering aspects. *Critical Reviews in Solid State and Materials Sciences* 31, : 111-22.

Li, Z., K. Greden, P. J. J. Alvarez, K. B. Gregory, and G. V. Lowry. 2010. Adsorbed polymer and NOM limits adhesion and toxicity of nano scale zerovalent iron to E. coli. *Environmental Science & Technology* 44, (9): 3462-7.

Liu, Y., and G. V. Lowry. 2006. Effect of particle age (Fe0 content) and solution pH on NZVI reactivity: H2 evolution and TCE dechlorination. *Environ.Sci.Technol* 40, (19): 6085-90.

Lyon, D. Y., L. K. Adams, J. C. Falkner, and P. J. J. Alvarez. 2006. Antibacterial activity of fullerene water suspensions: Effects of preparation method and particle size†. *Environ.Sci.Technol* 40, (14): 4360-6.

Macé, C., S. Desrocher, F. Gheorghiu, A. Kane, M. Pupeza, M. Cernik, P. Kvapil, R. Venkatakrishnan, and W. Zhang. 2006a. Nanotechnology and groundwater remediation: A step forward in technology understanding. *Remediation Journal* 16, (2): 23-33.

———. 2006b. Nanotechnology and groundwater remediation: A step forward in technology understanding. *Remediation Journal* 16, (2): 23-33.

Mackay, Douglas M., and John A. Cherry. 1989. Groundwater contamination: Pump-and-treat remediation. *Environmental Science & Technology* 23, (6): 630-6.

Mahendra, S., H. Zhu, V. L. Colvin, and P. J. Alvarez. 2008. Quantum dot weathering results in microbial toxicity. *Environmental Science & Technology* 42, (24): 9424-30.

Maier, Raina M., Ian L. Pepper, and Charles P. Gerba. 2009. *Environmental microbiology*. 2nd Edition ed. Amsterdam: Elsevier.

Matott, L. S., A. J. Rabideau, and J. R. Craig. 2006. Pump-and-treat optimization using analytic element method flow models. *Advances in Water Resources* 29, (5): 760-75.

McElroy, B., A. Keith, J. Glasgow, and S. Dasappa. 2003. The use of zero-valent iron injection to remediate groundwater: Results of a pilot test at the marshall space flight center *Remediation Journal* 13, : 145-53.

Monod, J. 1949. The growth of bacterial cultures. *Annual Reviews in Microbiology* 3, (1): 371-94.

Morones, J. R., J. L. Elechiguerra, A. Camacho, K. Holt, J. B. Kouri, J. T. Ramírez, and M. J. Yacaman. 2005. The bactericidal effect of silver nanoparticles. *Nanotechnology* 16, : 2346-53.

Mullet, Martine, Sophie Boursiquot, Mustapha Abdelmoula, Jean-Marie Génin, and Jean-Jacques Ehrhardt. 2002. Surface chemistry and structural properties of mackinawite prepared by reaction of sulfide ions with metallic iron. *Geochimica Et Cosmochimica Acta* 66, (5) (3/1): 829-36.

National Research Council. 1994. *Alternatives for ground water cleanup.* National Academy of Sciences, .

Neidhardt, F. C., P. L. Bloch, and D. F. Smith. 1974. Culture medium for enterobacteria. *Journal of Bacteriology* 119, (3): 736.

Nel, A., T. Xia, L. Madler, and N. Li. 2006. Toxic potential of materials at the nanolevel. *Science* 311, (5761): 622.

Nies, DH. 1999. Microbial heavy-metal resistance. *Applied Microbiology and Biotechnology* 51, (6): 730-50.

Nowack, B., and T. D. Bucheli. 2007. Occurrence, behavior and effects of nanoparticles in the environment. *Environmental Pollution* 150, (1): 5-22.

Nurmi, J. T., P. G. Tratnyek, V. Sarathy, D. R. Baer, J. E. Amonette, K. Pecher, C. Wang, J. C. Linehan, D. W. Matson, and R. L. Penn. 2005. Characterization and properties of metallic iron nanoparticles: Spectroscopy, electrochemistry, and kinetics. *Environmental Science & Technology* 39, (5): 1221-30.

O'Hannesin, Stephanie F., and Robert W. Gillham. 1998. Long term performance of an in situ "iron wall" for remediation of VOCs. *Ground Water* 36, (1).

Oki, Taikan, and Shinjiro Kanae. 2006. Global hydrological cycles and world water resources. *Science* 313, : 1068-72.

Page, C. A., M. L. Diamond, M. Campbell, and S. McKenna. 1999. LIFE-CYCLE FRAMEWORK FOR ASSESSMENT OF SITE REMEDIATION OPTIONS: CASE STUDY. *Environmental Toxicology and Chemistry* 18, (4): 801-10.

Pankow, James F., and James J. Morgan. 1979. Dissolution of tetragonal ferrous sulfide (mackinawite) in anoxic aqueous systems. 1. dissolution rate as a function of pH, temperature, and ionic strength. *Environmental Science & Technology* 13, (10): 1248-55.

Parkhurst, D. L., CAJ Appelo, and Geological Survey (US). 1999. *User's guide to PHREEQC (version 2): A computer program for speciation, batch-reaction, one-dimensional transport, and inverse geochemical calculations*US Geological Survey Reston, VA.

Phillips, DH, B. Gu, DB Watson, and Y. Roh. 2003. Impact of sample preparation on mineralogical analysis of zero-valent iron reactive barrier materials. *Journal of Environmental Quality* 32, (4): 1299.

Phillips, D. H., B. Gu, D. B. Watson, Y. Roh, L. Liang, and S. Y. Lee. 2000. Performance evaluation of a zerovalent iron reactive barrier: Mineralogical characteristics. *Environmental Science & Technology* 34, (19): 4169-76.

Phillips, D. H., T. Van Nooten, L. Bastiaens, M. I. Russell, K. Dickson, S. Plant, J. M. E. Ahad, T. Newton, T. Elliot, and R. M. Kalin. 2010. Ten year performance evaluation of a field-scale zero-valent iron permeable reactive barrier installed to remediate trichloroethene contaminated groundwater. *Environmental Science & Technology* 44, (10) (MAY 15): 3861-9.

Pre Consultants. 2006. *SimaPro 7.1*.

Reardon, E. J. 1995. Anaerobic corrosion of granular iron: Measurement and interpretation of hydrogen evolution rates. *Environmental Science & Technology* 29, (12): 2936-45.

Reardon, E. J., R. Fagan, J. L. Vogan, and A. Przepiora. 2008. Anaerobic corrosion reaction kinetics of nanosized iron. *Environmental Science & Technology* 42, (7): 2420-5.

Reinsch, B. C., B. Forsberg, R. L. Penn, C. S. Kim, and G. V. Lowry. 2010. Chemical transformations during aging of zerovalent iron nanoparticles in the presence of common groundwater dissolved constituents. *Environmental Science & Technology* 44, (9): 3455-61.

Rickard, D. R., and G. W. Luther. 2007. Chemistry of iron sulfides. *Chemical Reviews* 107, : 514-62.

Rickard, David. 2006. The solubility of FeS. *Geochimica Et Cosmochimica Acta,* 70, (23) (12/1): 5779-89.

Riondet, C., R. Cachon, Y. Wache, G. Alcaraz, and C. Divies. 2000. Extracellular oxidoreduction potential modifies carbon and electron flow in escherichia coli. *Journal of Bacteriology* 182, (3): 620.

Riondet, C., R. Cachon, Y. Waché, G. Alcaraz, and C. Diviès. 1999. Changes in the proton-motive force in escherichia coli in response to external oxidoreduction potential. *European Journal of Biochemistry* 262, (2): 595-9.

Robertson, W. D., J. L. Vogan, and P. S. Lombardo. 2008. Nitrate removal rates in a 15-year-old permeable reactive barrier treating septic system nitrate. *Ground Water Monitoring & Remediation* 28, (3): 65-72.

Scherer, Michelle M., Sascha Richter, Richard L. Valentine, and Pedro J. J. Alvarez. 2000. Chemistry and microbiology of permeable reactive barriers for in situ groundwater clean up. *Critical Reviews in Microbiology,* 26, (4): 221-64.

Schiavone, J. R., and HM Hassan. 1988. The role of redox in the regulation of manganese-containing superoxide dismutase biosynthesis in escherichia coli. *Journal of Biological Chemistry* 263, (9): 4269.

Schwegmann, Heiko, Andrew J. Feitz, and Fritz H. Frimmel. 2010. Influence of the zeta potential on the sorption and toxicity of iron oxide nanoparticles on S. cerevisiae and E. coli. *Journal of Colloid and Interface Science* 347, (1) (JUL 1): 43-8.

Scientific Applications International Corporation. 2006. *Life cycle assessment: Principles and practice.* EPA/600/R-06/060.

Sondi, I., and B. Salopek-Sondi. 2004. Silver nanoparticles as antimicrobial agent: A case study on E. coli as a model for gram-negative bacteria. *Journal of Colloid and Interface Science* 275, (1): 177-82.

Stackelberg, Paul E., Robert J. Gilliom, David M. Wolock, and Kerie J. Hitt. 2005. *Development and application of a regression equation for estimating the occurrence of atrazine in shallow ground water beneath agriculture areas of the united states.* U.S. Geological Survey, Scientific Investigations Report 2005-5287.

Stroo, H. F., M. Unger, C. H. Ward, M. C. Kavanaugh, C. Vogel, A. Leeson, J. A. Marqusee, and B. P. Smith. 2003. Remediating chlorinated solvent source zones. *Environmental Science & Technology* 37, (11) (JUN 1): 224A-30A.

Stumm, Werner, and James J. Morgan. 1996. *Aquatic chemistry: Chemical equilibria and rates in natural waters*. Environmental science and technology: A wiley-

interscience series of texts and monographs., eds. Jerald L. Schnoor, Alexander Zehnder. Third ed. New York: John Wiley & Sons, Inc.

Suer, P., S. Nilsson-Paledal, and J. Norrman. 2004. LCA for site remediation: A literature review. *Soil and Sediment Contamination (Formerly Journal of Soil Contamination)* 13, (4): 415-25.

Thill, A., O. Zeyons, O. Spalla, F. Chauvat, J. Rose, M. Auffan, and A. M. Flank. 2006. Cytotoxicity of CeO2 nanoparticles for escherichia coli. physico-chemical insight of the cytotoxicity mechanism. *Environ Sci Technol* 40, (19): 6151-6.

Tratnyek, P. G., and R. L. Johnson. 2006. Nanotechnologies for environmental cleanup. *Nano Today* 1, (2): 44-8.

Travis, Curtis C., and Carolyn B. Doty. 1990. Can contaminated aquifers at superfund sites be remediated? *Environmental Science & Technology* 24, (10): 1464-6.

U.S. EPA. National priorities list (NPL). in United States Environmental Protection Agency [database online]. 2007 [cited 3/19 2009]. Available from http://www.epa.gov/superfund/sites/npl/npl.htm.

———. 2002. *Field applications of in situ remediaiton technologies: Permeable reactive barriers.*

———. 1996. *Pump-and-treat ground water remediation: A guide for decision makers and practitioners.* EPA 625-R-95-005.

United Nations Environment Programme (UNEP). 2006. *Global international waters assessment: Challenges to international waters - regional assessments in a global perspective.*

USEPA. 2008. *Green remediation: Incorporating sustainable environmental practices into remediation of contaminated sites.* EPA 542-R-08-002.

Wang, Ai-Yu A. Y. 1994. The growth phase-dependent synthesis of cyclopropane fatty acids in escherichia coli is the result of an RpoS(KatF)-dependent promoter plus enzyme instability. *Molecular Microbiology* 11, (6) (-03): 1009-17.

Wang, Chuan-Bao, and Wei-xian Zhang. 1997. Synthesizing nanoscale iron particles for rapid and complete dechlorination of TCE and PCBs. *Environmental Science & Technology* 31, (7) (06/30/; 07/01/): 2154-6.

Wilkin, R. T., and R. W. Puls. 2003. *Capstone report on the application, monitoring, and performance of permeable reactive barries for groundwater remediation: Volume 1 performance evaluations at two sites.* Cincinnati, OH: Technical Report # EPA/600/R-03/045A.

Wilkin, Richard T., Robert W. Puls, and Guy W. Sewell. 2003. Long-term performance of permeable reactive barriers using zero-valent iron: Geochemical and microbiological effects. *Ground Water* 41, (4): 493-503.

Wilkin, R. T., C. M. Su, R. G. Ford, and C. J. Paul. 2005. Chromium-removal processes during groundwater remediation by a zerovalent iron permeable reactive barrier. *Environmental Science & Technology* 39, (12) (JUN 15): 4599-605.

Wolthers, Mariette, Sjierk Van der Gaast, and David Rickard. 2003. The structure of disordered mackinawite. *The American Mineralogist* 88, (11-12).

Xia, T., M. Kovochich, J. Brant, M. Hotze, J. Sempf, T. Oberley, C. Sioutas, J. I. Yeh, M. R. Wiesner, and A. E. Nel. 2006. Comparison of the abilities of ambient and manufactured nanoparticles to induce cellular toxicity according to an oxidative stress paradigm. *Nano Letters* 6, (8): 1794-807.

Xiu, Z., Z. Jin, T. Li, S. Mahendra, G. V. Lowry, and P. J. J. Alvarez. 2010. Effects of nano-scale zero-valent iron particles on a mixed culture dechlorinating trichloroethylene. *Bioresource Technology* 101, (4): 1141-6.

Yang, X., N. E. Le Brun, A. J. Thomson, G. R. Moore, and N. D. Chasteen. 2000. The iron oxidation and hydrolysis chemistry of escherichia coli bacterioferritin. *Biochemistry* 39, (16): 4915-23.

Zhang, L., Y. Jiang, Y. Ding, M. Povey, and D. York. 2007. Investigation into the antibacterial behaviour of suspensions of ZnO nanoparticles (ZnO nanofluids). *Journal of Nanoparticle Research* 9, (3): 479-89.

Zhang, Wei-xian. 2003. Nanoscale iron particles for environmental remediation: An overview. *Journal of Nanoparticle Research* 5, : 323-32.

Zwietering, MH, I. Jongenburger, FM Rombouts, and K. Van't Riet. 1990. Modeling of the bacterial growth curve. *Applied and Environmental Microbiology* 56, (6): 1875.